Mapping and functional characterization of two genes involved in root development of rice

2019. 1

En YU

Graduate School of Environmental and Life Science

Okayama University

Table of contents

Chapter 1 Introduction

Roots play important roles in anchoring the plants in soil, uptake of water and mineral elements. In addition, roots also can sense and respond to biotic and abiotic stresses (Fukai and Cooper, 1995; Cornwell and Grubb, 2003; Jung and McCouch, 2013). The root system is determined by genetic factors and environmental cues, such as low or high temperatures, soil water status, soil salinity and nutrient scarcity (López-Bucio et al., 2003; Yu et al., 2016). Therefore, understanding of the molecular mechanisms involved in root development and response to different environmental cues is very important to improve the crop productivity. During last decades, great progresses have been made in understanding of the physiological and molecular mechanisms of root development in different plant species.

1. Root structure and uptake system for mineral elements

Based on root developmental origin and branching patterns, plant root systems are mainly divided into taproot system and fibrous root system. The taproot system, which are seen in dicots such as *Arabidopsis thaliana*, pea (*Pisum sativa*) and tomato (*Solanum lycopersicum*), have a large, central, and dominant root from which other roots sprout laterally. While the fibrous root systems are formed by thin, moderately branching roots growing from the stem. This root system is often present in monocots such as rice (*Oryza sativa*), maize (*Zea mays*) and wheat (*Triticum aestivum*) (Atkinson et al., 2014; Coudert et al., 2010).

Rice, as a model plant of monocots is an important staple food for half of the world's population. Rice roots are characterized by having a fibrous root system, which consists of a

seminal root, adventitious roots (crown roots) and lateral roots (Fig. 1.1A). Furthermore, rice root is characterized by distinct anatomies; consisting of the epidermis, cortex (including exodermis, sclerenchyma and endodermis) and stele (including pericycle and vascular tissues) (Fig. 1.1B, C; Hoshikawa 1989). The rice root epidermal cells are capable of developing root hairs. The epidermis, exodermis and sclerenchyma cell layers are named together as root outer cell layers, which have been implicated in the resistance to various stresses, including drought, aluminum, heavy metal and salinity in soil (Huang et al., 2009; 2012). In mature root regions, almost all of the cortex cells between the exodermis and endodermis are destroyed, forming a highly developed aerenchyma (Fig. 1.1B). Furthermore, rice roots are characterized by two Casparian strips at both the exodermis and endodermis (Enstone et al., 2002).

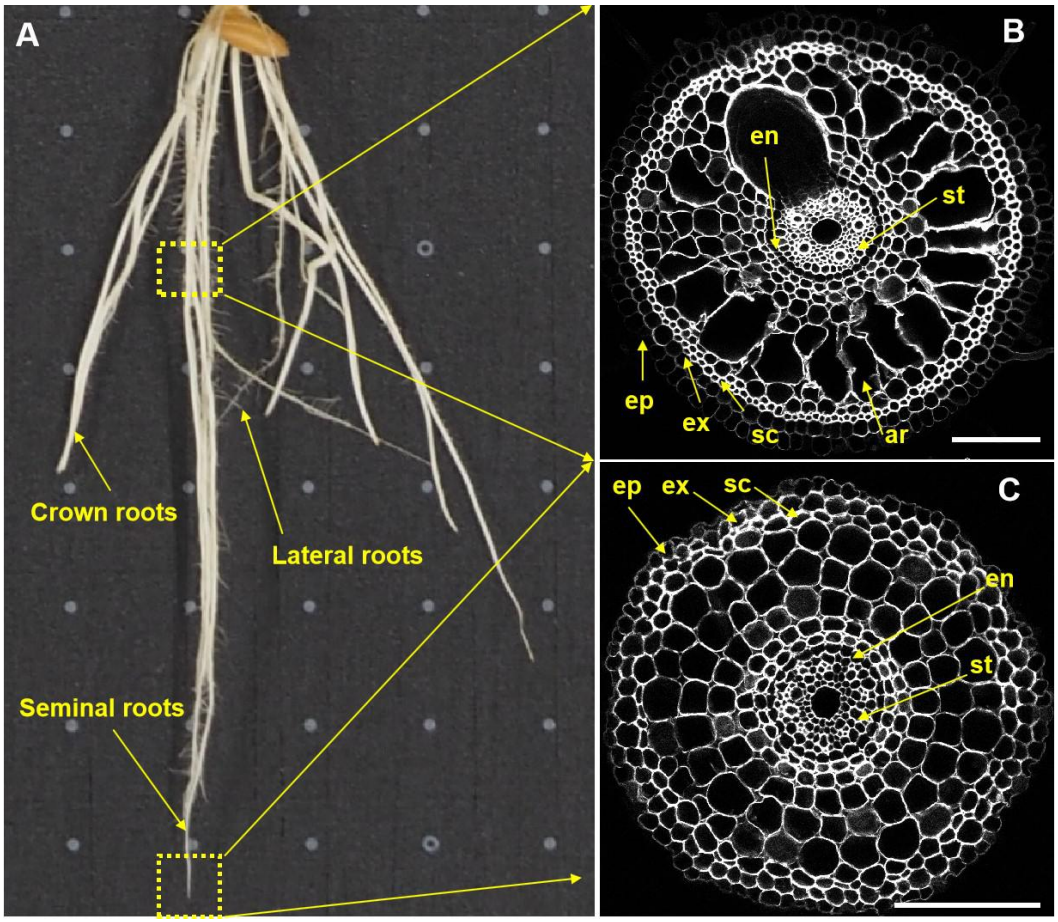

Figure. 1.1 Morphology and anatomy observation of rice roots. (A) Root morphology of rice seedlings grown in half-strength Kimura B solution. (B, C) Root cross section of rice seedlings at mature root region (B) and root tip region (C). Epidermis (ep), exodermis (ex), sclerenchyma (sc), arenchyma (ar), endodermis (en) and stele (st) cell layers are shown. Scale bars, 100 μm.

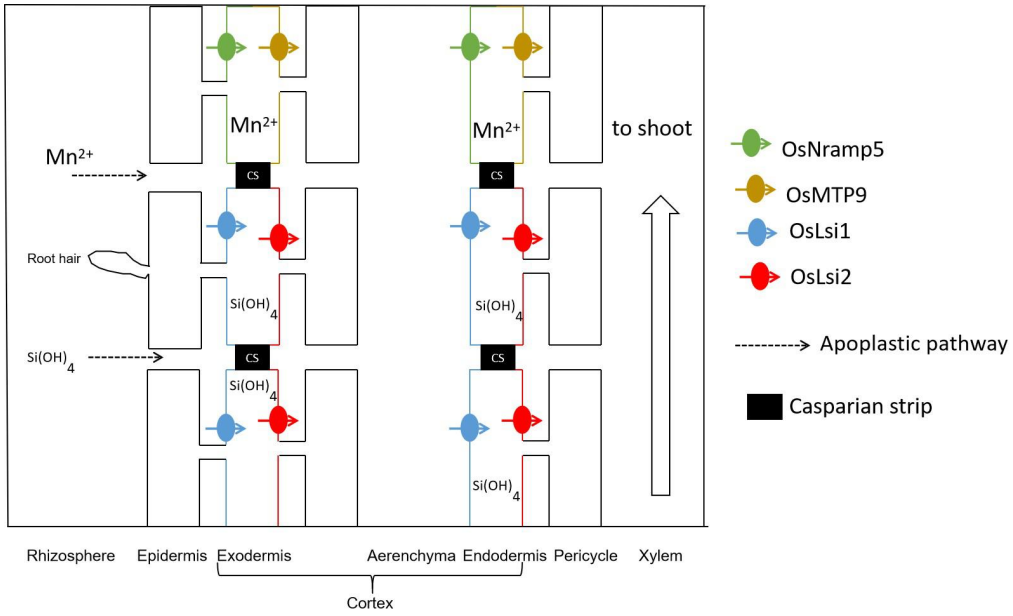

Figure. 1.2 Schematic presentation of an efficient uptake system for manganese (Mn) and silicon (Si) in rice root. The Mn uptake was mediated by OsNramp5 and OsMTP9, while the Si uptake is mediated by OsLsi1 and OsLsi2. Both OsNramp5 and OsLsi1 are influx transporters, and polarly localized at the distal side at both exodermis and endodermis cells, while OsMTP9 and OsLsi2 are efflux transporters and polarly localized at the proximal side of the same cell layers. (Based on Sasaki et al., 2016)

1.1 Role of Casparian strips in mineral element uptake

Casparian strip (CS) is a physical barrier localized at the endodermal cells. It consists of a ring-like impregnation of the primary cell wall with lignin (Naseer et al., 2012; Geldner, 2013) and embedded in the middle of anticlinal cell wall between endodermal cells. It plays an important role in preventing uncontrolled free diffusion of mineral elements from soil solution to root stele (vascular cylinder) and in blocking back leakage of mineral elements (Robbins et al., 2011). Recently, several key genes involved in CS formation in Arabidopsis

have been identified. The formation of lignin-based CS in Arabidopsis roots was initiated when the CS domain proteins (AtCASPs) moved to the CS membrane domain (CSD) (Roppolo et al., 2011). Two important factors including PER64 (Peroxidase 64, a respiratory burst oxidase homolog F) and ESB1 (Enhanced suberin 1) were recruited by CASPs to assemble the lignin polymerization machinery (Hosmani et al., 2013; Lee et al., 2013). A recent study indicated that MYB36, a transcription factor, positively regulated the expression of *CASP1*, *ESB1* and *PER64* during CS formation (Kamiya et al., 2015; Liberman et al., 2015). In contrast to Arabidopsis roots with only one CS at endodermis (Roppolo et al., 2011; Lee et al., 2013), rice roots have two CSs at the exodermis and endodermis cells. A recent study indicated that *OsCASP1* is required for CS formation at endodermis cells and knockout of *OsCASP1* resulted in a significant growth reduction and reduced the uptake of mineral elements, especially of Ca and Si (Wang et al., 2019). Due to distinct CS in rice roots, both influx and efflux transporters in both the exodermis and endodermis of the roots is required for the movement of mineral elements from the soil solution to the stele (Sasaki et al., 2016; Fig. 1.1B, C; Fig. 1.2).

2. Genetic factors regulating root development in rice

The root system is determined by endogenous genetic factors and external environmental cues. With the development of functional genomics, genetic factors controlling root development have been identified using mutant and quantitative trait loci (QTL) analysis. Using different mapping populations, a large numbers of QTL controlling rice root morphological parameters (including maximum root length, root thickness, root number, root

penetration index and root/shoot ratio) have been detected (Zhang et al., 2001; Zheng et al., 2003; Courtois et al., 2003; Li et al., 2005; Uga et al., 2015; Niones et al., 2015). For examples, 675 root QTL controlling 29 root parameters were detected in 12 mapping populations (Courtois et al., 2009). However, only a few root QTL have been cloned. *DRO1*, a deep-rooting QTL regulating root growth angle, is negatively regulated by auxin and involved in cell elongation in the root tip (Uga et al., 2011, 2013). *q*RT9, a QTL controlling root thickness and root length, was found to encode a basic helix-loop-helix (bHLH) transcription factor, *OsbHLH120* (Li et al., 2015b). In addition to those QTL genes, other genes involved in root development were isolated by rice root mutants as described below.

2.1 Molecular mechanisms of root elongation

Normal root elongation is required for plant growth and development. A number of genes involved in root elongation has been identified in rice. These genes encode key factors in different biological processes, including cell wall synthesis, sugar-related metabolism and phytohormone signaling pathway. For examples, *OsGLU3*, a putative membrane-bound endo-1,4-beta-glucanase, was reported to regulate root elongation by affecting the root cell wall loosening (Zhang et al., 2012). Map-based cloning revealed that *rl* (root growth inhibiting) is allelic to *Osglu3* (Inukai et al., 2012). Expansins, encoding by a large gene family, are cell wall proteins and play an important role in the control of plant growth via loosening of the extracellular matrix. One of them, *OsEXPA10* is expressed in the roots, which is regulated by a C_2H_2-type zinc finger transcription factor (*ART1*) in rice (Che et al., 2016). Loss-of-function mutant of *OsEXPA10* results in a decreased root elongation (Che et

al., 2016). Furthermore, *OsEXPA8* is critical for root system architecture. Knockout of this gene causes a shorter primary root and fewer lateral roots in rice (Wang et al., 2014a). These results show that the processes involved in cell wall synthesis can affect the root elongation.

Recent studies indicate that sugar-related metabolism pathways are also involved in root elongation. *OsCyt-inv1*, encoding an alkaline/neutral invertase, is homologous to Arabidopsis gene *AtCyt-inv1* (Qi et al., 2007). Knockout of this gene causes a short-root phenotype. In addition, the mutant accumulates more sucrose, while reduces the hexose concentration in the root. The root growth defects can be rescue by exogenous glucose supply (Jia et al., 2008). Another gene, *OsDGL1,* encoding the dolichyl-diphosphooligosaccharide-protein glycosyltransferase 48kDa subunit precursor, involves in rice root development. Mutation of this gene abolishes the N-glycosylation metabolism in the roots and causes a short root cell length and smaller root meristem and cell death in the root (Qin et al., 2012). Another study shows that OsMOGS, a putative mannosyl-oligosaccharide glucosidase, is highly expressed in rapidly cell-dividing tissues in rice roots (Wang et al., 2014b). Mutation of *OsMOGS* blocks N-glycan maturation and inhibits high-mannose N-glycan formation. The root elongation and root hair development are defected in *osmogs* mutant (Wang et al., 2014b). All these results indicate that sugar-related metabolism pathway paly an essential role in rice root elongation.

In addition, some hormone signaling pathways involved in auxin, ethylene, abscisic acid, gibberellic acid and strigolactones pathways have also been reported to be important for rice

root elongation (Qi et al., 2012; Yu et al., 2015; Mao et al., 2006; Xiao et al., 2016; Li et al., 2015a; Sun et al., 2016).

2.2 Genes involved in crown root development

The major root system of rice consists of crown roots (adventitious roots), which play an important role in water and nutrient elements uptake. Hormone signaling systems, especially auxin and cytokinin, involve in regulating crown root growth and development. To data, five auxin-related genes were reported to play critical roles in crown root development. In *crl1* (crown rootless 1)/*arl1* (adventitious rootless1), the first periclinal division is suppressed (Inukai et al., 2005; Liu et al., 2005). *CLR1*/*ARL1*, which encodes a member of the plant-specific AS2/LOB-domain protein family, is essential for crown root formation by regulating an auxin response factor in the auxin signaling pathway (Inukai et al., 2005; Liu et al., 2005). Knockout of this gene causes a reduced number of crown roots and lateral roots. In addition, lateral root formation in the mutant is not sensitive to auxin (Inukai et al., 2005). In addition, primordia initiation is damaged in *crl4* (crown rootless 4)/*Osgnom1* mutants (Kitomi et al., 2008; Liu et al., 2009). *CRL4*/*OsGNOM1* is a guanine nucleotide exchange factor for ADP-ribosylation factor, which involves in crown root development by affecting polar auxin transport (Kitomi et al., 2008; Liu et al., 2009). The *crl6* (crown rootless 6) mutant is also defect in the initiation and development of primordia. *CRL6*, a member of the CHD (chromodomain, helicase/ATPase, and DNA-binding domain) protein family, plays an important role in crown root development via auxin-related signaling pathway. The knockout line *crl6* had a low expression of *OsIAA* gene (Wang et al., 2016). Furthermore,

Cullin-associated and neddylation dissociated 1 *(OsCAND1)*, the Arabidopsis homologous gene *AtCAND1* (Cheng et al., 2004), involves in auxin signaling to maintain the G2/M cell cycle transition in crown root meristem. The knockout line *oscand1* showed a defect of visible crown root emergence (Wang et al., 2011). Recently, a squamosa promoter binding protein-like3 gene, *SPL3*, involves in crown root development by regulating OsmiR156-*SPL3*/*SPL12* module to directly activate a MADS-box transcription factor, *OsMADS50* (Shao et al., 2019). *SPL3*-*OsMADS50* might directly regulate auxin signaling-related genes, including *OsPIN2*, *OsPIN5a* and *OsPIN5c* (Shao et al., 2019). These genes involved in auxin signaling play an important role in crown root development in rice.

Cytokinins (CKs) are also essential for crown root development in rice, while CKs have negative effects on *de nove* auxin-induced root formation. A *WUSCHEL*-related homeobox (WOX) gene, *WOX11*, plays an important role in crown root development via CK-related signaling pathway (Zhao et al., 2009, 2015); knockout of this gene causes a reduced number of crown roots, while overexpression of *WOX11* substantially promotes crown root growth. *OsRR2* (*O. sativa* response regulator 2) is a type-A cytokinin-responsive regulator gene expressed in crown root primordia. *WOX11* directly represses *OsRR2* by binding to its promoter region (Zhao et al., 2009). The expression of *OsRR2* is also regulated by *OsERF3* (*O. sativa* ethylene-responsive factor3) during crown root initiation. *OsERF3* probably interacts with *OsWOX11* to repress the expression of *OsRR2* during crown root elongation (Zhao et al., 2015). The initiation of crown root primordia is impaired in *crl5* (crown rootless 5). *CRL5*, encoding a member of the large APETELA2/EFR transcription factor family protein, is expressed in crown root initiation region. The expression of *CLR5* is induced by

exogenous auxin treatment. The loss of *CLR5* function results in a reduced number of crown root because the initiation of its crown root primordia is impaired (Kitomo et al., 2011). The expression of the type-A CK response regulator is positively regulated by *CRL5*, which represses CK signaling to regulate crown root initiation in rice (Kitomi et al., 2011). The expression of *CKX4*, a cytokinin oxidase/dehydrogenase (CKX) family gene, is induced by exogenous auxin and cytokinin in the roots. The auxin response factor OsARF25 and the cytokinin response regulator OsRR2 and OsRR3 can directly bind to the promoter region of *CKX4*. The overexpression of *CKX4* enhances the root system development, while knockdown of *CKX4* displays a reduced crown root phenotype. *CKX4* involves in the crown root development by integrating the interaction between cytokinin and auxin (Gao et al., 2014). All these data indicate that the crown root development is coordinately regulated by auxin and CK signaling.

Except for auxin and CK, other plant hormones including brassinosteroids (BRs) and strigolactones (SLs) have also been implicated in crown root development (Mori et al., 2002; Arite et al., 2012; Sun et al., 2015).

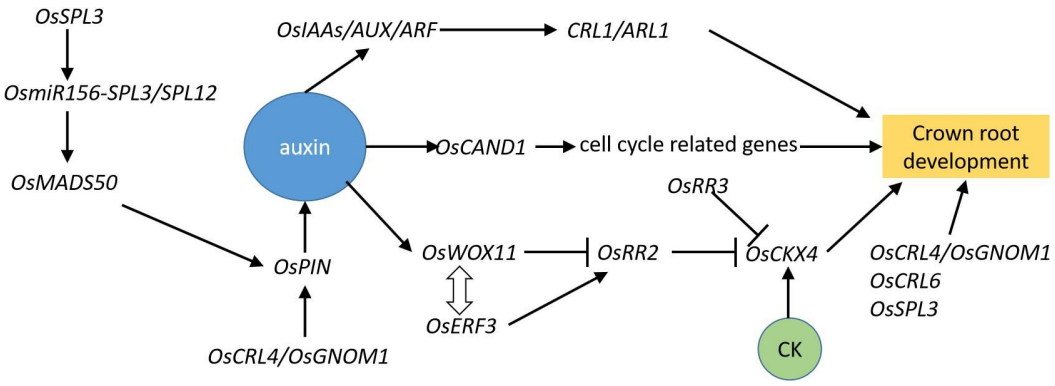

Figure 1.3 The molecular regulatory mechanisms of crown root development in rice. Arrows represent positive regulatory actions. Lines ending in a flat head indicate a negative regulatory action. Double-headed arrows indicate that two proteins interact.

2.3 Genes involved in lateral root formation

Lateral roots (LRs) are derived from a parental root and enable the plants to uptake more water and nutrients from the soil. Plant hormone signaling pathways play an essential role in formation of LRs. Several genes involved in LRs development though auxin-signaling pathway have been identified in rice. For examples, *OsCel9A*, encoding a member of glycoside hydrolase family 9 gene, is involved in regulating auxin-induced LR primordia formation (Yoshida et al., 2006). In addition, four *IAA* genes, *OsIAA3*, *OsIAA11*, *OsIAA13* and *OsIAA23*, were reported to regulate LR development (Nakamura et al., 2006; Ni et al., 2011; Kitomi et al., 2012; Zhu el al., 2012). The lateral root development is impaired in the gain-of-function mutants *osiaa3*, *osiaa11*, *osiaa13* and *osiaa23*. The number of crown roots is also decreased in *osiaa3* and *osiaa23*, but not in *osiaa11* and *osiaa13* (Nakamura et al., 2006; Ni et al., 2011; Kitomi et al., 2012; Zhu el al., 2012). Interestingly, *IPK2*, a rice inositol polyphosphate kinase, can directly interact with *OsIAA11* to repress its degradation and thereby inhibits lateral root development (Chen et al., 217). A cyclophilin gene, *OsCYP2*, is involved in LRs formation by interacting with the *OsTIR1* (*O. sativa* transport inhibitor response1) to degrade the auxin responsive protein, OsIAA11. The loss of *OsCYP2* function results in accumulation of OsIAA11 protein and inhibits the LR development (Zheng et al., 2013; Kang et al., 2013; Jing et al., 2015). In addition, *OsZFP*, encoding a C_2HC-type zinc

finger protein, is involved in regulating LR development by interacting with *OsCYP2* in the nucleus (Cui et al., 2017). All these results indicate that auxin signaling pathway play an essential role in LR development in rice.

Jasmonic acid (JA) and abscisic acid (ABA) signaling pathways are also reported to regulate LR development in rice (Chen et al., 2006; Chen et al., 2012; Hsu et al., 2013), but the molecular mechanism of JA/ABA-induced LR development is poorly understood compared with the auxin signaling pathways.

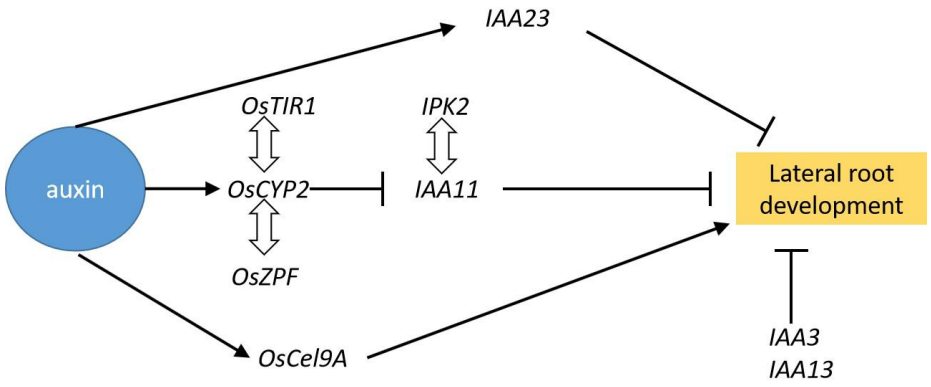

Figure 1.4 The molecular regulatory mechanisms of lateral root development in rice. Arrows represent positive regulatory actions. Lines ending in a flat head indicate a negative regulatory action. Double-headed arrows indicate that two proteins interact.

2.4 Genes involved in root hair formation

Root hairs, the tubular shaped unicellular cells extended from the surface of specialized epidermis cells, play an important role in water and nutrient uptake (Gilroy and Jones, 2000). Several genes involved in regulating root hair development have been isolated in rice. For examples, *OsCSLD1*, a cellulose synthase-like D1 gene, is involved in root hair elongation

but not initiation. Loss-of-function mutant of *OsCSLD1* shows a short root hair, while the root hair density and number of root hairs along their seminal root are the same as the wild-type plants (Kim et al., 2007). Furthermore, root hair elongation is impaired in *osrhl1-1* and *osrhl1-2* mutants (root hairless1-1 and root hairless1-2). *OsRHL1*, a bHLH transcription factor, is specifically expressed in root hair cells and required for root hair elongation. Mutation of *OsRHL1* does not affect the root length or the number of lateral roots and crown roots, which indicates that this gene functions specifically in root hair elongation (Ding et al., 2009). Another rice gene, OsEXPA17, encoding a root hair-specific expansin protein, is required for root hair elongation by remodeling cell wall (Yu et al., 2001).

Auxin signaling pathway is also involved in root hair development in rice. For examples, *OsWOX3A*, a member of WUSCHEL-related homeobox 3A family, was reported to be involved in root hair formation by regulating of auxin transport genes, probably by modulation the expression of *OsPIN* genes (Yoo et al., 2013). Mutation of *OsWOX3A* also affects the lateral root development (Yoo et al., 2013), which indicates that auxin signaling pathway plays an essential role not only in root hair but also in lateral root development.

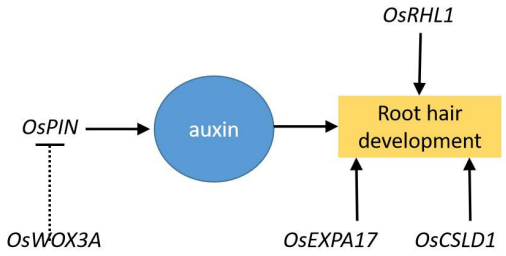

Figure 1.5 The molecular regulatory mechanisms of root hair development in rice. Arrows represent positive regulatory actions. Lines ending in a flat head indicate a negative

regulatory action. Dashed lines represent interactions that have not been experimentally confirmed .

2.5 Genes involved in root differentiation

Meristems control the development of plants organs by regulating cell proliferation and cell differentiation. Genes involved in root cell differentiation play an important role in regulating root development. For example, *OsDocs1*, a leucine-rich repeat receptor-like kinase, is required for the normal development of outer cell layer of both primary roots and lateral roots (Huang et al., 2012). In mutant of *OsDocs1*, some exodermal cells are transformed into additional sclerenchyma cells and became more sensitive to Al toxicity (Huang et al., 2009; 2012). In addition, *ROC4* and *ROC5* (*rice outermost cell-specific gene 4* and *5*), which belong to GL2-type homeobox genes are suggested to be involved in epidermis development (Ito et al., 2002; Ito et al., 2003). Their expression was significantly down-regulated in *OsDocs1* mutant, indicating that *ROC4* and *ROC5* might be regulated by *Docs1* (Huang et al., 2012).

3. Environmental cues regulating root development

3.1 Nutrients and nutrient starvation

Fourteen mineral elements are required for plant growth and development, which includes 6 macronutrients and 8 micronutrients (Marschner 2011). The availability and chemical forms of nutrients in the soils are changeable during the lifecycle of plants. For examples, the form of nitrogen (N) in upland condition is nitrate, while N is changed to ammonium under

flooded condition (Reddy et., 1984). The concentration of Fe in soil solution is hundred times higher in paddy soil than in upland soil (Wang et al., 2019). In addition, the N tends to be more abundant in deeper soil layers, while the phosphate (P) is more abundant in the upper soil (Giehl and von Wirén, 2014). The nutrients in deeper and upper soil layers require different root systems for acquisition. Therefore, plants need to optimize their root systems to respond to changing nutrients. Under N deficiency condition, the root growth is suppressed through the activation of the nitrate transporter (NRT1.1), which impedes auxin accumulation in lateral root primordia and inhibit their further development in Arabidopsis (Krouk et al., 2010; Araya et al., 2014). Alternatively, the N deficiency induced CEP, the C-terminally encoded peptides, are also involved in lateral root growth. CEP can be transported to the shoot to induce CEP downstream1(CEPD1) and CEPD2, then CEPDs are transported back to the root to induce *NRT1.1* and *NRT1.2* (Bouguyon et al., 2016; Tabata et al., 2014). Furthermore, P deficiency can also change the root system architecture. For example, P deficiency dramatically inhibits primary root growth in Arabidopsis (Williamson et al., 2001; Jiang et al., 2007), while this inhibited-root growth needs to combine several components together including blue light, malate, Fe^{2+}, Fe^{3+}, H_2O_2, low pH and low P (Zhang et al., 2019). The lack of any of these factors would abolish the inhibition of primary root growth under P deficiency condition (Zhang et al., 2019). *OsMYB1*, encoding an R2R3-type transcription factor, affects the primary root elongation in a P-dependent manner and lateral roots in a P-independent manner. In addition, the gibberellic acid (GA)-triggered lateral root elongation is largely suppressed under P deficiency condition, while this suppression is partially rescued

in *myb1* mutant. These results indicate that the cross-talk between P deficiency signaling and phytohormone pathways involves in root architecture development (Gu et al., 2017).

In addition to N and P, other mineral elements may also have effect on the root system development, but very little is known about the mechanism underlying.

3.2 Other factors

Many other factors also affect the root architecture, such as water, drought, salinity. Water is one of the most important components for plant growth and roots have developed a complicated system to forage for water. To cope with low water potentials, some types of roots have the ability to continue elongation, while the shoot growth is inhibited (Yamaguchi and Sharp, 2010). The ABA plays an important role in regulating root growth under water stress condition (Zhang et al., 2010). A study showed that ABA accumulation modulates auxin transport in the root tip, which can enhance proton secretion for maintaining primary root elongation and root hair development under moderate water stress (Xu et al., 2013). Salt stress disrupts homeostasis in water potential and ion distribution, which occurs at both the cellular and the whole plant levels (Zhu 2001; 2002). On the other hand, *OsCCC1*, encoding a cation-chloride cotransporter protein, plays an important role in the cell elongation by regulating ion (Cl^-, K^+ and Na^+) homeostasis to maintain cellular osmotic potential. The loss of *OsCCC1* function results in a growth defects of both the roots and shoots (Kong et al., 2011; Chen et al., 2016).

Understanding the molecular mechanisms of root development in rice will enable us to design the ideal root system and generate nutrient-efficient, high-yield and good-quality cultivars by marker-assisted selection or genetic modification.

Chapter 2 *OsGlu3* is required for cell elongation and differentiation of rice roots

1. Introduction

An ideal root system is determined by several parameters including root length, number and root configuration in the soil. Among these, the root length was considered as one of the most important features because it was related with various characters, such as the ability to absorb mineral nutrients and water from soils (Teo et al., 1995). Roots moved through the soil by elongation (Benfey et al., 1993). In recent decades, lots of genes involved in root elongation have been identified using different approaches as described in Chapter 1 (Meng et al., 2019). These genes play an important role in balancing not only the processes of cell division and cell differentiation, but also the processes of cell wall loosening and wall stiffening (Tsukagoshi et al., 2010; Cosgrove 2005; Boyer 2009). For example, *GLR3.1*, the Glu receptor-like gene, is essential for the maintenance of cell division in root apical meristem in rice (Li et al., 2006). A short-root phenotype accompanied by enhanced programmed cell death was observed in *glr3.1* mutant (Li et al., 2006). In addition, SHB, encoding an *AP2/ERF* transcription factor, is involved in regulating elongation and proliferation of meristem cells through activating *KS1*, the transcription of the GA biosynthesis (Li et al., 2015a).

On the other hand, the size and shape of plant cell was controlled by the cell wall. It was reported that there were four candidate agents involving in regulating cell wall loosening,

which included expansin, xyloglucan endotransglycolase (hydrolase), endo-1,4-beta-glucanase and hydroxyl radicals (Cosgrove 2005). For example, four expansin genes are reported to be involved in root growth and development in rice. Among them, *OsEXPA8* and *OsEXPA10* were involved in root elongation, while *OsEXPA17* and *OsEXPB2* were required for root-hair development (Wang et al., 2014a; Che et al., 2016; Yu et al., 2011; Zou et al., 2015). On the other hand, endo-1,4-beta-glucanase belongs to glycoside hydrolase family, of which there are 25 and 15 family members in Arabidopsis and rice, respectively (Cosgrove 2005; Zhou et al., 2006). *KORRIGAN1* (*KOR1*), encoding a putative membrane-bound endo-1,4-b-glucanase, was reported to play an important role in cytokinesis in Arabidopsis. Loss of function of *KOR1* caused a severely abnormal seedling morphology (Nicol et al., 1998; Zuo et al., 2000). In addition, the formation of cell plates and cell walls were aberrant (Zuo et al., 2000). In rice, there are at least three *KOR1* homologous genes including *OsGlu1*, *OsGlu2* and *OsGlu3* (Zhou et al., 2006). OsGlu1 was required for above-ground development (Zhou et al., 2006); the loss of *OsGlu1* function results a reduced cell elongation and a decreased cellulose content (Zhou et al., 2006). While the function of *OsGlu2* was still unclear. Previous studies revealed that *OsGlu3* was ubiquitously expressed in different tissues, especially strongly expressed in the root tip (Zhang et al., 2012). In *osglu3-1*/*rt* mutant, the root cell elongation was inhibited probably by affecting the root cell wall loosening (Zhang et al., 2012; Inukai et al., 2012). Although lots of genes involved in root development had been identified, the molecular mechanisms underlying root elongation and differentiation are still poorly understood in rice.

In this study, we isolated a rice mutant (*dice1*, *defective in cell elongation*) with short-root phenotype. We characterized this mutant in terms of morphological and anatomic aspects. We also mapped the responsible gene for the short-root phenotype. Furthermore, we compared the uptake of essential, beneficial and toxic elements between the mutant and wild-type rice and investigated the effect of root development on transporter expression and localization.

2. Materials and methods

2.1 Screening of rice short-root mutants

Seeds of 3000 lines for screening were provided by Kyushu University (http://shigen.nig.ac.jp/rice/oryzabase/strain/mutant/list). These lines were mutagenized by N-methyl-N-nitrosourea (MNU) from a japonica cultivar, Taichung 65 (T-65). Seeds of each line were geminated in a solution containing 0.5 mM $CaCl_2$ solution at 30ºC. After 7-day-growth, the mutants showing short root length were selected. In this study, we focused on one of the mutants isolated, *dice1* (*defective in cell elongation 1*).

2.2 Time-dependent root elongation

Seeds of T-65 and *dice1* mutant were soaked in water for 2 d at 30°C in the dark and then the germinated seeds were transferred on a net floating on a 0.5 mM $CaCl_2$ solution in a 1.2-liter plastic container. After 24 hours, the root length was measured with a rule at different days. Ten replicates were made for each line.

2.3 Morphological and anatomical analysis

To observe the morphological and anatomical differences between T-65 and *dice1*, 9-day-old seedlings were used for preparing longitudinal and transverse sections of the seminal root. The samples were imbedded into 5% agar and then were sectioned by a microslicer (100 μm thickness) (Linear Slicer PRO10; Dosaka EM). The sections were observed under a confocal laser scanning microscope (TCS SP8x; Leica Microsystems) using UV autofluorescence. More than 3 independent plants were used for the observation.

2.4 Positional cloning of the responsible gene

The mutant, *dice1* was crossed with its wild type to generate F_1. A total of 98 F_2 seedlings were used for genetic analysis. To map the candidate gene, a F_2 population was generated from a cross between *dice1* and Kasalath, an *indica* cultivar. Linkage analysis was performed using 86 polymorphic markers uniformly distributed on the whole rice genome. A total of 1075 F_2 seedlings was used for fine mapping using polymorphic molecular markers. The candidate gene was sequenced using a Big-Dye sequencing kit (Applied Biosystems, http://www.appliedbiosystems.com/) on the SeqStudio Genetic Analyzer.

To detect the transcripts of *OsGlu3* in WT and mutants, RNA and cDNA of the roots were prepared as described below. The transcripts were amplified by PCR using two primers at the 5'UTR and 3'UTR region. The PCR reaction consisted of 28 and 30 cycles (98°C for 10 sec, 60°C for 30 sec, and 68°C for 90 sec) for T-65 and *dice1*, respectively. The PCR products were analyzed by electrophoresis on 1% agarose gel. The target fragments were

isolated from the agarose and directly subjected to sequencing as described. The primers used for mapping and sequencing of *OsGlu3* were listed in Table 2.1.

Table 2.1 Primer sequences used for the mapping and sequencing of *OsGlu3*.

Primer name	Forward (5'---3')	Reverse (5'---3')	Note
M0404	AACGAATTCTATTTTGCGTC	TTCTTCTCATTTCAATTCGC	Mapping marker
M2288	AAATTGAACTTTTATGCGAGTCTTC	CAAGGAGGCAAATGCTAAACA	Mapping marker
M2378	GCGAGGAACAAAGGGATTAAG	CGTCCCAAAGCCTCCGTA	Mapping marker
M0405	CTTGAACCTGAGTGAGTGG	CGATGAAAATGATGTCTA	Mapping marker
M2481	GATTTGCCCTTTCCTTTTCC	GGCGACCAACCGAATAAAAT	Mapping marker
M2508	TCACGTTAGAAGCCAATAGCA	ATCCGATGGGAGCCTTTATC	Mapping marker
M2522	GCTCAGTGCTCAATGGAGAG	GCAAAGTGTTTCACCTTGGA	Mapping marker
M2577	CCAAAAGGAGCAAGCAAACT	GCACGATGATCTCACTGCAT	Mapping marker
M2588	CCACTCACAATCATCCCTCA	CTGAATTTCTCGAGGGCAGA	Mapping marker
M2625	ACGGAAACGTAGGTGGTCTG	GACAATAAACATCACTGGACACG	Mapping marker
M2722	TGGAAGATGAGTGAGAGAGAAGG	GGACGTCCGACGAAAATTAAA	Mapping marker
M2800	AACTACAGCGTCATGCCATT	CCGTGCTTCTGATGCCTTA	Mapping marker
F1	AGAATAGCACCCGCGTTTC		Sequence primer
F2	GTCATCATCGCCAAGTCCATC		Sequence primer
F3	AGTCTATAGCCAGGTGGGCA		Sequence primer
F4	GGGTTGATCCACCAGGAAAA		Sequence primer
R4		ACTCGATGTACTGGTTGCCG	Sequence primer
R3		ACCCTTGGTGAAGTTGAAGG	Sequence primer
R2		CTTGGTGTCCCTCCACTTGT	Sequence primer
R1		CAAACACCTTCGGAACCACT	Sequence primer

2.5 Ionomic analysis

To investigate the ionome profiles in wild-type rice (cv.T-65) and *dice1*, the seedlings (7-d-old) were transferred to a 3.5-liter plastic pot containing half-strength Kimura B solution (pH 5.6) (Yamaji et al., 2013). The Fe-EDTA (20 μM) in half-strength Kimura B solution was replaced with $FeSO_4$ (20 μM). The nutrient solution was renewed every 2 days. After one-week pre-culture, the seedlings were cultivated in different strength Kimura B solution (1/4 x, 1/2 x, 1 x and 2 x) in a 1.2-L pot, respectively. The treatment solution was changed

every 2 days. After 20 days, the seedlings were exposed to a solution containing 0.2 μM $CdSO_4$, 0.2 μM $NaAsO_2$ and 1 μM GeO_2 for 1 day before harvest. The roots were washed with 5 mM cold $CaCl_2$ three times and separated from the shoots with a razor. The biomass of shoots and roots were recorded after being dried at 70°C for 2 days in an oven. The shoots and roots were subjected to determination of element concentration as described below. All experiments were conducted with three biological replicates (2 plants per each sample).

2.6 Soil culture experiments

To compare agronomic trait differences between T-65 and *dice1* grown in soil condition, 30-day-old seedlings of both lines grown hydroponically as described above were transplanted to a 3.5-L plot containing around 3-kg soil. The plants were grown in a greenhouse till ripening under natural sunlight from July to November in 2018. At harvest, the roots were washed with tap water to remove soil and its dry weight was recorded. The tiller number, plant height, dry weight of straw and grain were also recorded.

2.7 Determination of metals in plant tissues

All samples including roots and shoots were dried at 70°C in an oven for at least 2 days. The dried samples were digested with 60% concentrated HNO_3 by heating up to 140°C. The element concentration in the digested solution was determined by inductively coupled plasma-mass spectrometer (7700X; Agilent Technologies) after appropriate dilution.

2.8 Exogenous glucose supplement experiment

Seeds of the wild type rice (T-65) and short-root mutant (*dice1*) were sterilized with 15% NaClO for 30 min and washed 5 times using sterile MilliQ water. The seeds were placed on 0.4% agar medium containing 2 x Kimura B nutrient solution (pH 5.6) in the presence of 0 and 3% (w/v) glucose in 300-ml transparent tubes. The tubes were incubated in a growth chamber at 30°C under a 24-h photoperiod and covered with silver paper. Root parameters were recorded after 7 days.

2.9 Gene expression analysis

The expression level of *OsLsi1*, *OsLsi2*, *OsNramp5,* and *OsMTP9* was investigated in both T-65 and *dice1*. 12-day-old seedlings were exposed to 1 x Kimura B solution for 21 days. Then roots were sampled for RNA extraction. To investigate the effect of exogenous glucose on the expression level of *OsLsi1*, *OsLsi2*, *OsNramp5*, and *OsMTP9* in both T-65 and *dice1,* both T-65 and *dice1* mutant were grown in 0.4% agar medium containing 2 x Kimura B nutrient solution (pH 5.6) in the presence of 0 and 3% glucose for 7 days. Subsequently, the roots were sampled for RNA extraction. To investigate the relationship between *OsDocs1* and *OsGlu3*, their expression was compared between the wild type and respective mutants (*dice1* and *C68*). Root samples for RNA extraction were taken from the seedlings grown in half-strength Kimura B solution for 21 days. Three independent replicates (2 plants per sample) were made.

Total RNA was extracted using an RNeasy Plant Mini Kit (Qiagen) and then was converted to cDNA using ReverTra Ace qPCR RT Master Mix with gDNA remover (Toyobo) according to the protocol supplied by the manufacturer. The expression of *OsLsi1*, *OsLsi2*,

OsNramp5, OsMTP9, *OsDocs1*, and *OsGlu3* was determined by quantitative RT-PCR using a Thunderbird SYBR qPCR mix (Toyobo) on CFX96 (Bio-Rad). *HistoneH3* was used as an internal standard. The primers used are shown in Table 2.2. The relative expression was normalized by the ΔΔCt method using the CFX Manager software (Bio-Rad).

Table 2.2 Primer sequences used for quantitative RT-PCR.

Gene name	Forward (5'---3')	Reverse (5'---3')
OsLsi1	CGGTGGATGTGATCGGAACCA	CGTCGAACTTGTTGCTCGCCA
OsLsi2	ATCTGGGACTTCATGGCCC	ACGTTTGATGCGAGGTTGG
OsNramp5	CAGCAGCAGTAAGAGCAAGATG	GTGCTCAGGAAGTACATGTTGAT
OsMPT9	AGGACCATTTCTTCGACGTG	TCCATCCACCATTTGTACCG
OsDocs1	CGGAAGTCCTTAATGCCCTTG	TGGCTCTATTATGAAGGATGATGAA
OsGlu3	AGTCTATAGCCAGGTGGGCA	ACTCGATGTACTGGTTGCCG
HistoneH3	AGTTTGGTCGCTCTCGATTTCG	TCAACAAGTTGACCACGTCACG

2.10 Immunostaining of OsLsi1

Immunostaining with an antibody against OsLsi1 used before was performed (Yamaji & Ma 2007). The root segments from 7-day-old and 44-day-old seedlings of both T-65 and *dice1* mutant were sampled for immunostaining, which was performed according to Yamaji and Ma (2007). Fluorescence of the secondary antibody (Alexa Fluor 555 goat anti-rabbit IgG; Molecular Probes, Eugene, OR, USA) was observed with confocal laser scanning microscopy (TCS SP8x; Leica Microsystems). To investigate the effect of exogenous glucose on the localization of Lsi1 in roots of the mutant, 7-day-old seedlings grown in the presence of glucose as described above were sampled for immunostaining for Lsi1.

2.11 Lignin, suberin and PI staining

Mature root part of seedlings (21-d-old) grown in half-strength Kimura B solution were used for lignin and suberin staining. Lignin was stained with 0.2% Basic Fuchsin according to Wang et al., (2019). Suberin staining was performed with Fluorol Yellow 088 according to Wang et al., (2019). 5-day-old seedlings grown in 0.5 mM $CaCl_2$ solution were used for PI staining. The PI (propidium iodide) penetration assay was performed as previously described (Wang et al., 2019). Fluorescence was observed with a confocal laser scanning microscope (TCS SP8x; Leica Microsystems).

2.12 Statistical analysis

Tukey test was applied to test differences among treatments at $P<0.05$ using the SPSS 22 (SPSS Inc., Chicago, IL, USA).

3. Results

3.1 Characterization of a short-root rice mutant

Based on seminal root length, a mutant showing short root phenotype was isolated from MNU-mutated seeds, which was designated as *dice1* (defective in cell elongation). The mutant showed a short-root phenotype at different growth stages compared with its wild type (WT), Taichung-65 (T-65) when grown in a nutrient solution (Fig. 2.1A-C). A time-dependent growth analysis showed that the seminal roots of the mutant did not elongate after germination (Fig. 2.1D), in contrast to the WT showing linear root elongation. In addition, the crown roots and lateral roots were also much shorter in the mutant than in the

WT (Fig. 2.1A-C). The shoot size of the mutant was also smaller than that of WT (Fig. 2.1A-C).

When cultivated under soil condition, the size of the whole plants was much smaller in the mutant compared with WT (Fig. 2.1E). Plant height, tiller number, grain yield per plant and dry weight of the roots and shoots, were significantly decreased in the mutant than in the WT (Fig. 2.1F-J). These results indicated the mutant showed a growth defect especially in the roots compared with the wild type.

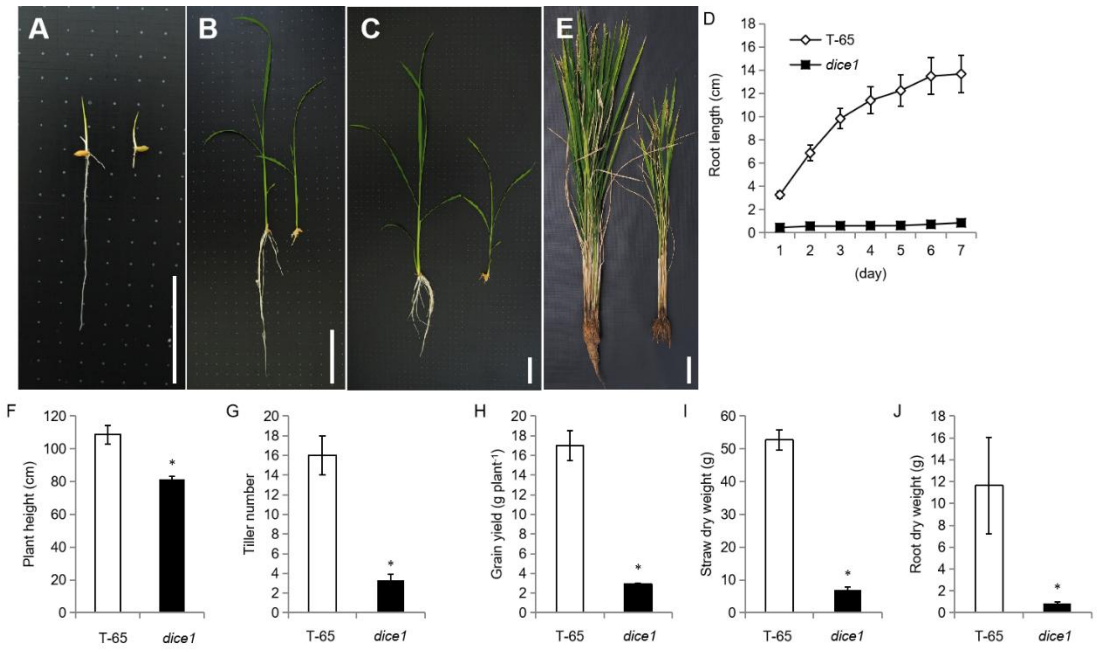

Figure 2.1 Phenotypic and growth parameters comparison of the wild-type rice (T-65) and short-root mutant (*dice1*). (A-C) Phenotype of the wild-type rice (T-65; left) and the mutant (*dice1*, right) grown hydroponically for 7 d (A), 15 d (B), 30 d (C). Bars = 5 cm.(D) Time-dependent root elongation. Germinated seedlings were exposed to a 0.5 mM $CaCl_2$ solution and the seminal root length was measured at different day. Error bars represent ± SD (n = 10). (E) Phenotype of the wild-type rice (left) and the mutant (right) grown in the

field. Photo was taken at harvest. Bar = 5 cm. (F-J) Growth parameters at harvest. Both T-65 and *dice1* were grown in soil till ripening. At harvest, plant height (F), tiller number (G), grain yield per plant (H), straw dry weight (I) and root dry weight (J) were recorded. The asterisk indicates significant differences compared with the wild type (*P<0.05 by Tukey's test).

3.2 Anatomical observation of mutant root

To observe the anatomical differences between the mutant and the wild type, we prepared both longitudinal and transverse sections of the seminal root using 9-day-old seedlings. Sequential sections revealed several differences between the mutant and the WT. Firstly, at the root tip region, the root cap was difficult to peel off from the epidermal cell layers in the mutant (Fig. 2.2A, F). Secondly, the epidermal cells at the root tips were much larger at radial direction in the mutant than in the WT (Fig. 2.2A, E, F, J). Thirdly, the epidermal cells and some exodermal cells at the basal root region were collapsed in the mutant (Fig. 2.2A, C, D, E, F, H, I, J). However, there were no clear anatomical difference in the stele of the roots between the mutant and the WT (Fig. 2.2C, D, H, I).

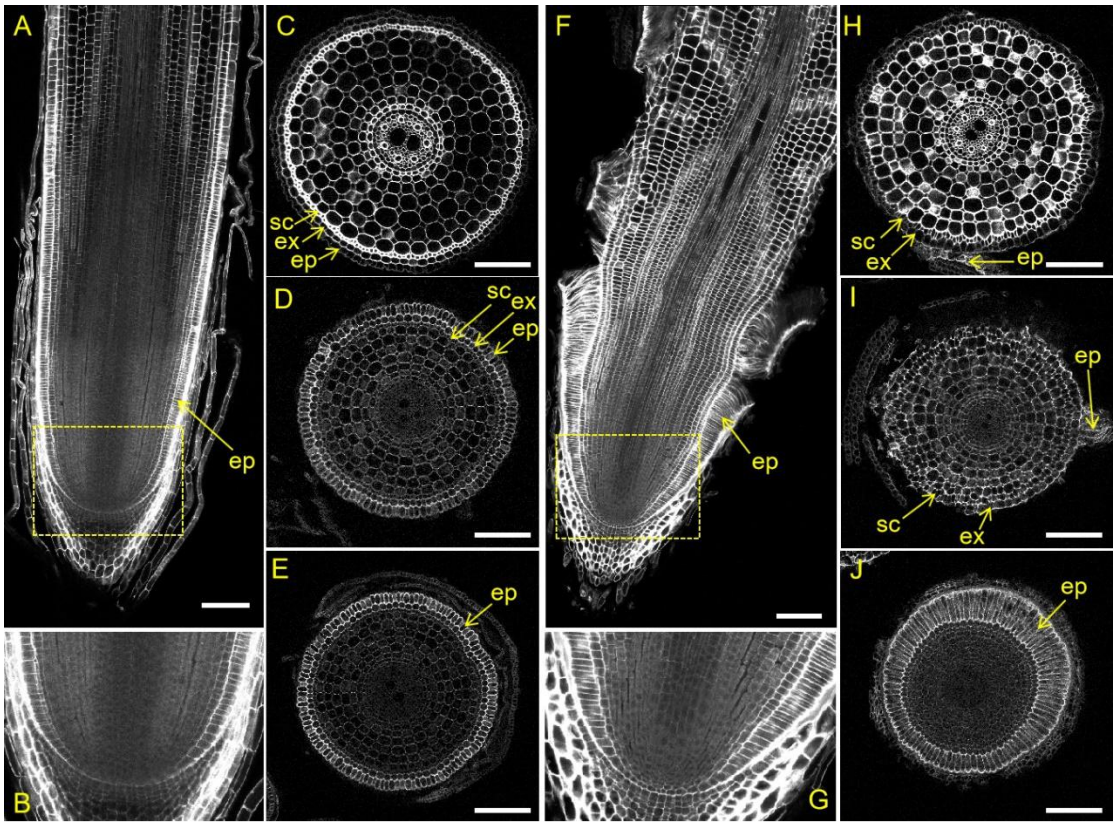

Figure 2.2 Anatomical difference between the wild-type rice and short-root mutant.

(A) Root longitudinal sections of 9-day-old seedlings of the wild type. (B) Magnified image of yellow dotted box in A. (C-E) Root sequential cross sections of 9-day-old seedlings of the wild type. (F) Root longitudinal sections of 9-day-old seedlings of the mutant. (G) Magnified image of yellow dotted box in F. (H-J) Root sequential cross sections of 9-day-old seedlings of the mutant. Epidermis (ep), exodermis (ex) and sclerenchyma (sc) cell layers were shown. Scale bars, 100 μm.

3.3 Lignin, suberin and PI staining

To investigate whether the cell identify of outer cell layer was altered in the mutant, we performed staining for lignin and suberin in the roots. Lignin deposition was observed in the exodermis and sclerenchyma in the WT (Fig. 3.3A-B). However, in the mutant, lignin

deposition was observed in the sclerenchyma-like cells and some cells next to sclerenchyma-like layer, but not in the exodermis (Fig. 3.3C-D).

Suberin staining showed that suberin deposition was observed at the exodermis and endodermis in the roots of the wild type (Fig. 3.3E-G), whereas it was observed at the endodermis but not at exodermis-like cells in the mutant (Fig. 3.3H-J). In the mutant, suberin deposition was also observed in some cells next to sclerenchyma-like layer. These results show that identity of the outer layer cells was altered in the mutant.

To examine whether the apoplastic barriers are damaged in the mutant, we performed propidium iodide (PI) penetration assay. In the wild type, the PI signal was weak in the root tip region (less than 1 mm from the root apex) (Fig. 3.4A, B). By contrast, the PI signal was very strong in the root tip region of the mutant (Fig. 3.4E-F). At the root mature region, the PI staining pattern became similar in the WT and mutant (Fig. 3.4C, D, G, H). These results indicate that the apoplastic barriers in root tip region were disrupted in the mutant.

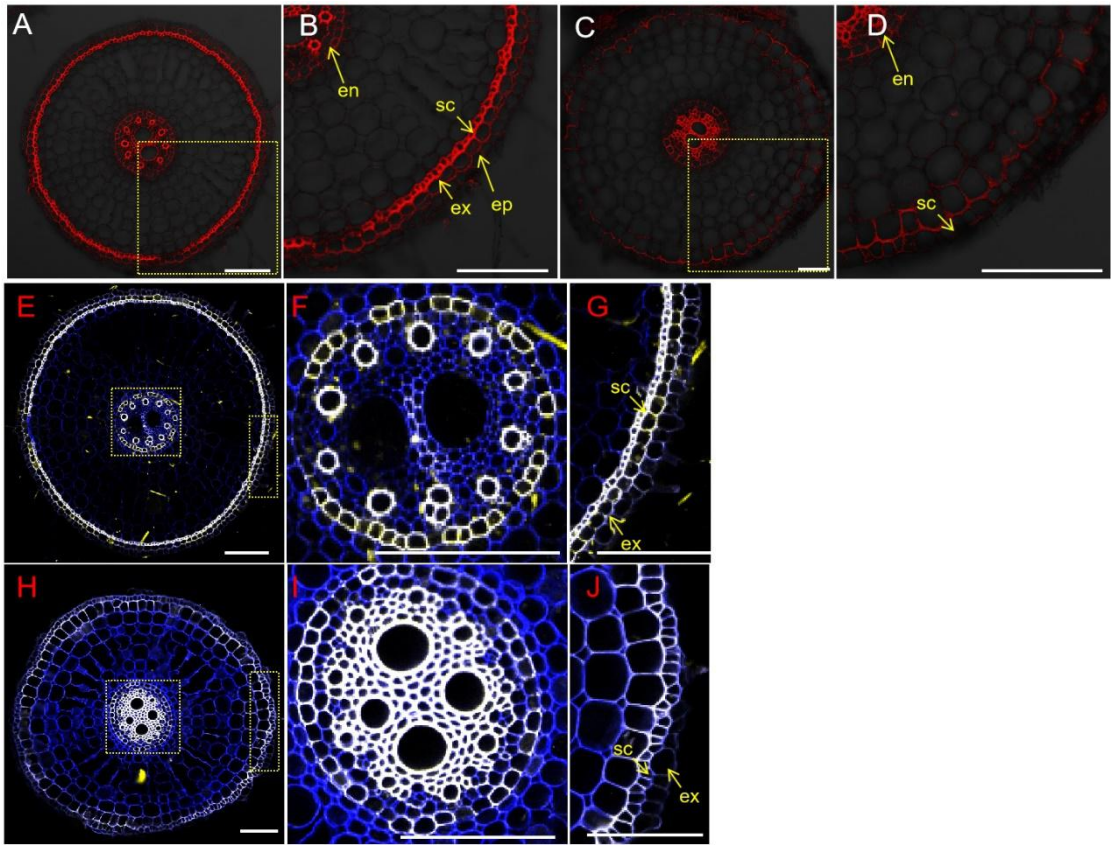

Figure 2.3 Lignin and suberin staining in the wild-type rice (T-65) and short-root mutant (*dice1*). Lignin staining was performed in the mature root region of wild-type rice (cv. T-65) (A) and *dice1* mutant (C). (B, D) Magnified image of yellow dotted box in A and C, respectively. Suberin staining was performed in the roots of T-65 (E) and dice1 (H). (F, G) and (I, J) Magnified image of yellow dotted box in E and H, respectively. The 21-day-old seedlings grown in half-strength Kimura B solution were used for lignin and suberin staining. Red and yellow shows signal of lignin and suberin, respectively. Endodermis (en), exodermis (ex), sclerenchyma (sc) and epidermis (ep) cell layers are shown. Bar = 100 µm.

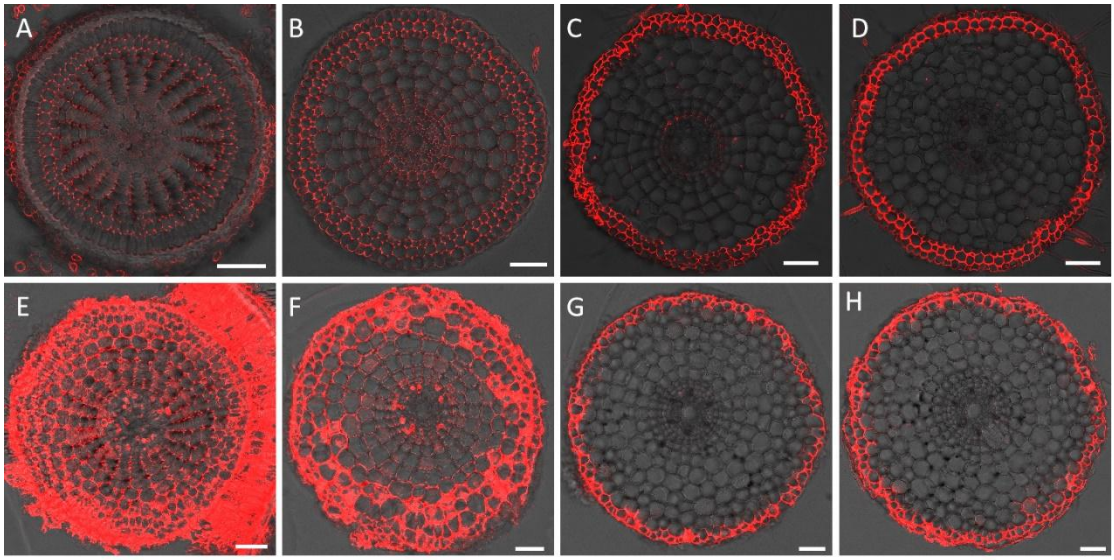

Figure 2.4 PI penetration test in roots of the wild-type rice (T-65) and short-root mutant (*dice1*). A PI (propidium iodide) penetration assay was performed in the roots of T-65 (A-D) and *dice1* mutant (E-H) at less than1 mm (A, B, E, F), more than 2 mm (G, H), 10 mm (C) or 20 mm (D) from the root apex. 5-day-old seedlings were exposed to PI in the dark for 40 min. Scale bars, 50 μm.

3.4 Mineral profile analysis of short-root mutant

To link the altered root structure with mineral element uptake, we first compared the growth between the mutant and the WT under different strength of the nutrient solution. With increasing the strength of nutrient solution, the growth of both the roots and shoots was significantly increased in the mutant although the difference between WT and mutant was still large (Fig. 2.5A, B, C). The growth of WT was also slightly improved with increasing nutrient strength (Fig. 2.5B, C). These results suggest that the inhibited growth of mutant is partly caused by insufficient nutrient uptake.

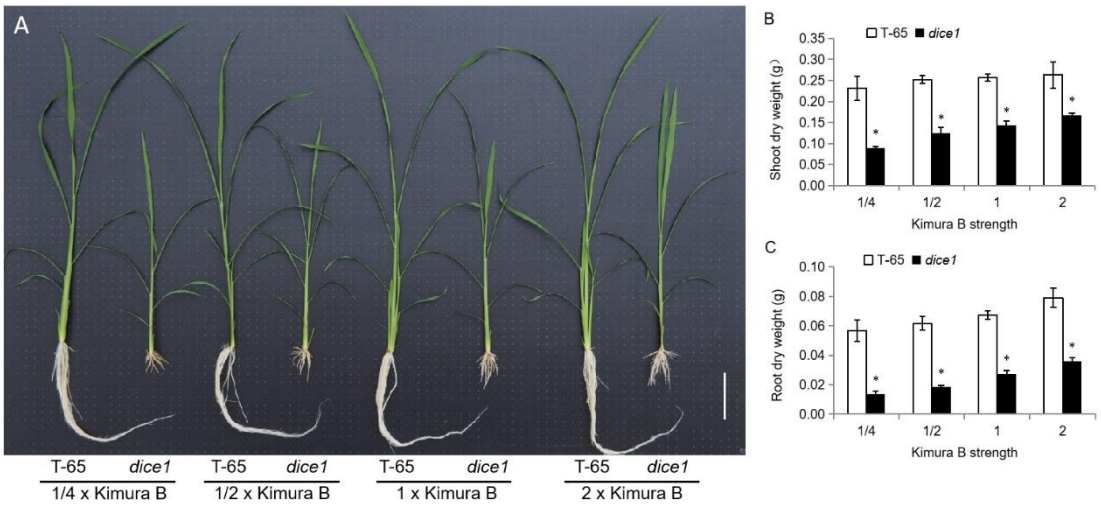

Figure 2.5 Effect of different nutrient solution strength on the growth of wild-type rice (T-65) and short-root mutant (*dice1*). (A) Growth of T-65 and *dice1*. Bar = 5 cm. (B, C) Dry weight of shoot (B) and root (C). Seedlings (12-d-old) were grown in 1/4, 1/2, 1 and 2 strength Kimura B solution for 21 days, respectively. Data are means ± SD (n = 3). The asterisk indicates significant differences between two lines (*P<0.05 by Tukey's test).

We compared the ionome profiles between the mutant and the WT grown in hydroponic solution. All elements tested except for K showed lower concentration in the shoots compared with WT (Fig. 2.6). Especially, one-day exposure to Ge (as an analog of Si), As and Cd significantly decreased their concentration in the shoots of the mutant compared with WT (Fig. 2.6I, J, K). In the roots, the concentration of mineral elements except Mg and As was also decreased in the mutant than in the WT at different extent (Fig.2.7).

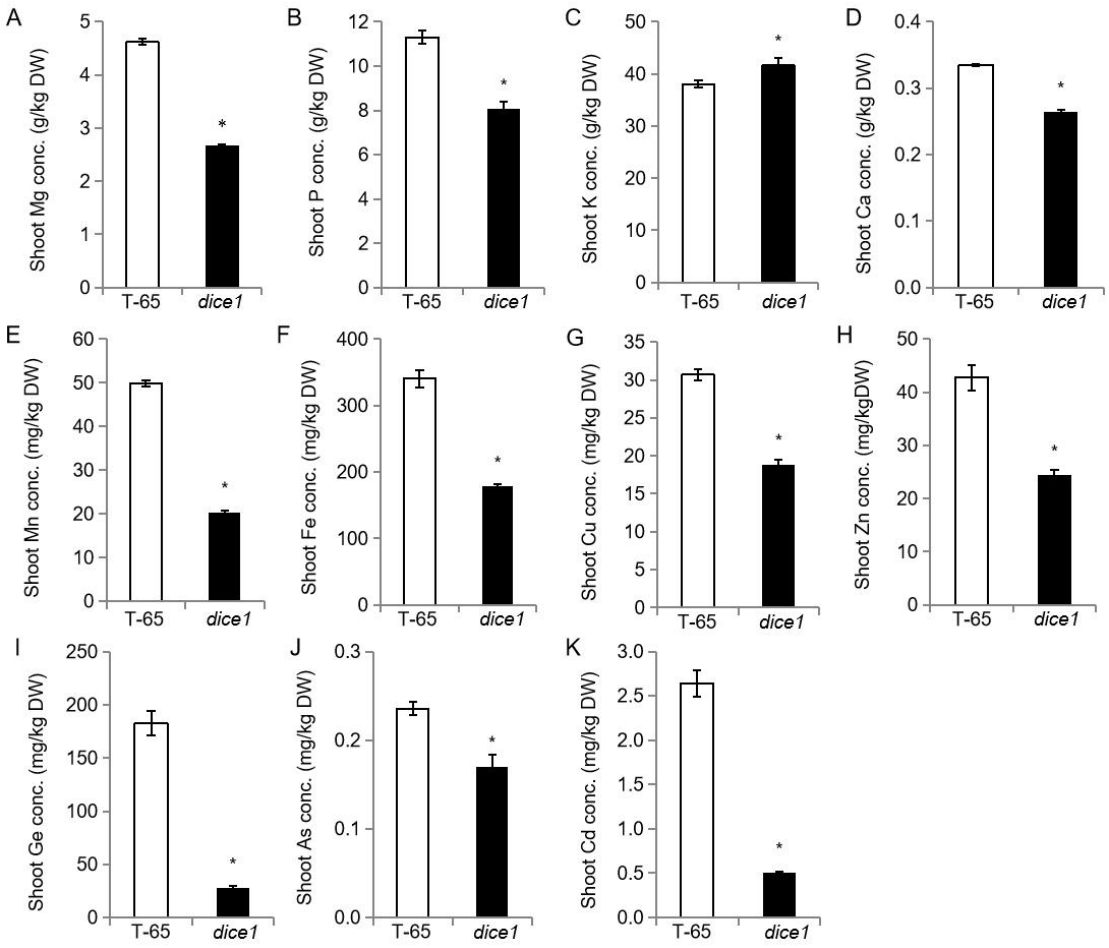

Figure 2.6 Mineral concentration in the shoots of the wild-type rice (T-65) and short-root mutant (*dice1*). Concentration of Mg (A), P (B), K (C), Ca (D), Mn (E), Fe (F), Cu (G), Zn (H), Ge (I), As (J), Cd (K) in the shoots of the wild-type rice and the mutant. 12-day-old seedlings were grown in 1 x Kimura B solution. After 20-d growth, the seedlings were exposed to a solution containing 0.2 μM $CdSO_4$, 0.2 μM As^{3+} and 1 μM Ge for another 1 day. Shoots were harvested for determination of element concentration by ICP-MS. Data are means ± SD (n = 3). The asterisk indicates significant differences between different lines (*P<0.05 by Tukey's test).

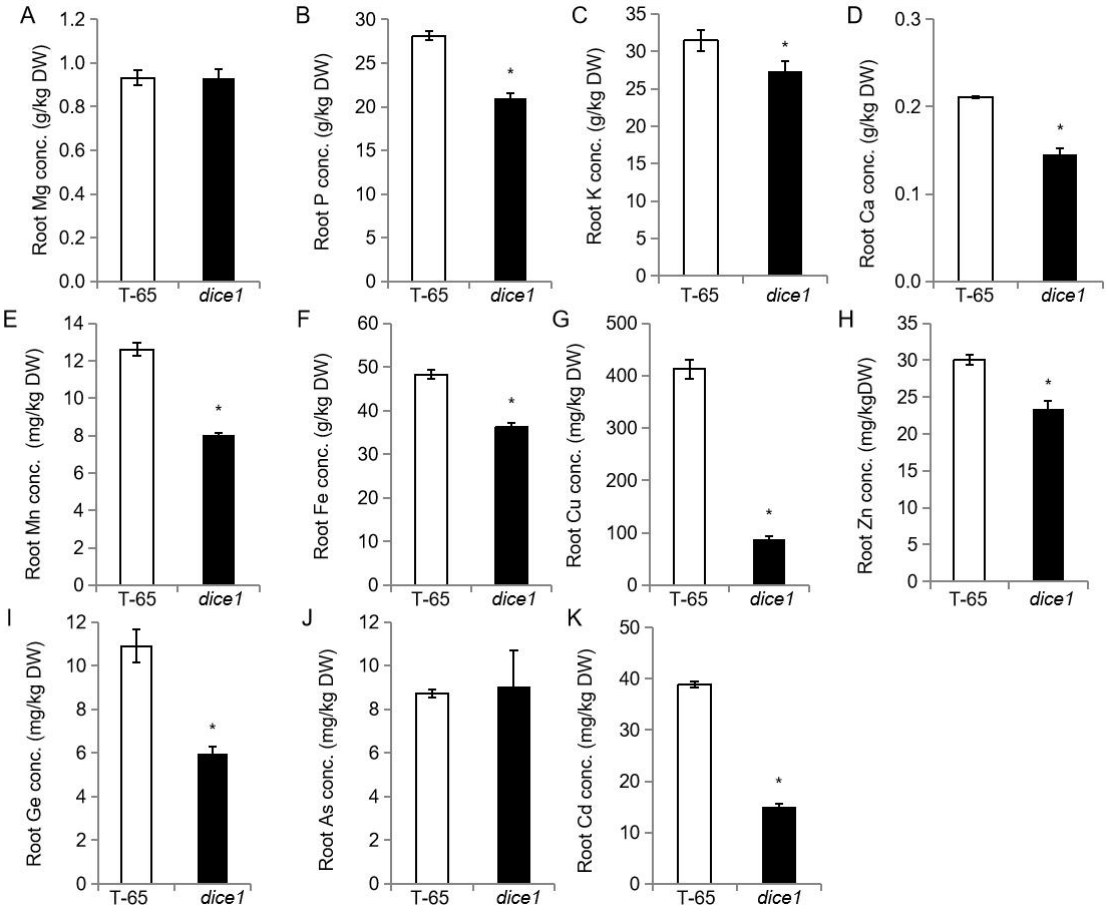

Figure 2.7 Mineral concentration in the roots of wild-type rice (T-65) and short-root mutant (*dice1*). Concentration of Mg (A), P (B), K (C), Ca (D), Mn (E), Fe (F), Cu (G), Zn (H), Ge (I), As (J), Cd (K) in the roots of wild-type rice and short root mutant. 12-day-old seedlings were grown in 1 x Kimura B solution. After 20-d growth, the seedlings were exposed to a solution containing 0.2 μM $CdSO_4$, 0.2 μM As^{3+} and 1 μM Ge for another 1 day. Roots were harvested for determination of element concentration by ICP-MS. Data are means ± SD (n = 3). The asterisk indicates significant differences between different lines (*P<0.05 by Tukey's test).

Since there was a large difference in the root biomass between WT and the mutant (Fig. 3.5C), we therefore calculated the uptake based on the root dry weight. As a result, the uptake of K and Ca was significantly increased and that of P was not changed in the mutant. In contrast, the uptake of Mg, Mn, Fe, Cu, Zn, Ge, As and Cd was significantly reduced in the mutant compared with the WT (Fig. 2.8).

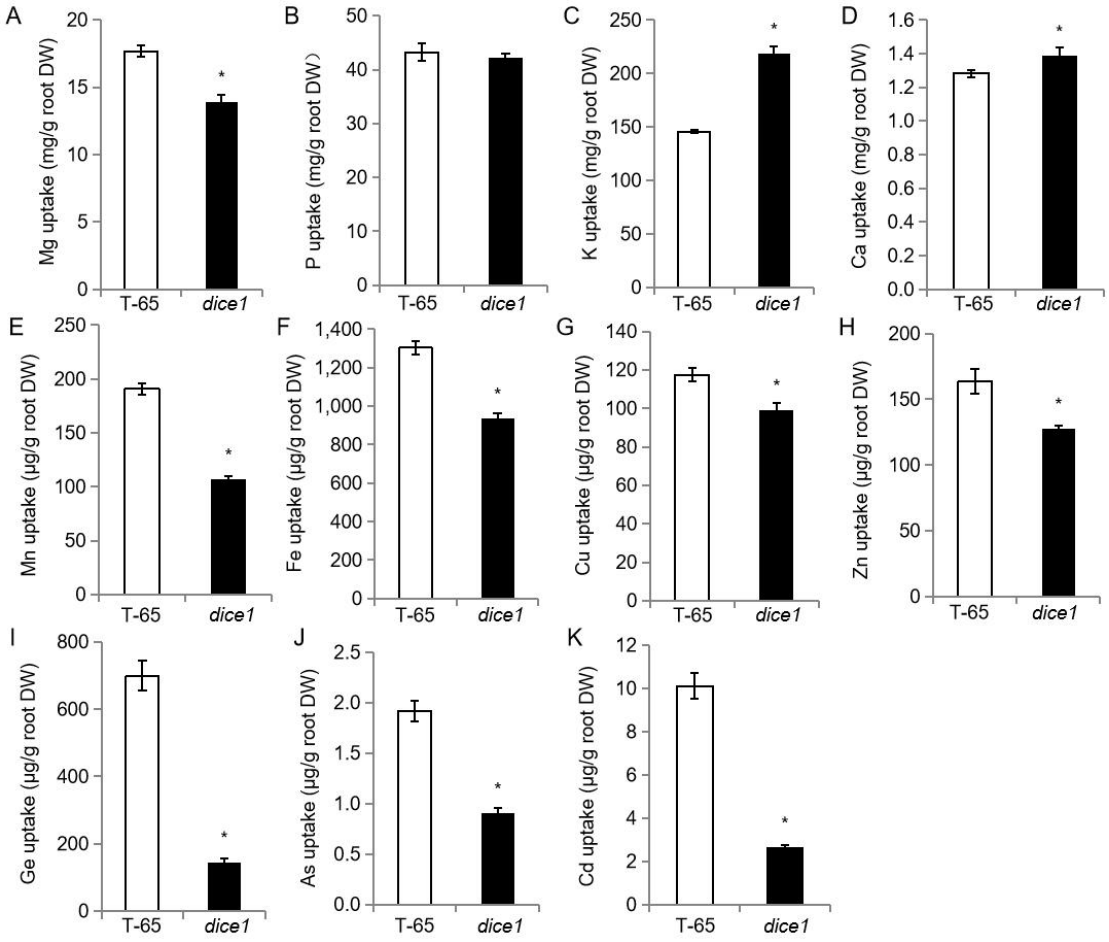

Figure 2.8 Uptake of mineral elements in the wild-type rice (T-65) and short-root mutant (*dice1*). Uptake of Mg (A), P (B), K (C), Ca (D), Mn (E), Fe (F), Cu (G), Zn (H), Ge (I), As (J), Cd (K) in the wild type rice and the mutant. Seedlings (12-day-old) were grown in 1 x Kimura B solution. After 20 days, the seedlings were exposed to the solution containing 0.2 μM $CdSO_4$, 0.2 μM As^{3+} and 1 μM Ge for another 1 day. The uptake was

calculated based on the root dry weight. Data are means ± SD (n = 3). The asterisk indicates significant differences between two lines (*P<0.05 by Tukey's test).

3.5 Map-based cloning of the responsible gene for the short-root phenotype

To isolate the gene responsible for the short-root phenotype in the mutant, we first generated an F_2 population by backcrossing the mutant with the wild type. Of 98 F_2 plants, 71 displayed the long-root phenotype similar to the wild type and 27 showed short-root phenotype similar to the mutant. This segregation ratio fitted to a 3:1, indicating that the short-root phenotype is controlled by a single recessive gene.

To map the responsible gene, we constructed an F_2 population by crossing the mutant with an *indica* cultivar 'Kasalath'. The phenotype was evaluated based on the seminal root length. Linkage analysis with 86 polymorphic markers uniformly distributed on the whole rice genome showed that two InDel markers M2378 and M2588 on chromosome 4 were linked to this gene (Fig. 2.9A). To fine mapping of the responsible gene, another 5 polymorphic markers and 1075 F_2 seedlings were used. Finally, the candidate gene was mapped to a 267-kb region between M2481 and M2508 on chromosome 4 (Fig. 2.9A). There are 44 predicted genes within this region including *OsGlu3* (Os04g0497200) based on the Rice Annotation Project Database (http://rapdb.dna.affrc.go.jp/) (Table 2.3). OsGlu3 encodes a putative membrane-bound endo-1,4-beta-glucanase (Inukai et al., 2012; Zhang et al. 2012). It has been reported to be involved in root cell elongation and cell division in rice (Inukai et al., 2012; Zhang et al., 2012). We then sequenced *OsGlu3* from the mutant and the WT and found that there was one point mutation (from G to A) occurring at the end of second intron.

This mutation resulted in two different transcripts, which have additional 29 and 589 nucleotides, respectively (Fig. 2.9C). Sequence analysis showed that partial or all part of second intron was remained during splicing process (Fig. 2.9C), generating a premature stop codon. As a result, the functional protein could not be translated (Fig. 2.9D), indicating that this is a loss-of-function mutant with novel allele of OsGlu3.

Table 2.3 List of candidate genes in the mapping region of chromosome 4.

Number	Locus ID	Annotation
1	Os04g0496150	Similar to H0306B06.2 protein.
2	Os04g0496300	Similar to H0306B06.4 protein.
3	Os04g0496400	RNA recognition motif, RNP-1 domain containing protein.
4	Os04g0496600	Similar to H0306B06.6 protein.
5	Os04g0496700	Similar to H0306B06.7 protein.
6	Os04g0496800	LETM1-like domain containing protein.
7	Os04g0497000	Similar to Allyl alcohol dehydrogenase.
8	**Os04g0497200**	***OsGlu3***
9	Os04g0497300	Similar to Atozi1 (Fragment).
10	Os04g0497350	Similar to H0306B06.12 protein.
11	Os04g0497400	Similar to 6,7-dimethyl-8-ribityllumazine synthase (Fragment).
12	Os04g0497600	Lupus La protein family protein.
13	Os04g0497700	Similar to CONSTANS-like protein.
14	Os04g0497900	Unknown protein with the N-terminal chloroplast transit peptide, Formation of thylakoid membranes.
15	Os04g0498000	Protein of unknown function DUF828, plant family protein.
16	Os04g0498500	Irgsp1_predicted_locus
17	Os04g0498600	S-adenosylmethionine decarboxylase, Polyamine biosynthesis, Salt and drought stresses, Abiotic stress.
18	Os04g0498700	Haem peroxidase family protein.
19	Os04g0498800	Similar to Cell division control protein 48 homolog B (AtCDC48b).
20	Os04g0498900	Similar to N-acetyltransferase ESCO1.
21	Os04g0499100	Biopterin transport-related protein BT1 family protein.
22	Os04g0499200	Enhancer of rudimentary family protein.
23	Os04g0499300	MIF4-like, type 1/2/3 domain containing protein; Similar to Eukaryotic initiation factor-like protein.

24	Os04g0499700	Irgsp1_predicted_locus
25	Os04g0499800	Hypothetical protein.
26	Os04g0500100	Irgsp1_predicted_locus
27	Os04g0500200	Conserved hypothetical protein.
28	Os04g0500300	Conserved hypothetical protein.
29	Os04g0500400	Similar to Hydroxyproline-rich glycoprotein DZ-HRGP precursor.
30	Os04g0500501	Irgsp1_predicted_locus
31	Os04g0500600	Hypothetical protein.
32	Os04g0500700	Similar to Hydroxyanthranilate hydroxycinnamoyl transferase 3.
33	Os04g0500900	Similar to H0311C03.1 protein.
34	Os04g0501000	Nucleotide-binding, alpha-beta plait domain containing protein.
35	Os04g0501100	Similar to Magnesium transporter MRS2-C.
36	Os04g0501200	Similar to H0311C03.4 protein.
37	Os04g0501500	BTB domain containing protein.
38	Os04g0501600	AT hook, DNA-binding, conserved site domain containing protein.
39	Os04g0501700	Spc97/Spc98 family protein.
40	Os04g0501800	Protein of unknown function DUF1068 family protein.
41	Os04g0502000	Irgsp1_predicted_locus
42	Os04g0502100	Similar to H0311C03.10 protein.
43	Os04g0502200	Transport protein Trs120 domain containing protein.
44	Os04g0502300	Similar to 40S ribosomal protein S11.

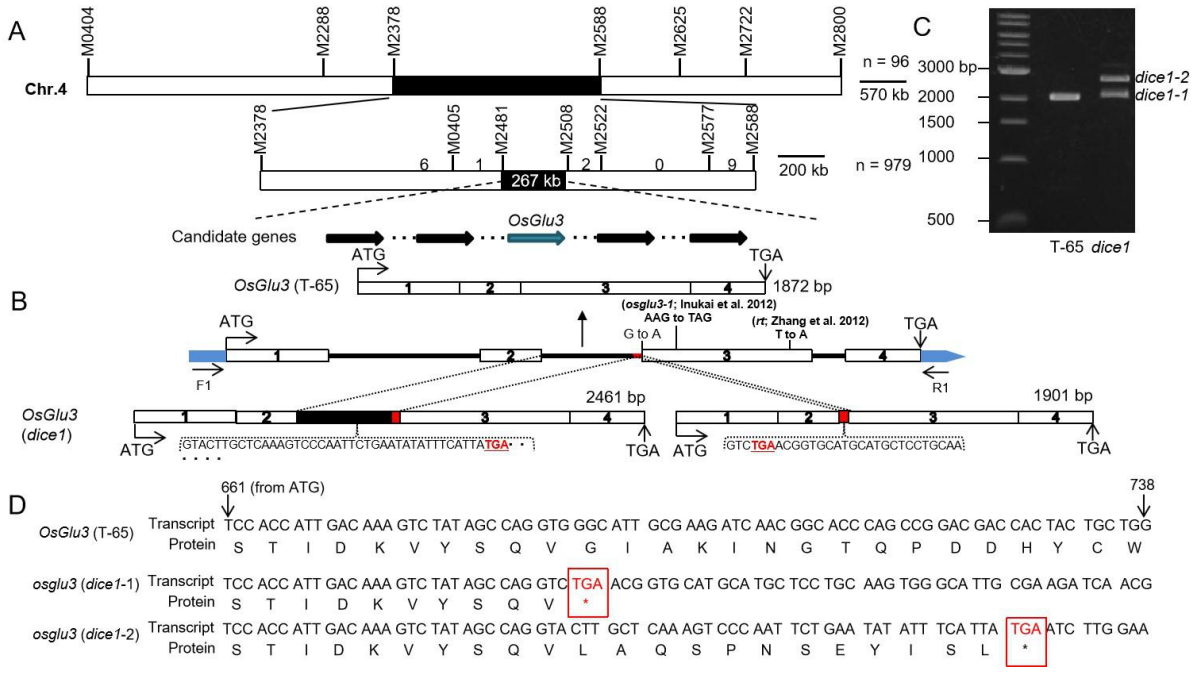

Figure 2.9 Map-based cloning of *OsGlu3* gene. (A) The candidate gene locus was mapped to 267-kb region on chromosome 4. The markers are listed at the top, and the numbers above the bars indicate the number of recombinants. (B) Gene structure of *OsGlu3*. Open boxes indicate exons and horizontal lines mean introns and blue boxes show UTR region, vertical line represents the point mutation of the *OsGlu3* in different alleles. Number shows the order of exons in *OsGlu3*. (C) Transcripts of *OsGlu3* in the wild-type rice (T-65) and *dice1* mutant. The transcripts were amplified by PCR using F1 and R1 primers shown in (B). PCR products with 28 cycles for T-65 and 30 cycles for *dice1* were subjected to electrophoresis. (D) Nucleotide and amino acid sequences flanking the stop codon of *OsGlu3*. Stop codon position is boxed with red color.

To assess whether the short-root phenotype was caused by mutation in *OsGlu3*, we added glucose in the growth media because *OsGlu3* knockout mutant phenotype was partially rescued by exogenous glucose (Zhang et al., 2012). The root elongation was only partially recovered in the *dice1* mutant in the presence of 3% glucose although the root elongation was inhibited in the WT (Fig. 2.10), consistent with that reported previously (Zhang et al., 2012). This result indicates that the short-root phenotype of *dice1* was caused by mutation of *OsGlu3*.

Figure 2.10 Effect of exogenous glucose on the root growth in the wild-type rice (T-65) and short-root mutant (*dice1*). Both T-65 and *dice1* mutant were grown in 0.4% agar medium containing 2 x Kimura B nutrient solution (pH 5.6) in the presence of 0 and 3% glucose for 7 days. Bar = 2 cm.

3.6 Transcriptional change of mineral transporter genes in mutant

To investigate the effect of root structure on expression of transporter genes involved in mineral element uptake, we selected four genes involved in Si/Ge/As uptake and Mn/Cd uptake for testing because uptake of Ge, As, Mn and Cd were mostly affected in the mutant (Fig. 2.8E, I, J, K). The expression level of *OsLsi1* and *OsLsi2* involved in Si/Ge/As uptake was significantly decreased in the mutant compared with the WT (Fig. 2.11A, B). The expression level of *OsNramp5* involved in Mn/Cd uptake was also significantly decreased (Fig. 2.11C), while that of *OsMTP9* was not changed in the mutant compared with the WT (Fig. 2.11D).

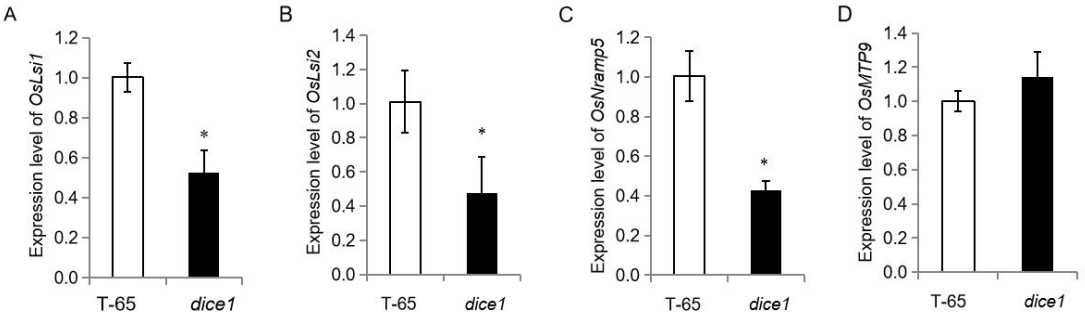

Figure 2.11 Expression of *OsLsi1*, *OsLsi2*, *OsNramp5*, and *OsMTP9* in the roots of wild-type rice (T-65) and short-root mutant (*dice1*). Expression of *OsLsi1* (A), *OsLsi2* (B), *OsNramp5* (C) and *OsMTP9* (D) in the roots of T-65 and *dice1*. Seedlings (12-day-old) were grown in 1 x Kimura B solution. After 21 days, the roots were sampled for RNA extraction. The expression level was determined by quantitative RT-PCR. Data are means ± SD (n = 3). The asterisk indicates significant differences between two lines (*P<0.05 by Tukey's test).

Since the root elongation was partially rescued in the presence of 3% exogenous glucose in the mutant (Fig. 2.10), we then compared the expression level of *OsLsi1*, *OsLsi2* and *OsNramp5* in the presence or absence of glucose. The results showed that the expression level of *OsLsi1* was significantly decreased by glucose in both the WT and *dice1* mutant (Fig. 2.12A), while the expression level of *OsLsi2* and *OsNramp5* was not changed by glucose in the mutant (Fig. 2.12B, C). However, their expression was decreased by glucose in the WT probably due to inhibited root elongation (Fig. 2.10).

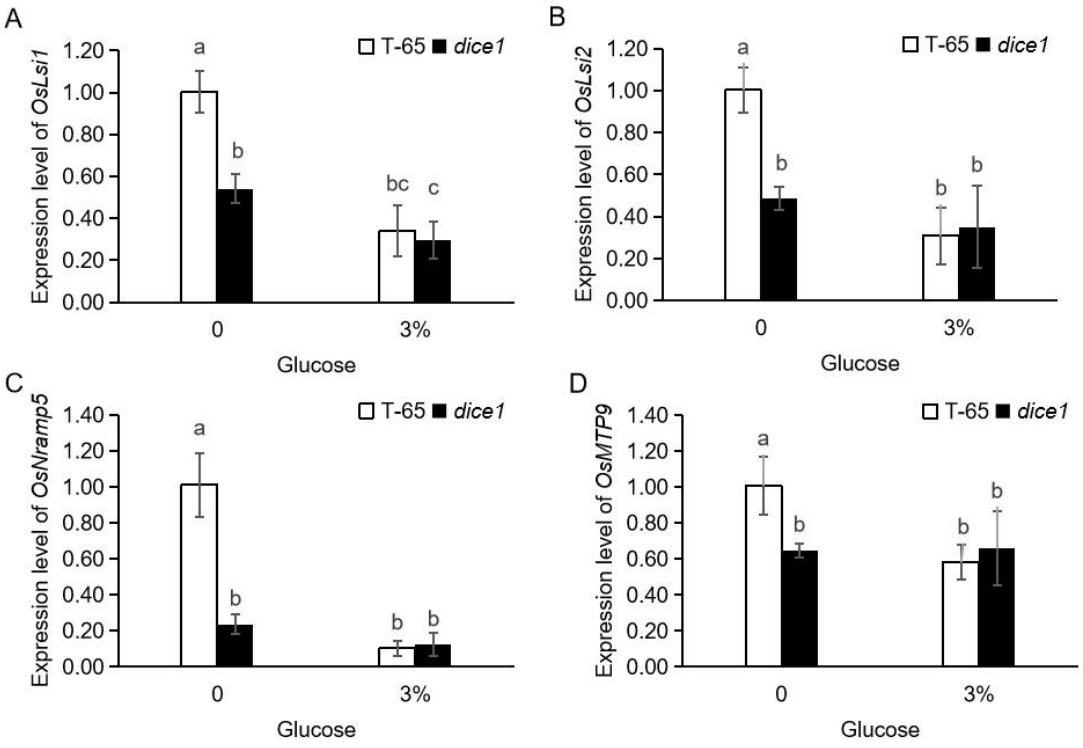

Figure 2.12. Effect of exogenous glucose on the expression of *OsLsi1*, *OsLsi2*, *OsNramp5*, and *OsMTP9* in the roots of wild-type rice (T-65) and short-root mutant (*dice1*). Expression of *OsLsi1* (A), *OsLsi2* (B), *OsNramp5* (C), and *OsMTP9* (D) in the roots of T-65 and *dice1*. Both T-65 and *dice1* mutant were grown in 0.4% agar medium containing 2 x Kimura B nutrient solution (pH 5.6) in the presence of 0 and 3% glucose for 7 days. The roots were sampled for RNA extraction. The expression level was determined by quantitative RT-PCR. Data are means ± SD (n = 3). Significant difference was determined by Tukey test and labeled with different letters ($p < 0.05$).

3.7 Tissue and cellular localization of transporters in the mutant

To investigate the effect of root structure on tissue and cellular localization of transporters involved in mineral element uptake, we selected Si transporter OsLsi1 and performed its

immunostaining. In the WT, OsLsi1 were localized at the distal side of exodermis and endodermis, which is consistent with a previous study (Fig. 2.13A-B, F, Ma et al., 2006). However, in the mutant, OsLsi1 signal was partially localized at the two outer cell layers (second and third cell layers, corresponding to sclerenchyma and a following cortex cell layer in WT) although the polarity was not altered (Fig. 2.13C-E, G-H, K). The localization of OsLsi1 at the endodermis was not altered in the mutant (Fig. 2.13C-E, G-L).

We also compared the Lsi1 localization between the WT and the mutant grown in the presence or absence of glucose in agar plate. In the absence of glucose, the Lsi1 localization was altered in the mutant, which was similar to that observed in plants grown hydroponically (Fig. 2.13C-E, G, H, K). However, in the presence of glucose, the Lsi1 localization in the mutant was largely restored to the exodermis although the expression level was not recovered (Fig.2.13I, J, L, Fig. 2.12A).

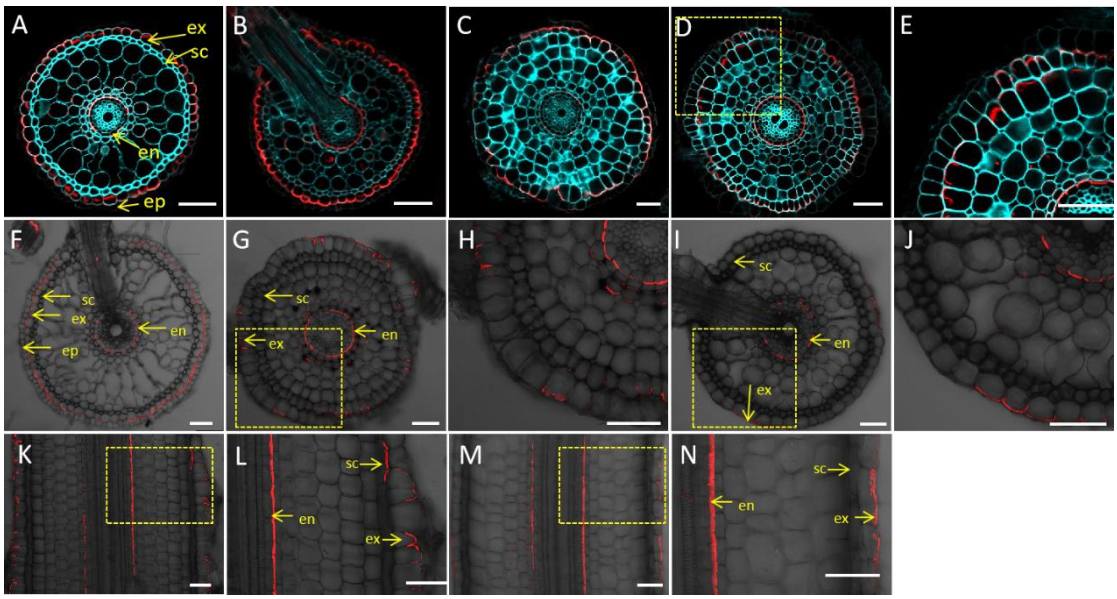

Figure 2.13 Cellular localization of OsLsi1 protein in roots of wild-type rice (T-65) and short-root mutant (*dice1*) and effect of glucose on Lsi1 localization. (A-E) Lsi1 localization in the wild type and *dice1*. Root cross section of 7-day-old (A, C) and 44-day-old (B, D) seedlings of the wild type (A, B) and mutant (C, D) grown hydroponically was used for immunostaining of OsLsi1 (red color). Blue color showed cell wall ultraviolet autofluorescence. (E) Magnified image of yellow dotted box in D.

(F-N) Effect of glucose addition on Lsi1 localization. Root cross sections of the wild type (F) and the mutant (G, I), and root longitude section of the mutant (K, M) were prepared from seedling grown in agar in the absence of (F, G, K) or presence of 3% glucose (I, M) for 7 days. (H, J, L, N) Magnified image of yellow dotted box in G, I, K and M, respectively. Epidermis (ep), exodermis (ex) and sclerenchyma (sc) and endodermis (en) cell layers are shown. Scale bars = 50 μm.

3.8 Expression of *Glu3* in *Docs1* mutant

OsDocs1 encodes a leucine-rice repeat receptor-like kinase and mutation of this gene resulted in defect in outer cell layer formation similar to *dice1* (Huang et al., 2012, Fig. 2.2). To investigate the possibility that *OsGlu3* expression is regulated by *OsDocs1*, we compared the expression level of *OsGlu3* in the wild type and Docs1 mutant (*C68*). The result showed that there was no difference in the expression between two lines (Fig. 2.14A). In addition, there was also no difference in the *OsDocs1* expression between wild type and *dice1* mutant (Fig. 2.14B).

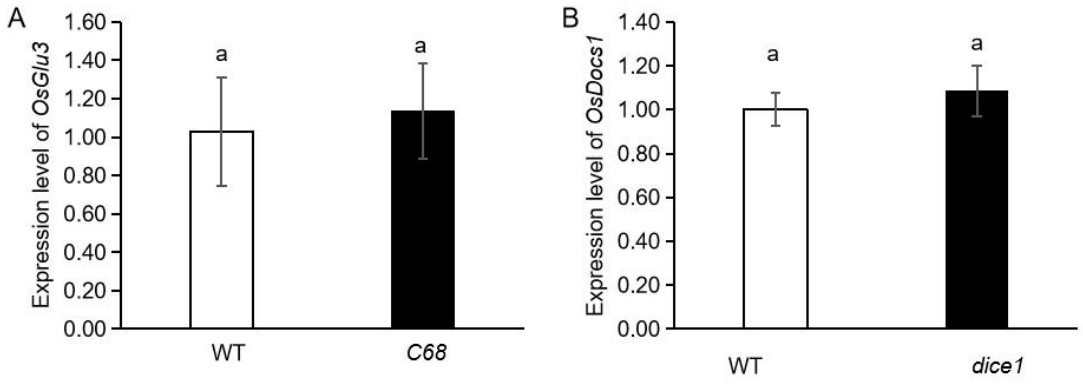

Figure 2.14. Expression of *OsDocs1* and *OsGlu3* in the roots of the wild-type rice and mutant. (A) Expression of *OsGlu3* in the roots of the wild type and *C68* mutant. (B) Expression of *OsDocs1* in the roots of the wild type and dice1 mutant. Seedlings (21-day-old) were grown in half-strength Kimura B solution and the roots were sampled for RNA extraction. The expression level was determined by quantitative RT-PCR. Data are means ± SD (n = 3). Significant difference was determined by Tukey test and labeled with different letters ($p < 0.05$).

4. Discussion

4.1 *dice1* mutant is defective in both root cell elongation and differentiation

Through screening of MNU-mutated seeds, we obtained a rice mutant, *dice1*, which showed extremely shorter seminal, lateral and crown roots at both vegetative and reproductive stage (Fig. 2.1A-C). This mutant is not only defective in root cell elongation, but also in root outer cell differentiation (Fig. 2.1D, Fig. 2.2F-J). Molecular mapping revealed that the short-root phenotype is caused by a point-mutation of *OsGlu3* at the end of second intron, resulting in splicing disorder in the mutant (Fig. 2.9B-D). Splicing site mutation can abolish the function

of a gene (Lorković et al., 2000; Yuan et al., 2009). *OsGlu3* encodes a putative membrane-bound endo-1,4-beta-glucanase, which involves in the loosening of root cell wall and modulates root cell division and elongation in rice (Zhang et al., 2012; Inukai et al., 2012). Two mutants (*osglu3-1* and *rt*) reported showed similar phenotype as *dice1* isolated in this study, including defect of cell elongation, collapse of epidermal and some cortex cells (Zhang et al., 2012; Inukai et al., 2012). However, the phenotype of *dice1* was more severe compared with *osglu3-1* (Fig. 2.1A-C, E, Zhang et al., 2012). This could be attributed to the different mutation. In *osglu3-1* mutant, a point mutation from T to A occurred at nucleotide position 2,715 bp of the coding sequence, resulting in an amino acid change (from Leu to His) at a position of 451 (Fig. 2.9B, Zhang et al., 2012). This mutated OsGlu3-1 may still possess some enzyme activity. In contrast, *rt* mutant, a single nucleotide substitution at Lys291 (AAG to TAG) occurred, generating a premature stop codon (Fig. 2.9B, Inukai et al., 2012). While splicing site disorder occurred in *dice1* (Fig. 2.9C), generating two different transcripts of *OsGlu3* with a premature stop codon (Fig. 2.9D). Therefore, both *dice1* and *rt* were loss-of-function mutants showing severe phenotype.

4.2 Alternation of root structure affects both expression and localization of transporter for uptake of mineral elements

Although one of the most important roles of roots is to take up mineral nutrients from soil, less has been investigated on the association between root system and mineral element uptake. Uptake of mineral elements is mediated by various different transporters, therefore, abundance of transporters in the roots is closely associated with uptake ability. Root length,

number, diameter and root configuration in the soil profile may affect the transporter abundance (Wang et al., 2006). However, we found that root structure also plays a crucial role in regulating expression and localization of transporters through detailed analysis of *dice1* mutant in this study. *dice1* showed reduced uptake of many mineral elements, especially Mn, Ge, As and Cd (Fig. 2.8E, I, J, K). Germanium (Ge), an analogue of Si, is taken up by rice roots in a manner similar to that of Si (Takahashi et al., 1976a; Takahashi et al., 1976b). Rice is a typical Si accumulating plant and its high Si accumulation is achieved by high expression of OsLsi1 and OsLsi2 transporters (Ma et al., 2006; Ma et al., 2007). OsLsi1 and OsLsi2 are localized at the distal and proximal side of both the exodermis and endodermis in the roots. In *dice1* mutant, the expression of both *OsLsi1* and *OsLsi2* was significantly decreased (Fig. 2.11A-B), probably due to lacking or damage of the exodermis cells in the mutant root. Furthermore, the localization of OsLsi1 was also changed in *dice1* mutant (Fig. 2.13C-E, G-H); localizing to outer two cell layers corresponding to sclerenchyma and a following cortex cell layer in WT (Fig. 2.13C-E, G-H). This localization change is probably caused by altered cell identity, which was demonstrated by lignin and suberin staining (Fig. 2.3). This is supported by glucose addition experiment. When the root elongation was partially rescued by addition of glucose in the medium (Fig. 2.10), the exodermis cell formation and Lsi1 localization became normal as wild type (Fig. 2.13I, J). Although the apoplastic barriers in the root tip region (less than 1 mm from the root apex) was probably damaged in *dice1* mutant (Fig. 2.4E, F, I), the Si uptake are mainly from the root mature region where the apoplastic barriers were functional as that in the WT (Fig. 2.4C,

D, G, H), indicating that the reduced Si uptake was mainly caused by low expression and abnormal localization of Lsi1 transporter in *dice1*.

According to mathematic modelling, polar localization of OsLsi1 and OsLsi2 at the exodermis and endodermis is the most efficient combination for Si uptake across the two Casparian strips (Sakurai et al., 2015). Therefore, altered localization of OsLsi1 in the mutant reduces the efficiency of Si uptake in addition to decreased expression. Since arsenite uptake is also mediated by OsLsi1 and OsLsi2 (Ma et al., 2008), its uptake was also similarly reduced in the mutant as Si (Fig. 2.8J).

Rice is also a Mn-accumulating plant (Yamaji et al., 2013). Mn uptake is mediated by OsNramp5 and OsMTP9 localized at the distal and proximal side, respectively, of root exodermis and endodermis (Sasaki et al., 2012; Ueno et al., 2015, Shao et al., 2018). Similar to Lsi1 and Lsi2, a cooperative transport by OsNramp5-OsMTP9 is required for efficient Mn uptake. The expression of *OsNramp5* was also reduced in the *dice1* mutant although that of *OsMTP9* was not changed (Fig. 2.11C, D). Therefore, similar to Si, decreased Mn uptake in *dice1* mutant is likely caused by decreased expression of *OsNramp5*. Since OsNramp5 is also a major transporter for Cd (Sasaki et al., 2012), this explains why Cd uptake was also greatly reduced like Mn in the mutant (Fig. 2.8K). The uptake of other elements including Mg, P, Fe, Cu, Zn was also significantly reduced in *dice1* mutant (Fig. 2.8A, B, F, G, H) and some (e.g. K in the roots) was unchanged. However, since the uptake system for these elements is not as clear as Si and Mn in rice, the effect of root structure on transporters of these elements remains to be investigated in future.

In conclusion, we isolated a rice short-root mutant with new allele of *OsGlu3*. In addition to reduced cell elongation reported before, the outer cell layers were not well formed and cell identify was altered in the mutant. These alternations of root structure affect uptake of mineral elements through reducing expression and changing localization of transporters at least for Mn, Cd, Si (Ge) and As (III). This study provides a link between root structure and mineral element uptake in rice.

Chapter 3 *OsLKRT1* is required for normal root elongation in rice

1. Introduction

Rice (*Oryza sativa*) is able to grow under both flooded and upland conditions, where both the concentration and chemical forms of mineral elements are greatly different as well as oxygen concentration (Wang et al., 2019). To cope with these different conditions, rice roots have developed a distinct morphology and anatomy as described in Chapter 1. For example, rice roots have two Casparian strips at the exodermis and endodermis. Furthermore, in the root mature region, aerenchyma is formed to release oxygen from above-ground part. Although several genes involved in rice root development have been identified as described in Chapters 1 and 2, our understanding of rice root system formation is still poor. To further understand the molecular mechanisms underlying root development of rice, I functionally characterized another short-root mutant (*dice2*) isolated from screening of MNU-mutated rice seeds. Map-based cloning combined with complementation test revealed that the short-root phenotype was caused by a point mutation of a gene being annotated to encode Lysine Ketoglutarate Reductase Trans-Splicing related 1 (*OsLKRT1*), resulting in a premature stop.

2. Materials and methods

2.1 Plant materials and growth conditions

A short-root mutant (referring to *dice2* for *defective in cell elongation 2*) was isolated through screening 3000 lines of MNU-mutated seeds provided by Kyushu University as described in the Chapter 2. The screening method and growth condition were same as described in the Chapter 2.

2.2 Soil culture experiments

To compare agronomic trait differences between T-65 and *dice2* grown in soil condition, 21-day-old seedlings of both lines grown hydroponically as described in the Chapter 2 were transplanted to a 3.5-L pot containing 3.5 kg soil taken from paddy field of Institute of Plant Science and Resources, Okayama University. Six gram of fertilizer (N-P_2O_5-K_2O) for each pot was applied. The plants were grown in a greenhouse until ripening under natural sunlight from June to October in 2019. At harvest, the plant height, tiller number, grain weight per plant and dry weight of straw were recorded. Nine biological replicates were made for this experiment.

2.3 Physiological, morphological and anatomical analysis

All plants grown hydroponically were used for morphological observation at different time points. To compare the root elongation difference between the wild type (cv. T-65) and *dice2* mutant, germinated seedlings were grown in a 0.5 mM $CaCl_2$ solution at 30°C, and the root length was measured with a rule at different days. Ten replicates were made for each line. To observe the anatomical differences between T-65 and *dice2*, 4-day-old seedlings grown in a 0.5 mM $CaCl_2$ solution at 30°C. were used for preparing longitudinal and transverse cross

sections of the seminal root. To compare the anatomical differences between T-65 and *dice2* at different temperature treatment, 27-day-old seedlings were used for preparing longitudinal and transverse cross sections of crown roots. Samples of the roots were sectioned by a microslicer (100 μm thickness) (Linear Slicer PRO10; Dosaka EM). Then the sections were observed under a confocal laser scanning microscope (TCS SP8x; Leica Microsystems) using UV autofluorescence. For measurement of cell length in the root elongation region, longitudinal sections (>20 mm from root apex) of the main roots were used. The size of the cortex cells was determined from 10 roots each with 10 cells (n= 100).

2.4 Ionomic analysis

To compare the ionome profiles in wild-type rice (cv.T-65) and *dice2*, 7-day-old seedlings were cultivated in a 1.2-L plot containing half strength Kimura B solution (pH 5.6) (Yamaji et al., 2013). After 20 days, the seedlings were exposed to a solution containing 0.2 μM $CdSO_4$ for 1 day before harvest. The roots were then washed with 5 mM cold $CaCl_2$ three times and separated from the shoots with a razor. All the samples were dried at 70°C for 2 days in an oven and used for metal measurement as described below.

2.5 Positional cloning of the responsible gene

The mutant, *dice2* was crossed with its wild-type rice (T-65) to generate F_1. A total of 96 F_2 seedlings were used for genetic analysis. For positional cloning of the mutated gene, the short root mutant was crossed with ‘Kasalath‘, an *indica* cultivar. First, a bulked segregant analysis was used to identify the polymorphic markers linked to *dice2*. Then 192 F_2 seedlings were

used to roughly map the gene. To further map this gene, more than 3000 F_2 seedlings were used for fine mapping using polymorphic molecular markers listed in Table 3.1. The candidate gene was sequenced using a Big-Dye sequencing kit (Applied Biosystems, http://www.appliedbiosystems.com/) on the SeqStudio Genetic Analyzer using primers listed in Table 3.1.

Table 3.1 Primer sequences used for the mapping and sequencing of *OsLKRT1*.

Primers name	Forward (5'---3')	Reverse (5'---3')	Note
M0221	TTCTTCTTCGTATTCTCTCGACAC	TCTTCACACCACATCCTCACCT	Mapping marker
M1115	CATGTTATATGTCCGCAAGCTG	CATAGGCACATGCAAAGAGC	Mapping marker
M1319	CTTTGCTGGAAATGGAAGACA	ACCGATGAGCTGGACAGAAT	Mapping marker
M0204	GCAGCAAAGTGCGGAGTA	CAGGTGAATTGCCAATTT	Mapping marker
M1152	CGCTGACGCCAACAATTC	CTGCACCTTCATGCTGTGTT	Mapping marker
M1201	TGATGACTTTTTGGGGTCTTG	AGGAGGACTGCGCCTTATTT	Mapping marker
M1265	AATTCTGCCAGCGAAGACC	ATCTCGGATCACATCCGTTT	Mapping marker
M1126	AGCTCACAGAGATTCAAGCAAT	CACAAAATCATGCCGTGAAA	Mapping marker
M1130	CAATTGCATGCGGTAGTTTTT	AAACCTAGCTGCCGTTGGAT	Mapping marker
M1136	CACCAGTTACTACCCCTTACTTCTG	AGGTTCCATATGCCGTGGTA	Mapping marker
M1138	CCGAGGACAGTCACACAACA	TTGTCGACACCTCCTGGATT	Mapping marker
M1141	CAATGGTAGTAGGTAGCTGAATGA	TTGTTACATCGTAGCGGGTTC	Mapping marker
M1146	CATTAGGTAGATCGTGCTGTGG	TGACGCGCAGTACATACACA	Mapping marker
F1	CGCTGCAGCTCTACAGGTTT		Sequencing
F2	AGGACCTGAGTAGCGAACCA		Sequencing
F3	AAGATTGGAGTCGTCGATGC		Sequencing
R1		CCAGCTAGGTTGCCGAAAT	Sequencing

2.6 Complementation test

For the complementation test of *dice2* mutant, we constructed two transformation constructs. One includes the whole genomic DNA of *OsLKRT1*, which contained 2889 bp promoter before the ATG, 3151 bp genomic DNA and 1157 bp downstream sequence (after the translational stop site), which were amplified from the wild-type genomic DNA. Another one

contained 1206 bp coding sequence, but promoter (2889 bp), downstream sequence (1157 bp) were the same. These two fragments were inserted into pPZP2H-lac (with NOS terminator). The constructs were introduced into the calluses of *dice2* via the *Agrobacterium tumefaciens*-mediated transformation method (strain EHA101; Hiei et al., 1994). Sequence information for the primers used for construct preparation is shown in Table 3.2.

Table 3.2 Primer sequences used for complementation test

Forward (5'---3')	Reverse (5'---3')	Note
GGGCCCCGTAAGCCGGATAGCATAGG	CCCGGGATGAACTGCGAATCTTCCCCTC	Promoter of *OsLKRT1*
CCCGGGATGGCAAAACCTGCTAATAGC	GAGCTCCTAAACTAGGGTCGAGTTG	Genome of *OsLKRT1*
CCCGGGATGGCAAAACCTGCTAATAGC	ACTAGTCTAAACTAGGGTCGAGTTG	ORF of *OsLKRT1*
GAGCTCAAGAACACACGAACACGACAC	GAGCTCGGCAGATGATCATGGAGAGG	Terminator of *OsLKRT1 (G)*
ACTAGTAAGAACACACGAACACGACAC	GAGCTCGGCAGATGATCATGGAGAGG	Terminator of *OsLKRT1* (C)

2.7 Subcellular localization of OsLKRT1

To determine the subcellular localization of *OsLKRT1*, *OsLKRT1*-GFP and GFP-*OsLKRT1* fusions were introduced into rice protoplasts and onion (*Allium cepa* L.) epidermal cells. The full-length open reading frame of *OsLKRT1* with or without the stop codon was amplified by PCR from the wild-type rice (cv. T-65) root cDNA for GFP-*OsLKRT1* and *OsLKRT1*-GFP fusions, respectively. The ORF was inserted between cauliflower mosaic virus 35S promoter and GFP–NOS terminator in the pBluescript vector. The primers used were listed in Table 3.3. The rice leaves of 14-day-old seedlings grown in half-strength Kimura B solution were used to isolate the protoplasts, which were used for transformation by the polyethylene glycol method as described previously (Chen et al., 2006). In addition, *OsLKRT1*-GFP and DsRed-monomer (Clontech), GFP-*OsLKRT1* and DsRed-monomer, and DsRed-monomer

alone were introduced into onion epidermal cells, respectively according to Yokosho et al (2016). GFP fluorescence was observed under a confocal laser scanning microscope (TCS SP8x; Leica Microsystems).

Table 3.3 Primer sequences used for investigating subcellular localization.

Forward (5'---3')	Reverse (5'---3')	Note
TCCGGAATGGCAAAACCTGCTAATAGC	TCCGGACTAAACTAGGGTCGAGTTG	GFP-OsLKRT1
TCCGGAATGGCAAAACCTGCTAATAGC	TCCGGAAACTAGGGTCGAGTTGGGTG	OsLKRT1-GFP

2.8 Tissue-specificity of expression of *OsLKRT1*

To investigate the tissue-specificity expression of *OsLKRT1*, we generated transgenic rice lines carrying the *OsLKRT1* promoter fused with GFP. The 2887 bp promoter region of *OsLKRT1* (-2888 to -1 before ATG) was amplified from T-65 genomic DNA by PCR using primers listed in Table 3.2. Then the promoter fragment was subcloned into the binary vector pPZP2H-sGFP (Fuse et al., 2001). The derived construct was subsequently introduced into calluses (cv. T-65) by *Agrobacterium tumefaciens*-mediated transformation (strain EHA101; Hiei et al., 1994). Immunostaining with an antibody against GFP was performed in the roots, leaf sheath and leaf blade of the T2 transgenic lines harboring p*OsLKRT1*-GFP and the wild-type rice as a negative control as described previously (Yamaji and Ma., 2007). The signal was observed under a confocal laser scanning microscope (TCS SP8x; Leica Microsystems).

2.9 Effect of temperature on root growth

To investigate the effect of different temperature on the root growth, germinated seedlings of both the WT and mutant were exposed to a 0.5 mM $CaCl_2$ solution in a growth chamber under a 14-h/10-h photoperiod regime at 23°C and 32°C, respectively. After 5 days, the seedlings were transferred to a 3.5-L plot containing half strength Kimura B solution at the same growth condition. After 27-day growth, the seedlings were used for morphological observation and mineral element determination as described below.

2.10 Determination of metals in plant tissues

All samples were dried at 70°C in an oven for at least 2 days. The dried samples were digested with 60% concentrated HNO_3 at a temperature up to 140°C. The element concentration in the digested solution was determined by inductively coupled plasma-mass spectrometer (7700X; Agilent Technologies).

2.11 RNA-sequence analysis

Roots from 14-day-old seedlings grown in half-strength Kimura B solution in a greenhouse from Aug 3 to Aug 17 in 2019 were used for RNA extraction. The temperature in the green house ranged from 25°C to 35°C during the growth period. Total RNA of each sample was extracted using an RNeasy Plant Mini Kit (Qiagen). RNA-seq was performed by using an Illumina HiSeq 2500 system (Illumina, San Diego, CA, USA). A total of 20M–23M stranded paired-end (2×125 bp) sequences was obtained for each sample. The sequence and expression of some target genes of *OsLKRT1* was compared between *dice2* mutant and the WT based on the RNA-seq data. Three biological replicates were made for each line.

2.12 Gene expression analysis

To investigate the expression pattern of *OsLKRT1* in different organs at different growth stages, the cDNA of Nipponbare grown in a paddy field prepared previously was used (Yamaji et al., 2013). The expression of *OsLKRT1* was determined by quantitative RT-PCR using a Thunderbird SYBR qPCR mix (Toyobo) on CFX96 (Bio-Rad). *HistoneH3* was used as an internal standard. The primers used are shown in Table 3.4. The relative expression was normalized by the ΔΔCt method using the CFX Manager software (Bio-Rad).

Table 3.4 Primers used for quantitative RT-PCR.

Forward (5'---3')	Reverse (5'---3')	Note
TGACTAGCTGCGATGTAAGTAG	AGTAATGGGAATCAATGCAACG	*OsLKRT1*
AGTTTGGTCGCTCTCGATTTCG	TCAACAAGTTGACCACGTCACG	*Histone H3*

2.13 Phylogenetic analysis

The amino sequence alignments of *OsLKRT1* with its homologs in *Oryza sativa* were performed with ClustalW using default settings (http://clustalw.ddbj.nig.ac.jp/). The phylogenetic tree was constructed using the neighbor-joining algorithm with 1000 bootstrap trials in MEGA 7 (Kumar et al., 2016).

2.14 Statistical analysis

Tukey test was applied to test differences among treatments at $P<0.05$ using the SPSS 22 (SPSS Inc., Chicago, IL, USA).

3. Results

3.1 Phenotypic characterization of a short-root rice mutant, *dice2*

During screening of MNU-mutated seeds, we obtained another short-root mutant, *dice2* (*defective in cell elongation 2*). The *dice2* mutant showed a shorter length of seminal root, crown roots at different growth stages compared with the WT (Fig. 3.1A-C). A time-dependent experiment revealed that the growth of the seminal root stopped in *dice2* mutant at day 4 after germination (Fig. 3.1D). The shoot size of *dice2* mutant was also smaller compared with the WT (Fig. 3.1A-C). When cultivated in soil in a greenhouse under natural sunlight, the mutant showed much smaller size of the whole plants (Fig. 3.1C). The plant height, tiller number and straw dry weight were significantly decreased in the mutant than those of the WT (Fig. 3.1E, F, G). In addition, the grain weight per plant was also greatly decreased in the mutant (Fig. 3.1H). However, the fertility was almost same between the mutant and the WT (Fig. 3.1I). These results indicated the *dice2* mutant showed a growth defect compared with the wild type.

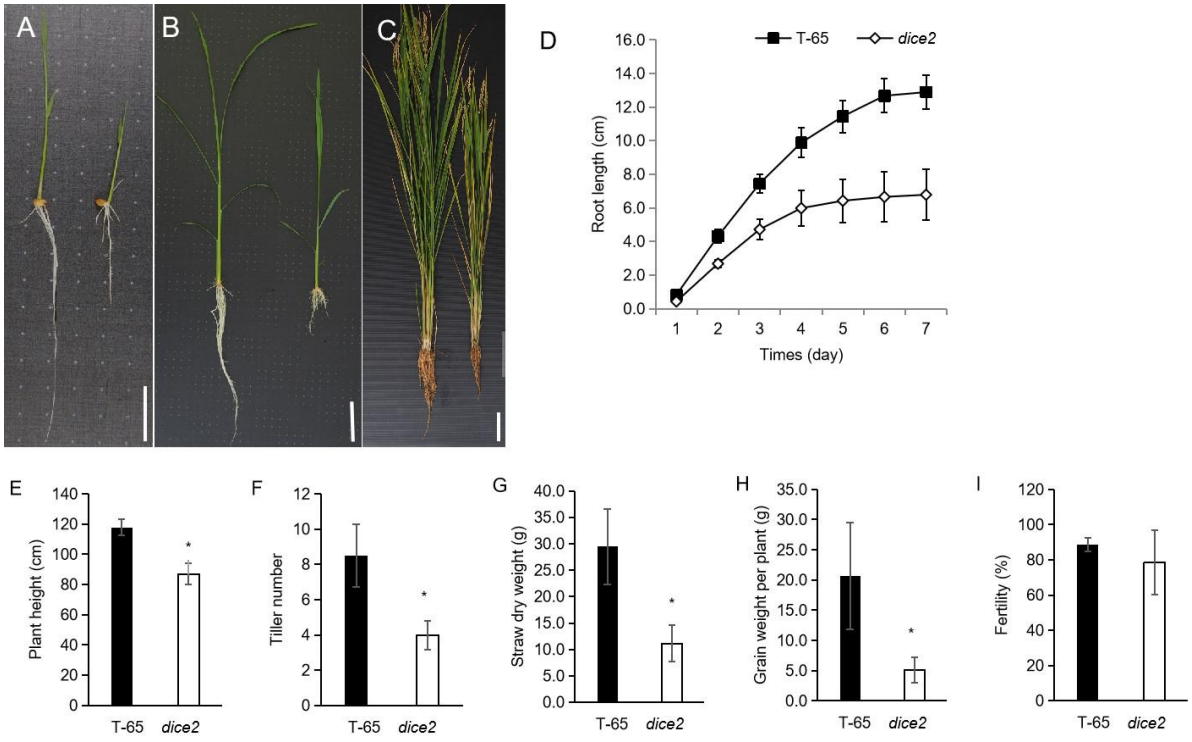

Figure 3.1. Comparison of the phenotype between the wild-type rice and *dice2* mutant. (A, B) Phenotype of the wild-type rice (T-65; left) and the short-root mutant (*dice2*; right) grown hydroponically for 7 d (A) and 30 d (B) in a greenhouse. (C) Phenotype of the wild-type rice (left) and the mutant (right) grown in soil condition. Photo was taken at harvest. (D) Time-dependent root elongation. Germinated seedlings were exposed to a 0.5 mM $CaCl_2$ solution and the seminal root length was measured at different day. Error bars represent ± SD (n = 10). (F-J) Growth parameters at harvest. Both T-65 and *dice2* were grown in soil till ripening. At harvest, plant height (E), tiller number (F), straw dry weight (G), grain yield per plant (H) and fertility (I) were recorded. Error bars represent ± SD (n = 9). Scale bars, 2 cm (A), 5 cm (B) and 10 cm (C). The asterisk indicates significant differences compared with the wild type (*P<0.05 by Tukey's test).

3.2 Anatomical observation of mutant root

To observe the anatomical differences between the *dice2* mutant and the WT, we prepared both longitudinal and transverse sections of the seminal root using 4-day-old seedlings. The results revealed that there was no clear anatomical difference at root tip region between mutant and WT (Fig. 3.2A, B). In addition, both WT and mutant roots had similar radial structures including epidermis, cortex (exodermis, sclerenchyma and endodermis), pericycle and central cylinder at different root regions (Fig. 3.2 E-H). However, the cell length of root cortical cells of mutant in the elongation region (2 mm from root apex) was significantly reduced compared with WT (Fig. 3.2C, D, I). The width of root cortical cells was similar between mutant and WT (Fig. 3.2E-H, J). All those results indicated that the short-root phenotype of *dice2* was caused by a reduced cell length.

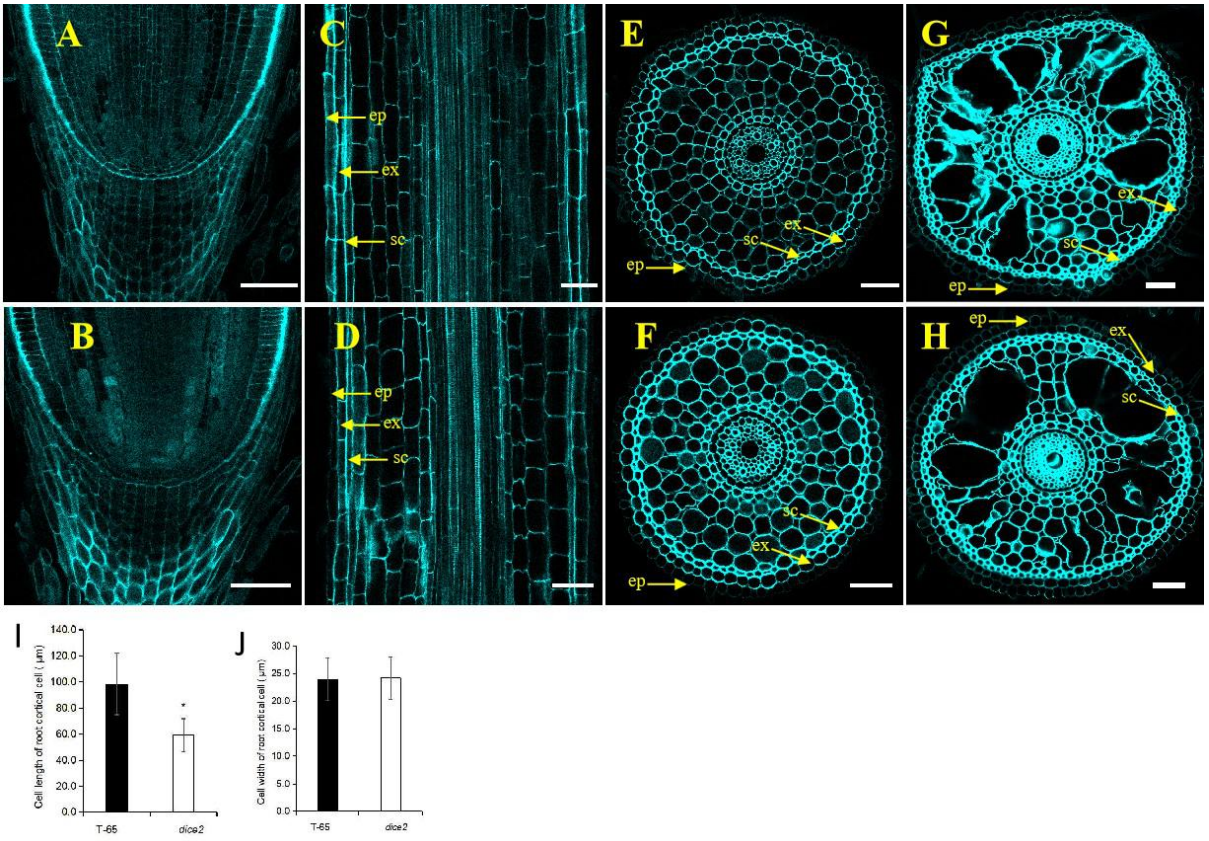

Figure 3.2 Anatomical features of the short-root mutant. Root longitudinal sections of 4-day-old seedlings of the wild type (A, C) and mutant (B, D). (E-F) Transverse sections of wild-type (E) and mutant (F) at around 2 mm from the root apex. (G-H) Transverse sections of wild-type (G) and mutant (H) at around 15 mm from the root apex. (I) Longitudinal cell length of cortical cells in the elongation region of the roots (2 mm from the root apex; n = 100). (J) Transverse cell width of cortical cells in the mature region of the root (10-15 mm from the apex; n = 100). Epidermis (ep), exodermis (ex) and sclerenchyma (sc) cell layers were shown. Scale bars, 50 μm. Blue color showed cell wall ultraviolet auto fluorescence. The asterisk indicates significant difference between different lines (*P<0.05 by Tukey's test).

3.3 Mineral element profile analysis of the short-root mutant

We compared the ionome profiles between the mutant and the WT grown in hydroponic solution. All elements tested showed lower concentration in the shoots compared with WT at different extent (Fig.3.3B, C). In the roots, the concentration of Mg, Mn, Fe and Zn was slightly but significantly increased, and that of P and Ca was not changed in the mutant compared with the WT (Fig. 3.3D, E). In contrast, the root concentration of K, Cu and Cd was significantly decreased in the mutant compared with the WT (Fig. 3.3D, E). Since there was a large difference in the root biomass between WT and the mutant (Fig. 3.3A), we therefore calculated the uptake based on the root dry weight. As a result, the uptake of most elements were similar between mutant and WT (Fig. 3.4A, B).

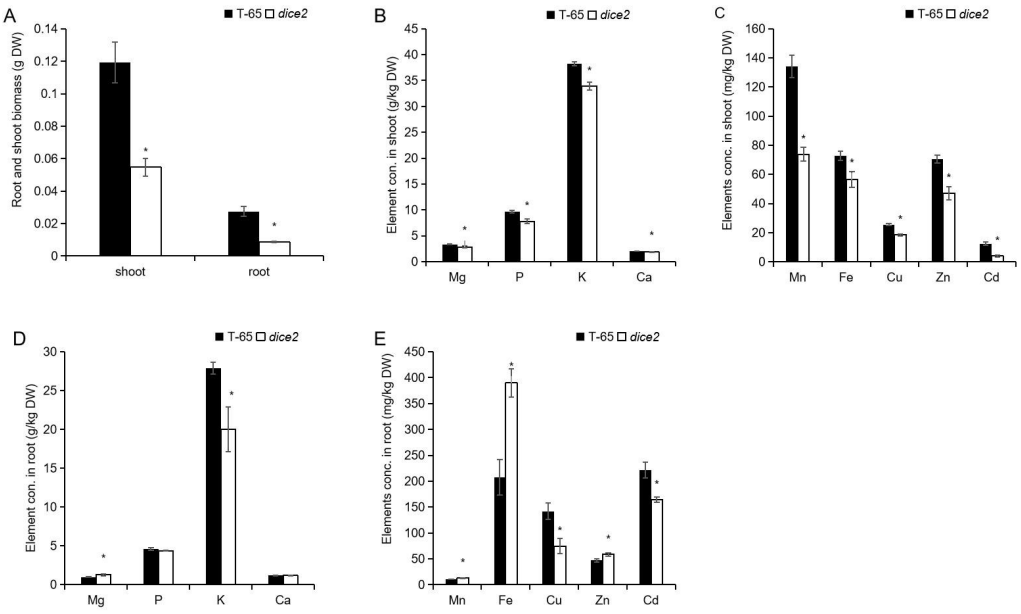

Figure 3.3 Mineral concentration in shoot and root of the wild-type rice (T-65) and short-root mutant (*dice2*). (A) Root and shoot biomass. (B-E) Shoot (B, C) and root (D, F) element concentration. 7-day-old seedlings were grown in half-strength Kimura B solution. After 20-d growth, the seedlings were exposed to a solution containing 0.2 μM $CdSO_4$ for another one day. Shoots and roots were separately harvested for determination of element concentration by ICP-MS. Data are means ± SD (n = 3). The asterisk indicates significant differences between different lines (*P<0.05 by Tukey's test).

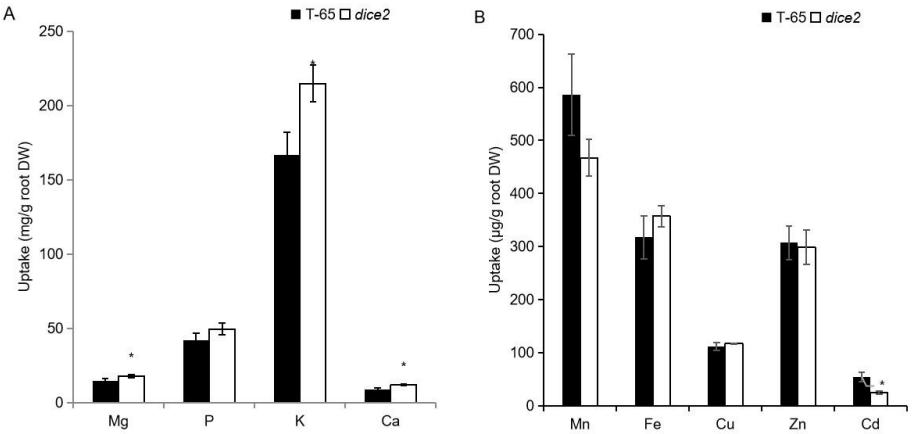

Figure 3.4 Uptake of mineral elements in the wild-type rice (T-65) and short-root mutant (*dice2*). (A) Uptake of Mg, P, K and Ca in the wild-type rice and the mutant. (B) Uptake of Mn, Fe, Cu, Zn and Cd in the wild-type rice and the mutant. 7-day-old seedlings were grown in half-strength Kimura B solution. After 20-d growth, the seedlings were exposed to a solution containing 0.2 μM $CdSO_4$ for another one day. The uptake was calculated based on the root dry weight. Data are means ± SD (n = 3). The asterisk indicates significant differences between two lines (*P<0.05 by Tukey's test).

3.4 Map-based cloning of the responsible gene for the short-root phenotype in *dice2*

We first performed a genetic analysis using an F_2 population by backcrossing the mutant with the wild type (cv T-65). Among 89 seedlings tested, 68 seedlings showed the wild-type root phenotype, while 21 displayed the short-root phenotype similar to the mutant ($\chi^2 = 0.0337$; $P < 0.05$). The segregation of the short root phenotype in the population showed a ratio of 3:1, indicating that a single recessive gene was responsible for the mutant phenotype.

To isolate the responsible gene, another F_2 population derived from a cross between the mutant and an *indica* cultivar 'Kasalath' was generated. Linkage analysis showed that the short-root phenotype of *dice2* mutant was tightly linked with two InDel markers M0221 and M0204 on chromosome 2 (Fig. 3.5A). For fine mapping of the responsible gene, another 11 polymorphic markers and 3 000 F_2 seedlings were used. Finally, the candidate gene was narrowed down to a 33-kb region between M1138 and M1141 on chromosome 2 (Fig. 3.5A). This region contains 5 predicted genes based on the Rice Genome Annotation Project (RGAP) (http://rice.plantbiology.msu.edu/) (Table 3.5). The expression level of LOC_Os02g19510

was very high in the root according to RiceXPro database (http://ricexpro.dna.affrc.go.jp/), while no information for another 4 candidate genes is available. Sequence of LOC_Os02g19510 in both WT and mutant was then compared. The results showed that a point mutation (from G to A) occurring at nucleotide position 1119 bp of the coding sequence (from ATG) within the last exon of the gene resulted in a premature stop (Fig. 3.5B). According to RGAP database (http://rice.plantbiology.msu.edu/), this gene was annotated to *OsLKRT1* (*Lysine Ketoglutarate Reductase Trans-splicing related 1*). *OsLKRT1* contains 14 exons and 13 introns (Fig. 3.5B), encoding a peptide of 402 amino acids according to RGAP. The sequence of entire open reading frame was confirmed from cDNA of rice root (cv T-65).

In rice genome, there are ten *LKRT1* homologous genes (Fig. 3.6), but none of them has been functionally characterized.

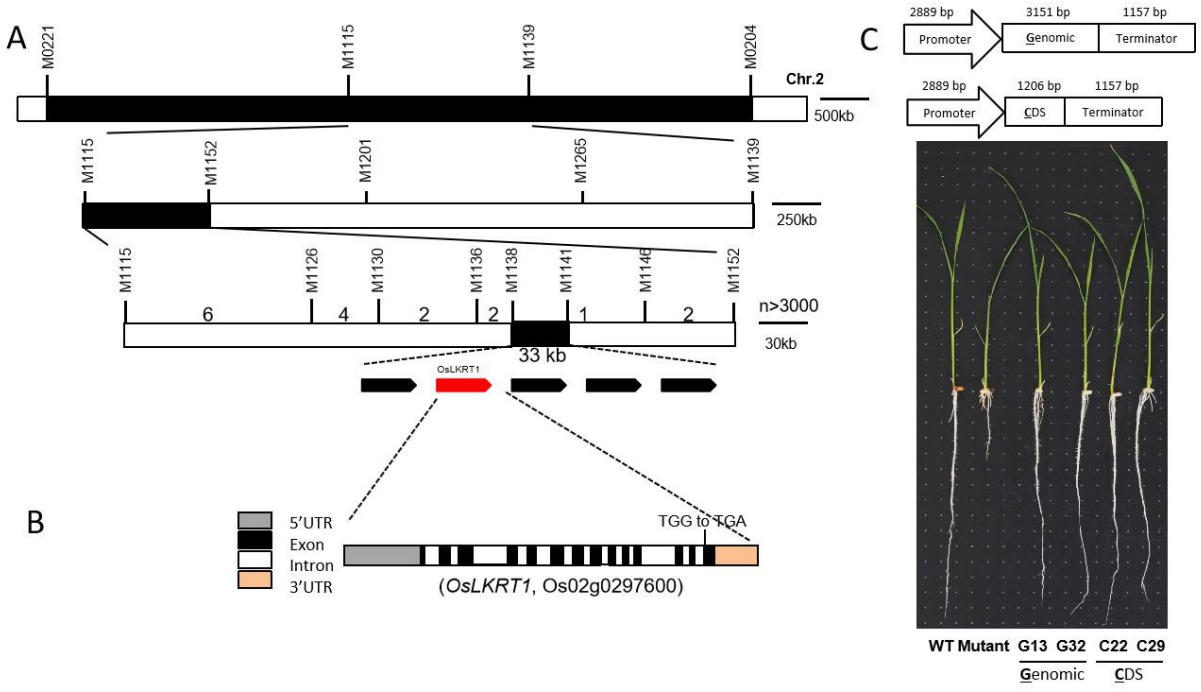

Figure 3.5 Map-based cloning and phenotypic complementation test. The candidate gene locus was mapped to 33-kb region on chromosome 2. The markers are listed at the top, and the numbers above the bars indicate the number of recombinants. (B) Gene structure of *OsLKRT1*. Vertical line represents the point mutation of *OsLKRT1*. (C) Complementation test of *dice2*.

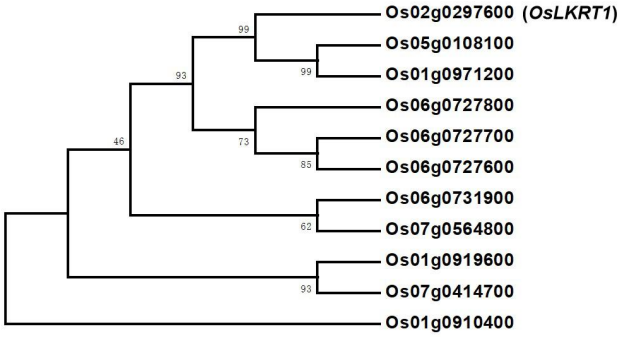

Figure 3.6 Phylogenetic tree of OsLKRT1 homolog proteins in *Oryza sativa*. The amino acid sequences were aligned by ClustalW.

Table 3.5 List of candidate genes in the mapping region of chromosome 2.

Gene name	Annotated information
LOC_Os02g19490	retrotransposon protein, putative, unclassified, expressed
LOC_Os02g19510	lysine ketoglutarate reductase trans-splicing related 1, putative, expressed
LOC_Os02g19520	transposon protein, putative, unclassified, expressed
LOC_Os02g19530	lectin-like receptor kinase, putative, expressed
LOC_Os02g19540	OsFBX47 - F-box domain containing protein, expressed

3.5 Complementation test

A complementation test was performed to confirm whether the mutation in *OsLKRT1* was responsible for the short-root phenotype by using genomic DNA and cDNA of *OsLKRT1*. A total of 7 individual lines for genomic DNA and 6 individual lines for cDNA were obtained.

Both constructs were able to rescue the short-root phenotype in *dice2* (Fig. 3.5C), indicating that the short-root phenotype in *dice2* is caused by the point mutation in *OsLKRT1*.

3.6 Effect of temperature on root growth of *dice2*

During experiments in green house, I occasionally found that the root growth of *dice2* changed with seasons. This suggests that the root growth of *dice2* is affected by temperature. I therefore compared the root growth in grown chamber at different temperature between WT and *dice2*. At 23°C, the root length of *dice2* was only 14.5% of that of wild-type rice after 27-day growth (Fig. 3.7A, B). However, at 32°C, the root growth of *dice2* increased to 64.7% of WT (Fig. 3.7A, B). A similar result was observed for shoot growth of *dice2* mutant (Fig. 3.7A). At 23°C, the shoot length of *dice2* was 43.1% of that of the WT, while the shoot growth of *dice2* increased to 72.1% of WT at 32°C (Fig. 3.7A, C). These results indicate that the defect in root and shoot growth of *dice2* could be partially rescued at high temperature.

A morphological observation showed that the root tip color of *dice2* was brown when grown at 23°C, while the color became to be white at 32°C (Fig. 3.8A-D). In addition, the length and intensity of root hairs were deceased in *dice2* mutant than that in WT at 23°C (Fig. 3.8 E, F), while these defects could be partially reduced by high temperature (Fig. 3.8 G, H).

We also compared the anatomic difference between mutant and WT at different temperature. The longitudinal sections of root elongation region (2 mm from root apex) showed that the cortex cell length was significantly shorter in the mutant than that in the wild type at both 23°C and 32°C, while the cell length in *dice2* mutant was significantly increased at 32°C compared with that at 23°C (Fig. 3.9A-D, M). In contrast, the root radial structure

and the cell width of root cortical cell was similar between the WT and mutant at both 23°C and 32°C (Fig. 3.9-L, N).

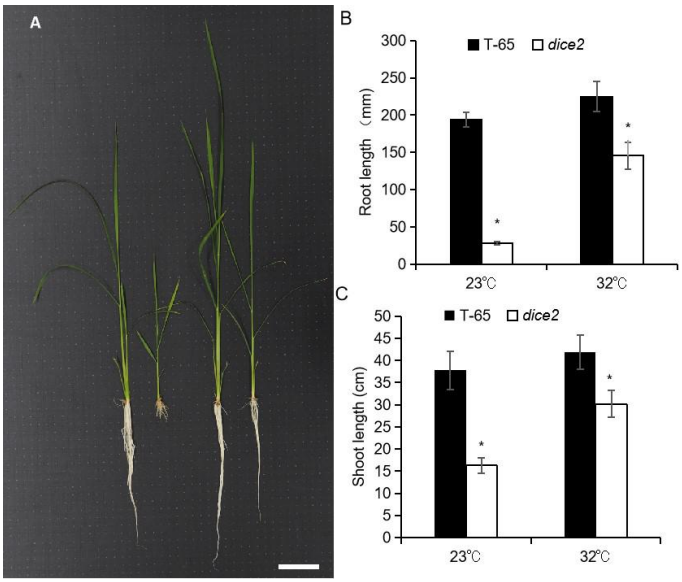

Figure 3.7 Phenotypic characterization of short-root mutant at different temperature treatments. (A) Effect of temperature on root growth. From left to right, WT and mutant at 23°C, WT and mutant at 32°C. Bar = 5 cm. Germinated seedlings were exposed to half-strength Kimura B solution for 27 days in a growth chamber at 23°C and 32°C, respectively. (B-C) Root (B) and shoot (C) length.

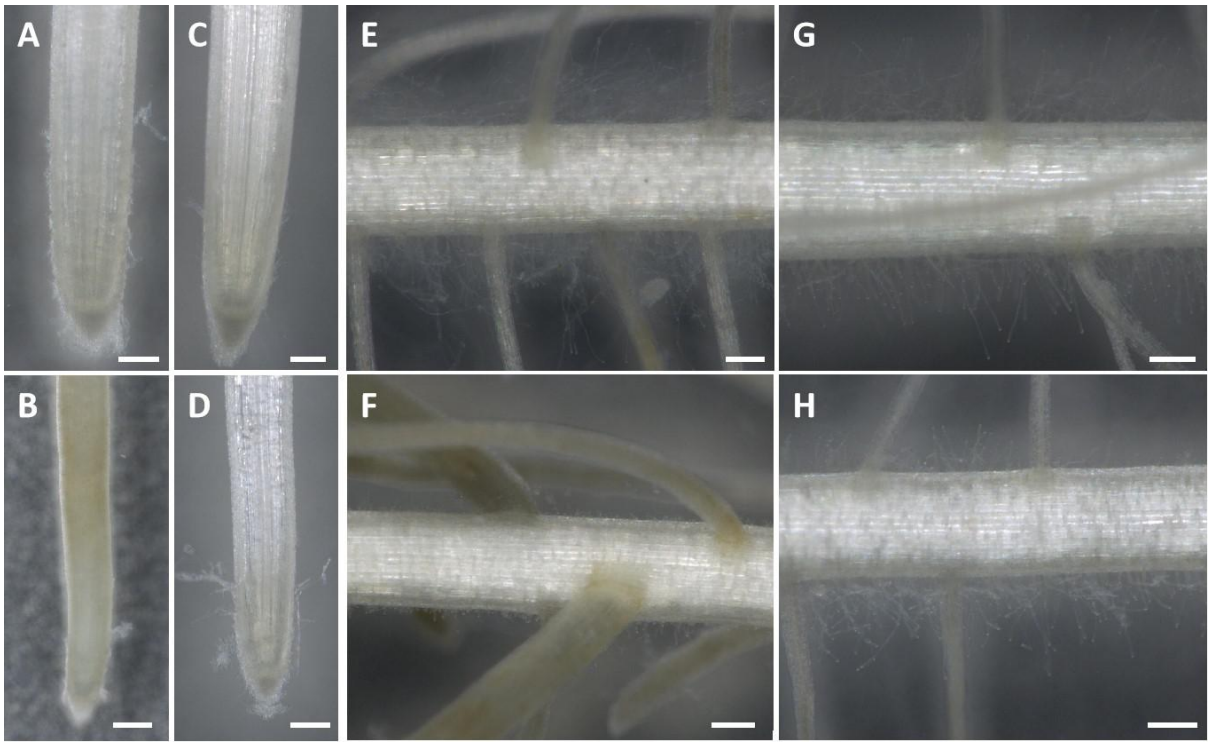

Figure 3.8 Morphological observation of short-root mutant at different temperature treatments. (A-D) Root tip color of WT (A, C) and short-root mutant (B, D). Bar = 100 μm. (E-H) Root hairs on primary roots of wild type (E, G) and short-root mutant (F, H). Bar = 100 μm. Germinated seedlings were exposed to half-strength Kimura B solution for 27 days in a growth chamber at 23°C and 32°C, respectively. (A, B, E, F) and (C, D, G, H) are from 23°C and 32°C, respectively.

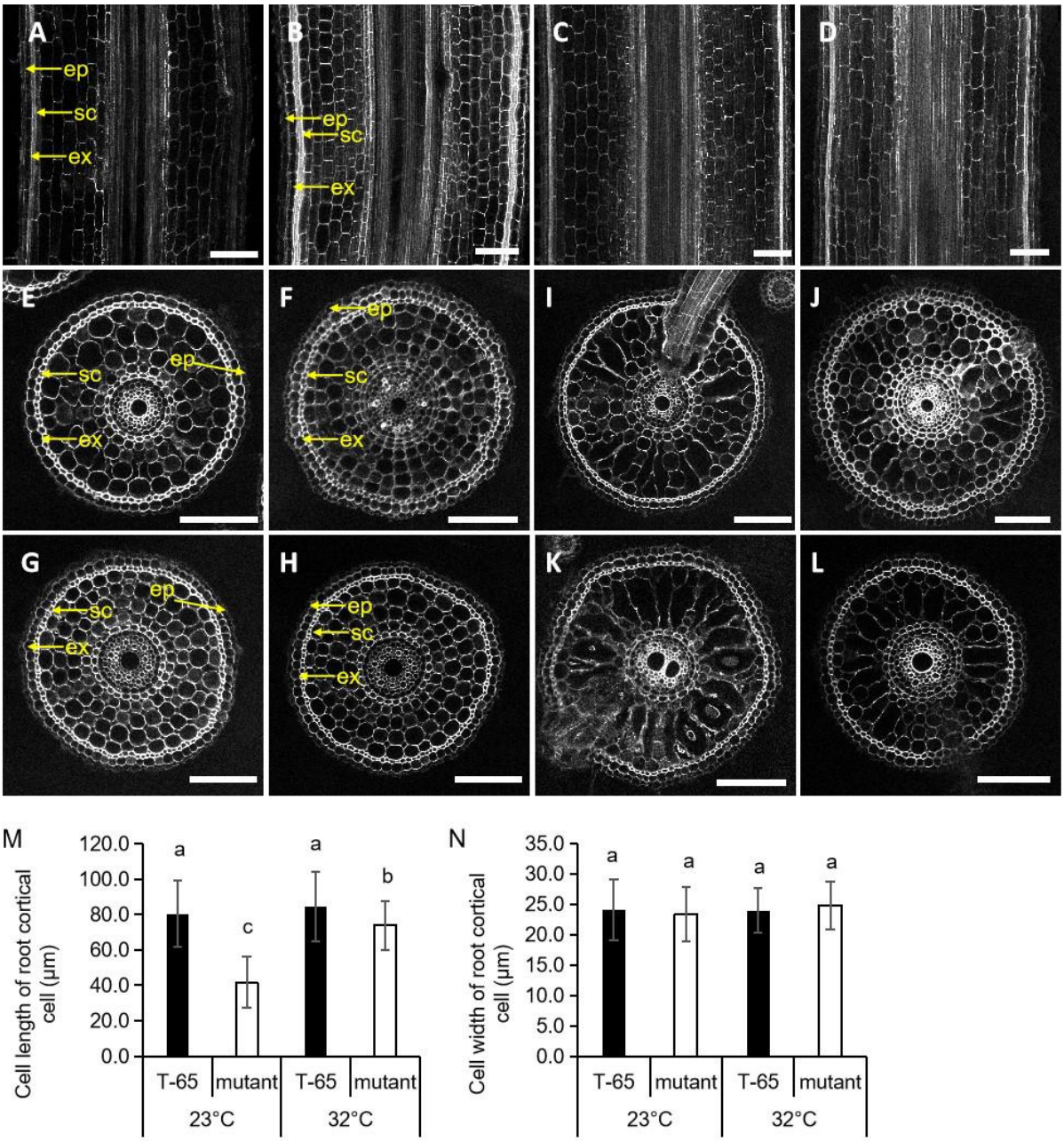

Figure 3.9 Anatomical features of the short-root mutant at different temperature treatments. Root longitudinal sections of 27-day-old seedlings of the wild type (A, C) and mutant (C, D). (E-H) Transverse sections of wild-type (E, G) and mutant (F, H) at around 2 mm from the root apex. (I-L) Transverse sections of wild-type (I, K) and mutant (J, L) at around 15 mm from the root apex. (M) Longitudinal cell length of cortical cells in the elongation region of the roots (2 mm from the root apex; n = 100). (N) Transverse cell width

of cortical cells in the mature region of the root (10-15 mm from the apex; n = 100). (A, B, E, F, I, J) and (C, D, G, H, K, L) are from 23°C and 32°C, respectively. Epidermis (ep), exodermis (ex) and sclerenchyma (sc) cell layers were shown. Scale bars, 100 µm.

3.7 Expression analysis of *OsLKRT1*

The expression pattern of *OsLKRT1* was investigated in different organs at different growth stages of rice grown in a paddy field. The expression level of *OsLKRT1* was similar in various organs including root, basal stem, leaf sheath and leaf blade at both tilling and booting stage, while the expression level of *OsLKRT1* was much higher in node I and immature panicle compared with other tissues at booting stage. At flowering and grain filling stage, the expression of *OsLKRT1* was also detected at different organs (Fig. 3.10).

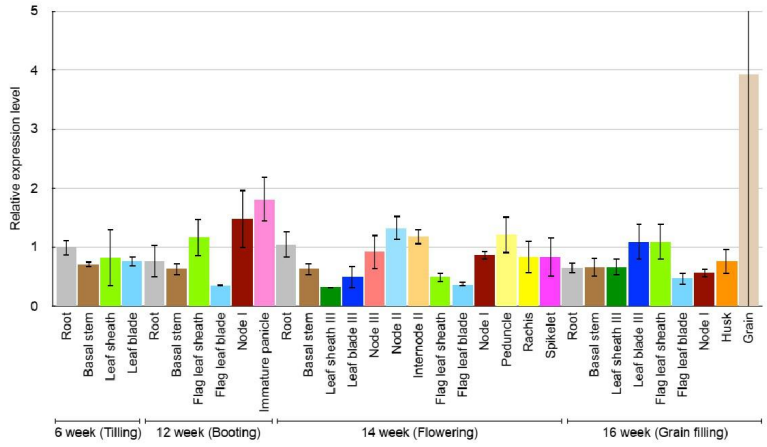

Figure 3.10 Expression analysis of *OsLKRT1*. Relative expression of *OsLKRT1* in various organs at different growth stages. Rice was grown in a paddy field until ripening and various organs were sampled at different growth stage.

3.8 Subcellular localization of *OsLKRT1*

To investigate the subcellular localization of *OsLKRT1*, the ORF of *OsLKRT1* was fused with GFP at both the C-terminus and the N-terminus under the control of 35S promoter. The signal of GFP alone was observed in the cytosol and nucleus in the rice protoplast (Fig. 3.11A-D). By contrast, both *OsLKRT1*-GFP and GFP-*OsLKRT1* were localized to the cytosol in rice protoplast (Fig. 3.11E-L). When the fused fragments were expressed in onion epidermal cells, similar localization in the cytosol was observed (Fig. 3.12).

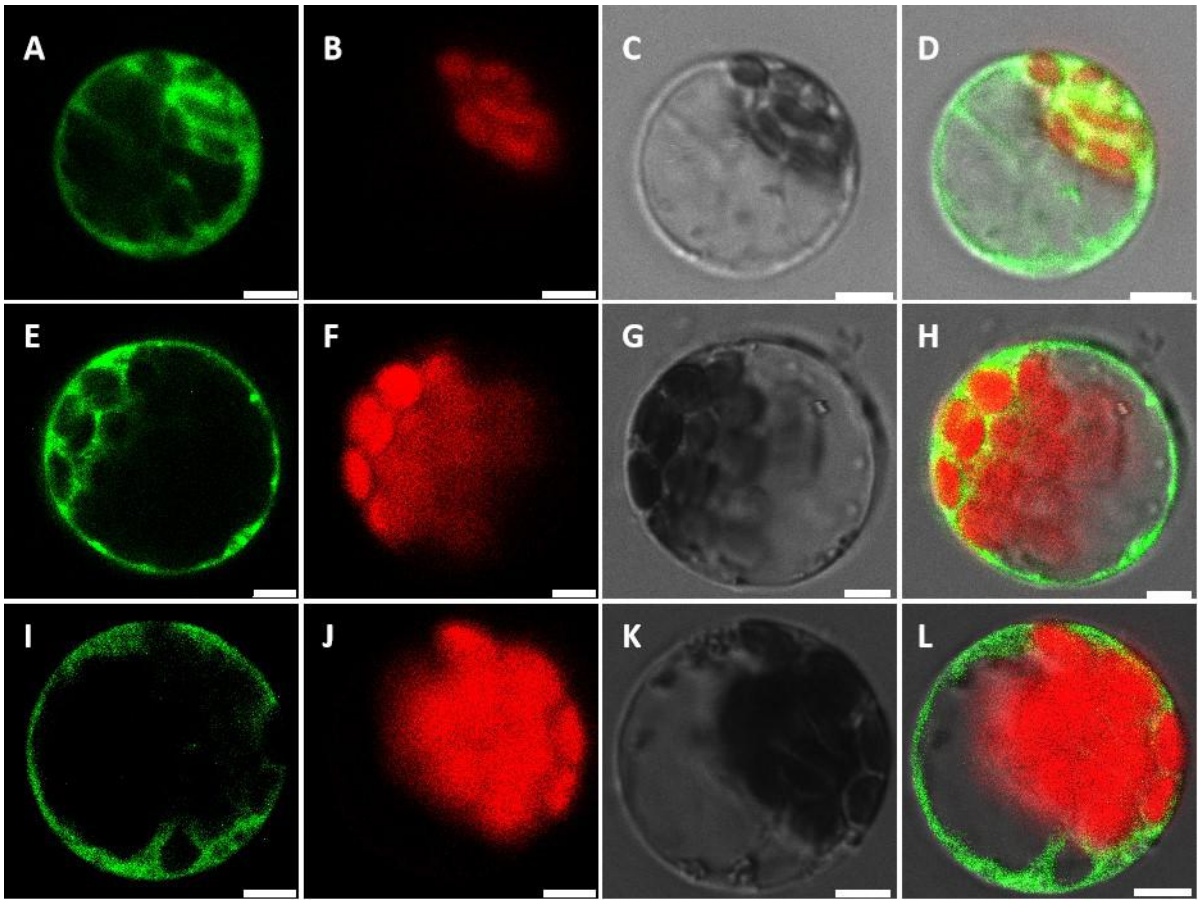

Figure 3.11 Subcellular localization of *OsLKRT1* in rice protoplasts. GFP alone (A-D) or *OsLKRT1* fused with GFP at C-terminus (E-H) and N-terminus (I-L) was transiently transformed into rice protoplasts by the polyethylene glycol method. GFP signal (A, E, I),

chlorophyll image (B, F, J), bright field (C, G, K) and merged image (D, H, L) are shown. Scale bars, 5 μm.

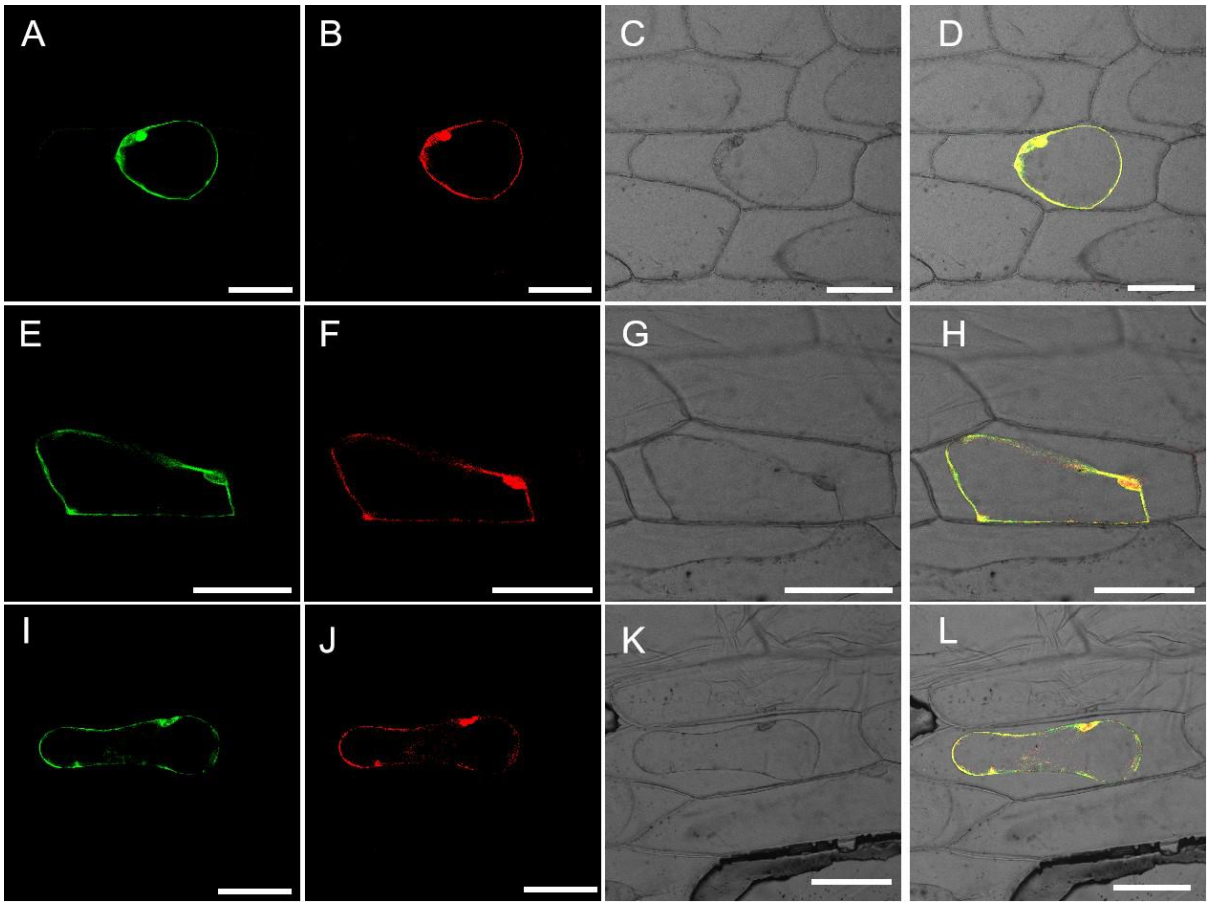

Figure 3.12 Subcellular localization of *OsLKRT1*. GFP alone (A-D) or *OsLKRT1* fused with GFP at C-terminus (E-H) and N-terminus (I-L) was co-transformed with 35S:DsRed into onion epidermal cells by particle bombardment. GFP signal (A, E, and I), DsRed signal (B, F, and J), bright field (C, G, and K) and a merged image (D, H, and L) are shown. The cells were plasmolyzed by 1 M mannitol. Bars are 100 μm.

3.6 Tissue-specific expression of *OsLKRT1*

To investigate tissue-specific expression of *OsLKRT1*, we generated transgenic rice lines carrying GFP under the control of the *OsLKRT1* promoter (2889 bp from the ATG). Immunostaining of the T_2 transgenic rice with a GFP antibody showed that *OsLKRT1* promoter was expressed in all root cells of the root tip (Fig. 3.13A-E). At the mature root region (more than 20 mm from the root apex), a stronger signal was observed central cylinder (Fig.3.13B, E). In the leaf blade, the signal was also expressed in all cells (Fig. 3.13F). No signal was observed in the roots and leaf blade of non-transgenic wild type (Fig. 3.13G, H), indicating the specificity of the antibody.

Since high temperature can partially recover the short-root phenotype in *dice2* mutant (Fig. 3.7A, C), we therefore compared the effect of low and high temperature on the tissue-specific expression of *OsLKRT1*. The results indicated that the *OsLKRT1* promoter was expressed at both low and high temperature treatment with a similar expression pattern (Fig. 3.14A-H).

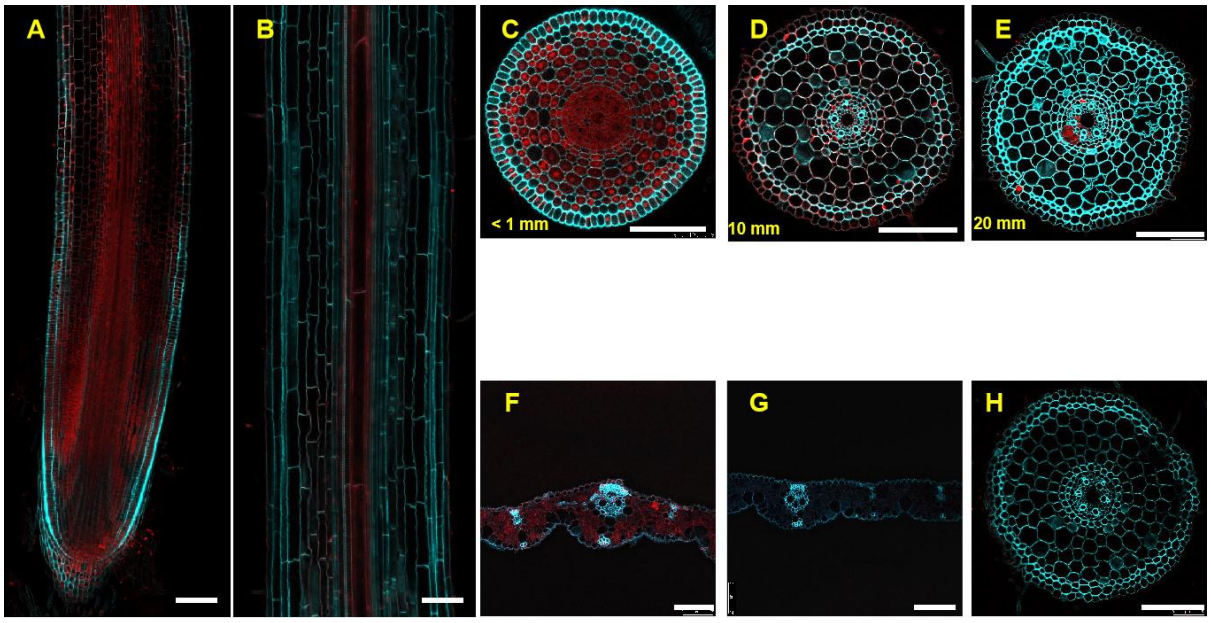

Figure 3.13 Tissue specificity of *OsLKRT1* expression. Immunostaining with an anti-GFP antibody was performed in different tissues of pOsLKRT1-GFP transgenic rice (A-F) and wild-type rice (G-H), including longitudinal section of root tip (A) and root mature zone (B). Cross sections at less than 1 mm (C), 10 mm (D) and 20 mm (E, H) and leaf sheath (F, G). Red color shows the GFP antibody-specific signal and blue color indicates cell wall autofluorescence. Scale bars = 100 μm.

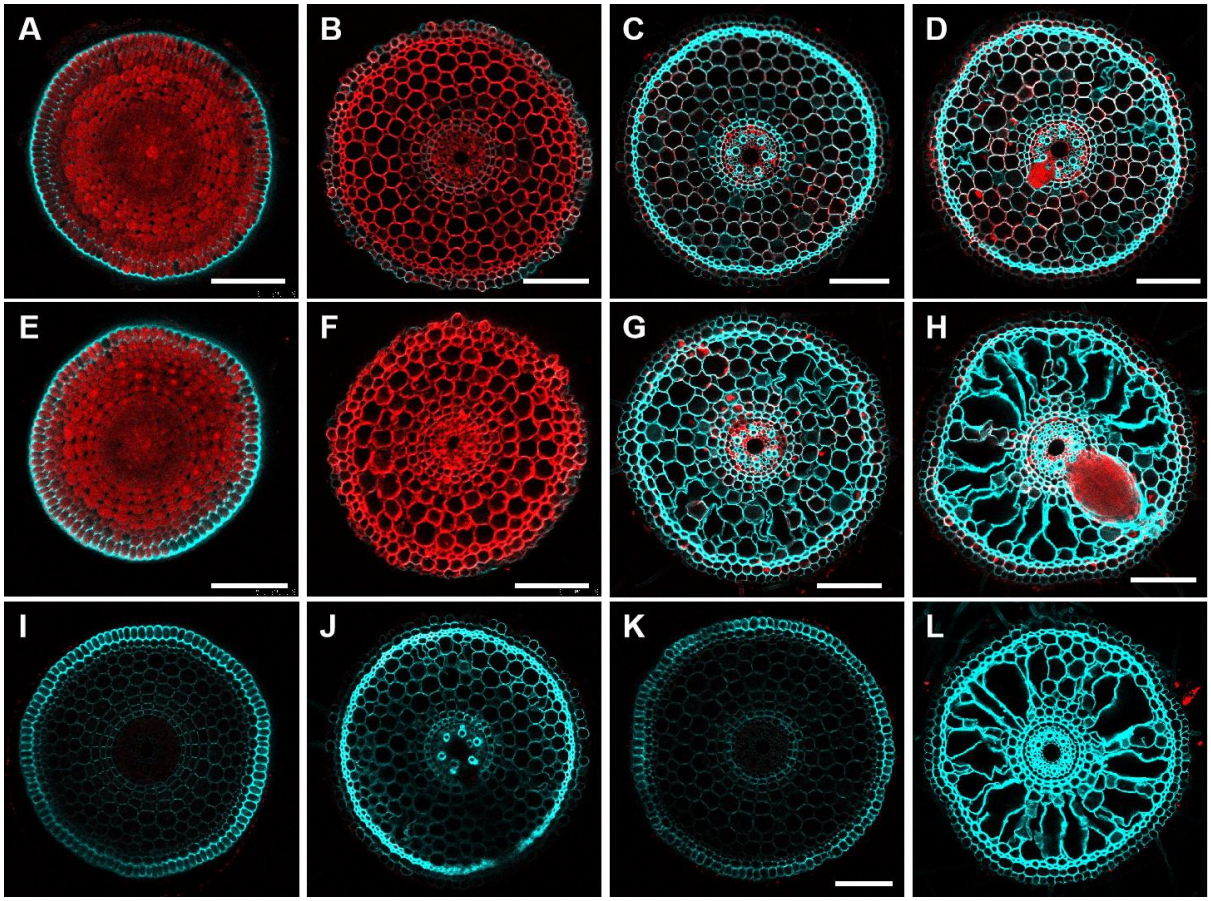

Figure 3.14 Effect of temperature on tissue specificity of *OsLKRT1* expression. Immunostaining with an anti-GFP antibody was performed in roots of p*OsLKRT1*-GFP transgenic rice (A-H) and wild-type rice (I-L). Cross sections at less than 1 mm (A, B, E, F, I,

K), 10 mm (C, G) and more than 15 mm (D, H, J, L). (A-D, I, J) and (E-H, K, L) are from seedlings grown at 23°C and 32°C, respectively. Bars are 100 μm.

3.10 Transcriptomic analysis of *dice2* mutant

To identify target genes of *OsLKRT1*, we carried out an RNA-seq analysis for the whole roots of the WT and the *dice2* mutant. Compared with WT, the expression of genes exhibited more than twofold change in the mutant were selected. As a result, there were 369 and 815 genes that were significantly down-regulated and up-regulated, respectively, in the mutant (Fig. 3.15A) .

To classify the functions of the up- and down-regulated genes in mutant, we performed the gene ontology (GO) enrichment analysis. The results showed that the defense response, response to wounding and response to biotic stimulus were the top 3 of GO enrichment in up-regulated genes, while the hydrogen peroxide catabolism process, hydrogen peroxide metabolic process and oxidation-reduction process were the top 3 of GO enrichment in down-regulated genes (Fig. 3.15B, C).

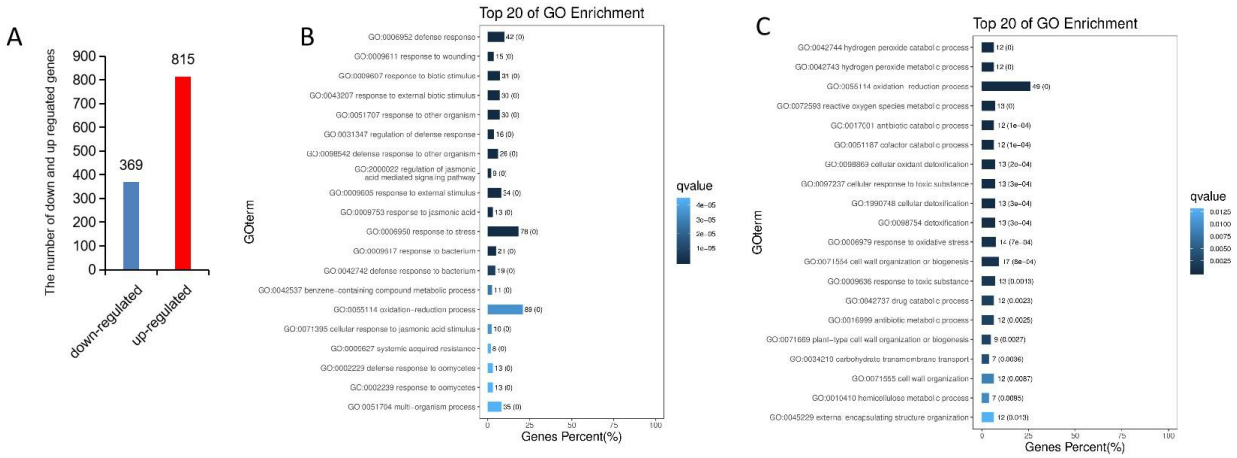

Figure 3.15 Enriched gene functions in roots of *dice2*. (A) The number of down- and up-regulated genes in *dice2* mutant compared with the WT. (B-C) Functional classification of the genes specifically up-regulated (B) and down-regulated (C) in the roots of *dice2* and the wild-type rice. Gene ontology (GO) categories related to biological process represents enriched GO terms using the omics-share platform (https://www.omicshare.com/).

3.11 Sequence and expression comparison of candidate genes of *OsLKRT1*

According to the annotated information of *OsLKRT1* and temperature-sensitive root growth feature of *dice2* mutant, we speculated that *OsLKR/SDH* and *OsGNA1* might be the target genes of *OsLKRT1* because *OsLKR/SDH* encoded a bifunctional lysine-degrading enzyme (Kawakatsu and Takaiwa, 2010) and *OsGNA1* was involved in regulating root growth in a temperature-dependent manner (Jiang et al., 2005). We subsequently compared the sequence of these genes as well as *OsLKRT1* between *dice2* and WT (Fig. 3.16). The sequence of *OsLKR/SDH* and *OsGNA1* did not differ between WT and the mutant (Fig. 3.16A). The expression of *OsLKR/SDH* was slightly but significantly increased in *dice2* mutant compared with the WT, and that of *OsGNA1* and *OsGlu3* was not changed in *dice2* mutant (Table 3.6). This suggests that *OsLKR/SDH* and *OsGNA1* are not the target of *OsLKRT1*. On the other hand, a point mutation of *OsLKRT1* was observed at the last exon in the mutant, which was consistent with the mapping results (Fig. 3.16C, D; Fig. 3.5B).

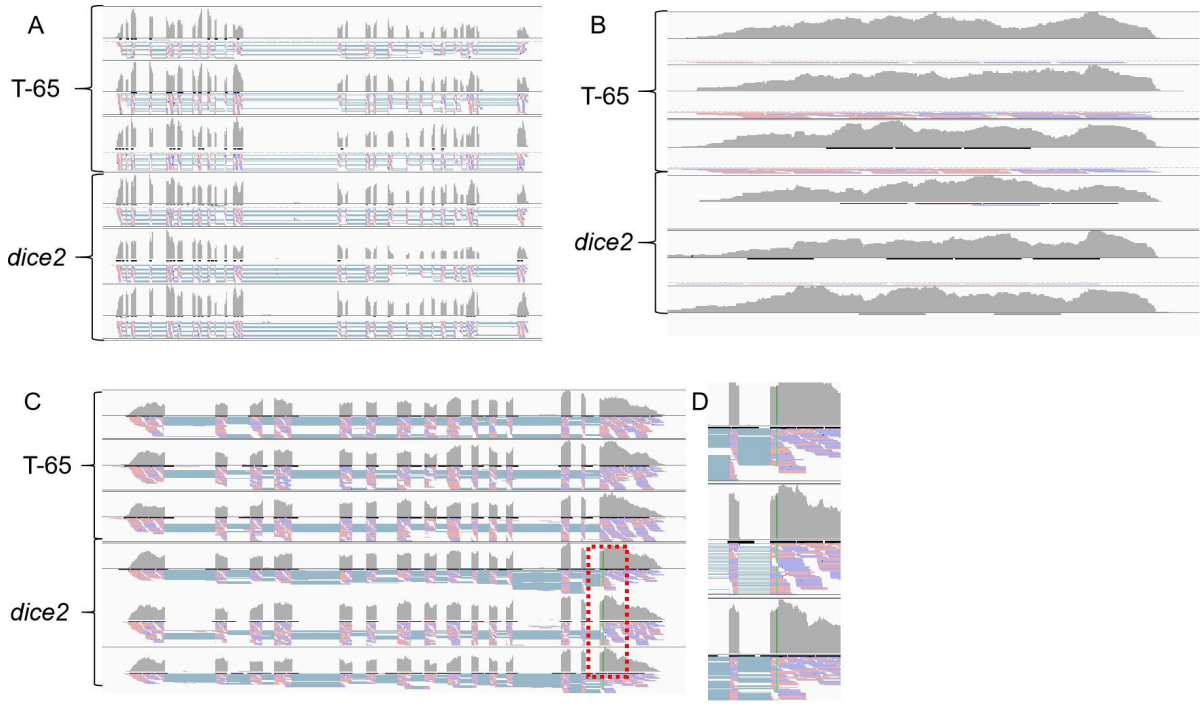

Figure 3.16 Sequence of candidate target genes of *OsLKRT1* between *dice2* and WT. The sequence comparison of *OsLKR/SDH* (A), *OsGNA1* (B) and *OsLKRT1* (C) between *dice2* mutant and WT. (D) Magnified image of red dotted box in C. Three independent replicates were used for both *dice2* and WT, the gray peaks indicate the exons and green vertical line represent the point mutation in *OsLKRT1*.

Table 3.6 The expression of candidate target genes of *OsLKRT1* between *dice2* and WT.

Gene ID	T-65_FPKM	*dice2*_FPKM	Log_2(fold change)	q value	Significant	Annotation
Os04g0497200	109.4	112.0	0.0	0.9	no	*OsGlu3*
Os09g0488000	13.8	13.8	0.0	1.0	no	*OsGNA1*
Os02g0783700	13.3	19.3	0.5	0.0	yes	*OsLKR/SDH*

4. Discussion

Through screening of MNU-mutated seeds, we obtained another rice mutant, *dice2*, which showed a shorter seminal root and crown roots at different growth stages (Fig. 3.1A-C). This mutant is defective in root cell elongation but not in root cell differentiation (Fig. 3.1D; Fig. 3.2). The uptake of mineral elements was not affected in the mutant although the concentration of mineral elements in the shoots was lower in the mutant due to reduced root biomass (Fig. 3.3； Fig. 3.4). This result indicates that the function of mineral element uptake was not altered in the mutant.

Map-based cloning combined with complementation test revealed that the short-root phenotype was caused by a point mutation of a gene being annotated to encode Lysine Ketoglutarate Reductase (LKR) Trans-Splicing related 1 (*OsLKRT1*), resulting in a premature stop in *dice2* mutant (Fig. 3.5B). There are 10 *OsLKRT1* homologous genes in rice genome (Fig. 3.6), but none of them has been functionally characterized. Trans-splicing is the precise joining of RNA exons from two discontiguous primary transcripts, while the cis-splicing is joining of RNA exons originated from the same primary transcript (Agabian 1990; Lasda et el., 2011). In plants, pentatricopeptide repeat (PPR) proteins, chloroplast RNA splicing and ribosome maturation (CRM) proteins are reported to be involved in trans-splicing event (Barkan et al., 2007). For example, *OTP43*, a PPR gene, is required for trans-splicing of the mitochondrial *nad1* intron 1 in Arabidopsis. Loss of function of *OTP43* resulted in severe defects in seed development, germination and to a lesser extent in plant growth (Falcon de Longevialle et al., 2007). On the other hand, *PPR4* was reported to be involved in trans-splicing of plastid *rps12* transcripts in maize, rice and Arabidopsis

(Schmitz-Linneweber et al., 2006; Cheng et al., 2016; Lee et al., 2019). Recently, *Zmlkrts*, the homologous gene of *OsLKRT1*, was reported to regulate lysine level via its role in the lysine catabolic pathway (Wen et al., 2018). Overexpression of *Zmlkrts* could increase the lysine content in maize mature leaf (Wen et al., 2018). Lysine could be catabolized into acetyl CoA and several molecules of glutamate (Glu) (Galili et al., 2001). LKR, the first enzyme in the lysine catabolic pathway, condensed lysine and α-ketoglutarate into saccharopine, which is then converted by the second enzyme saccharopine dehydrogenase (SDH) into α-amino adipic semialdehyde and Glu (Tang et al., 2002). In rice, *OsLKR/SDH*, which encoded a bifunctional lysine-degrading enzyme, was involved in Lys catabolism (Kawakatsu and Takaiwa, 2010). I therefore compared the sequence of *OsLKR/SDH* between *dice2* mutant and the WT. However, the coding sequence of *OsLKR/SHD* was identical between *dice2* mutant and the WT according to RNA-seq database although the expression level of *OsLKR/SDH* was significantly increased in *dice2* mutant (Fig. 3.16A; Table 3.6). These results suggest that *OsLKR/SDH* is not the target gene of trans-splicing by *OsLKRT1* in rice.

On the other hand, the root growth of *dice2* exhibited a temperature-sensitive feature, which was similar to *gna1* mutant (Jiang et al., 2005). *OsGNA1*, a glucosamine-6-P acetytransferase, was reported to be involved in normal root cell metabolism and cell shape by affecting the de novo UDP-N-acetylglucosamine biosynthesis (Jiang et al., 2005). The root growth was inhibited in *gna1* mutant under low temperature (25°C), while this inhibited root growth was partially abolished by high temperature (32°C) (Jiang et al., 2005). We therefore speculate that *OsGNA1* might be the target gene of *OsLKRT1*, however the

sequence of *OsGNA1* transcript was the same between *dice2* mutant and the WT in RNA-seq database (Fig. 3.16B), indicating that *OsLKRT1* is involved in regulating the root elongation in a *OsGNA1*-independent pathway.

OsLKRT1 was located in the cytosol (Fig. 3.11; Fig. 3.12), while the *PPR*-mediated trans-splicing occurs in mitochondria or chloroplast (Falcon de Longevialle et al., 2007; Schmitz-Linneweber et al., 2006). These findings suggest that OsLKRT1 mediated trans-splicing has a novel function or OsLKRT1 was not involved in trans-splicing event as annotated. Attempt was further made to identify the target genes of *OsLKRT1* by comparing transcript profiles between WT and *dice2* mutant using RNA-seq data. However, although hundreds of genes were up- and down-regulated in the mutant compared with the WT (Fig. 3.15A), the target genes could not be extracted. The exact molecular function of OsLKRT1 needs to be further investigated in future.

The interesting phenotype of *dice2* mutant is that its root growth was partially recovered at high temperature (Fig. 3.7A). The exact mechanism for this phenomenon is unknown, but one possibility is that other genes involved in root development complemented the phenotype of the mutant at high temperature.

In addition to the roots, *OsLKRT1* was also expressed in other organs including basal stem, leaf sheath, leaf blade, node and immature panicle through whole growth period (Fig. 3.10). In fact, the shoot growth of *dice2* was smaller than that of the WT (Fig. 3.7A, D). Furthermore, the shoot growth was also partially recovered in the mutant (Fig. 3.7 A, B, D). These findings suggest that OsLKRT1 is also required for shoot growth.

In summary, our results show that *OsLKRT1* is required for normal cell elongation of rice roots. It encodes a cytosol-localized protein, which is annotated to Lysine Ketoglutarate Reductase (LKR) Trans-Splicing related 1. However, the exact function of *OsLKRT1* remains to be investigated in future.

Chapter 4 General discussion

An ideal root system is a very important agronomic trait controlling crop production (Coudert et al., 2010; Meng et al., 2019). Rice roots have a unique root morphology and anatomy. Therefore, understanding of the molecular mechanisms of root development in rice will enable us to design the ideal root system and generate nutrient-efficient, high-yield and good-quality cultivars by marker-assisted selection or genetic modification. In this study, two rice mutants (*dice1* and *dice2* for *defective in cell elongation 1* and *2*) with short-root phenotype were isolated through screening of N-methyl-N-nitrosourea (MNU)-mutated seeds. Molecular mapping revealed that the short-root phenotypes in *dice1* and *dice2* are caused by loss-of-function of *OsGlu3* and *OsLKRT1*, respectively. Through detailed analysis, I found that these two genes are required for root development. Furthermore, I found that *OsGlu3* is involved in root cell elongation and differentiation, while *OsLKRT1* is required for root cell elongation, but not involved in cell differentiation.

4.1 Different roles of *OsGlu3* and *OsLKRT1* in root development of rice

Cell wall loosening is an important event for root cell elongation (Cosgrove, 2005). So far, several genes involved in cell wall loosening have been reported. For example, two members from expansin family, *OsEXPA8* and *OsEXPA10* were involved in root elongation by loosening the cell wall (Wang et al., 2014a; Che et al., 2016). OsGlu3 identified in this study is also probably involved in cell wall loosening process although its exact role is unknown. There are two hypothesizes on the role of OsGlu3 in root development. One is that OsGlu3 might hydrolyze the matrix polysaccharides or the links between matrix

polysaccharides and together with cell wall-loosening enzymes, create space for new cellulose synthesis, which is required for root elongation (Zhang et al., 2012). However, exogenous glucose did not completely rescue the root structure of the mutant although the root elongation was improved some (Fig. 2.10), indicating that exogenous glucose may exert the effect indirectly. The other one is that OsGlu3 is involved in digestion of noncrystalline amorphous cellulose and release of the hemicellulose tightly bound to cellulose microfibrils (Inukai et al., 2012). Knockout of this gene resulted in decreased plastic extensibility of the cell wall for root cell elongation due to strong cellulose-hemicellulose network (Inukai et al., 2012). This is also supported by defect in smooth exfoliation of root cap cells from the epidermal cell layer in the mutant (Fig. 2.2F, Inukai et al., 2012).

In *dice1* mutant, the differentiation of the outer cell layer was also altered (Fig. 2.2; Fig. 2.3). Different from other plant species, the outer cell layers of rice roots comprise the epidermis, exodermis and sclerenchyma (Rebouillatet al., 2008). These cell layers have been implicated in the resistance to various stresses such as drought, aluminum (Al), heavy metal and salinity in soil (Huang et al., 2009). However, the mechanism underlying the specification of these layers is still poorly understood. *Docs1*, encoding a leucine-rich repeat receptor-like kinase (LRR RLK) is involved in differentiation of our cell layers of rice roots (Huang et al., 2012). Furthermore, *Roc4* and *Roc5* encoding GL2-type homeodomain proteins may be the target of *Docs1* because their expression was down-regulated in *docs1* mutant (Huang et al,, 2012). Therefore, there is a possibility that *OsDocs1* is the upstream gene controlling *OsGlu3*. However, there was no difference in the *OsGlu3* expression

between the WT and the *C68* mutant (Fig. 2.14A), suggesting that *OsDocs1* and *OsGlu3* don't share the same pathway.

On the other hand, *OsLKRT1* is only involved in cell elongation of rice roots, but not in cell differentiation (Fig. 3.1D; Fig. 3.2). *OsLKRT1* was annotated to encode Lysine Ketoglutarate Reductase (LKR) Trans-Splicing related 1 (*OsLKRT1*) (Fig. 3.5B). However, the exact function of *OsLKRT1* and its homologs in rice is unknown. Trans-splicing is the precise joining of RNA exons from two discontiguous primary transcripts (Lasda et el., 2011). According to this annotation information, the sequence of its possible target, *OsLKR/SHD* were compared between *dice2* mutant and the WT by RNA-seq. However, the transcript sequence of *OsLKR/SHD* was identical between *dice2* mutant and the WT (Fig. 3.16A). Further work on identification of target genes of *OsLKRT1* is being undertaken.

In *dice2* mutant, the expression level of *OsGlu3* was similar to the WT (Table 3.6), suggesting that *OsGlu3* and *OsLKRT1* are involved in different processes independently.

On the other hand, *dice2* showed a temperature-sensitive short-root phenotype (Fig. 3.7A, B); the root growth defect could be partially rescued by high temperature (Fig. 3.7A). Previously, several temperature-sensitive rice root mutants have been reported. For example, *gna1* mutant exhibited a retarded root growth under low temperature (25°C), while this inhibited root growth was partially abolished by high temperature (32°C). *OsGNA1* encoding a glucosamine-6-P acetytransferase, was the responsible gene for the short root phenotype in *gna1* mutant (Jiang et al., 2005). OsORC3 was reported to be involved in DNA replication, cell proliferation and viability, which was proposed to regulate the lateral root (LR)

development by balancing the cell-cycle progression (Chen et al., 2013). The *orc3* mutant exhibited a temperature-dependent LR development defect. At 34°C, LRs failed to develop, while LRs development was normal at 26°C (Chen et al., 2013). However, it is unlikely that *OsGNA1* is the target gene of *OsLKRT1* because the sequence and expression of *OsGNA1* was same between *dice2* and WT (Fig. 3.17B; Table 3.6). Since the length of primary root and crown roots was not affected by temperature in *orc3* mutant, *OsORC3* could not be the target gene of *OsLKRT1*. Mechanisms underlying temperature-controlled root growth need to be further investigated in future.

2. Root structure and mineral element uptake

One of the most important roles of the roots is uptake of mineral nutrients from soil. Rice roots have developed an efficient uptake system for mineral element uptake (Sasaki et al., 2016). Due to unique anatomy of rice roots, both influx and efflux transporters localized at the exodermis and endodermis are required for transporting a mineral element from soil solution to the central stele. According to previous studies in rice, a mineral element is first transported from the soil solution to the aerenchyma across the exodermal cells, and subsequently from apoplastic solution in aerenchyma to stele across the endodermal cells (Ma & Yamaji, 2015; Che et al., 2018). Recently, this co-operative uptake system has been reported for Si and Mn in rice (Shao et al., 2017; Che et al., 2018). OsLsi1 (influx) and OsLsi2 (efflux) are responsible for Si uptake (Ma et al., 2006; Ma et al., 2007), OsNramp5 (influx) and OsMTP9 (efflux) are required for efficient Mn uptake (Sasaki et al., 2012; Ueno et al., 2015). These transporters are located at the exodermis and endodermis of mature root zones of rice (Ma et al., 2006; Ma et al., 2007; Sasaki et al., 2012; Ueno et al., 2015) and

knockout either of them results in significant decrease of root Si or Mn uptake. However, less has been investigated on the association between root system and mineral element uptake. In the present study, through detailed analysis of mineral element uptake in two mutants, it was found that both the root biomass and structures are important for mineral element growth. In *dice2* mutant, the mineral element accumulation in the shoots was significantly decreased due to small root biomass although the uptake was hardly affected (Fig. 3.3; Fig. 3.4). In *dice1* mutant, both the shoot accumulation and uptake was decreased (Fig. 2.6; Fig. 2.8). This is attributed to altered root structure (Fig. 2.2). Transporters for mineral element uptake require to be properly localized at specific cells (such as exodermis and endodermis in rice). It seems that altered root structure affect the expression and localization of transporters.

Summary

Plant roots not only play important roles in structural support of above-ground parts and uptake of water and mineral nutrients from soil, but also are important for sensing environmental changes. Rice, as a model plant of monocots is characterized by having a fibrous root system and a distinct root anatomy. In addition, rice is an important staple food for half the world's population. Understanding the molecular mechanisms of root development in rice will enable us to design the ideal root system and generate nutrient-efficient, high-yield and good-quality cultivars by marker-assisted selection or genetic modification. In this study, I isolated two rice mutants (*dice1* and *dice2* for *defective in cell elongation 1* and *2*) with short-root phenotype through screening of N-methyl-N-nitrosourea (MNU)-mutated seeds. I physiologically and anatomically characterized these mutants and mapped the genes responsible for the short-root phenotypes. I further functionally characterized these genes in terms of expression pattern, cellular or subcellular localization. Finally, I investigated the effect of root structure on uptake of mineral elements by comparing the mutants with their wild-type rice (WT).

dice1 exhibited a retarded root growth compared with WT at both seedlings and reproductive stages. A time-dependent root elongation indicated that the root growth was almost stopped after germination in *dice1* mutant, in contrast to the WT showing linear root elongation. Anatomical analysis showed that the root cap was difficult to peel off from the epidermal cell layers, and the epidermal cells and some exodermal cells at the basal root region were collapsed in *dice1*. Lignin and suberin staining indicated that the identity of the

outer layer cells was altered in *dice1*. Molecular mapping revealed that the short-root phenotype is caused by a single nucleotide substitution of a gene encoding a membrane-anchored endo-1,4-beta-glucanase (*OsGlu3*), resulting in splicing disorder in *dice1* mutant. To link the altered root structure with mineral element uptake, I compared the ionome profiles between *dice1* mutant and the WT grown in hydroponic solution. The results indicated that all elements tested except for K showed lower concentration in the shoots compared with WT. Especially, the uptake of Mn, Cd, As, Ge was significantly decreased in *dice1* compared with WT. Further analysis showed that the expression level of transporter genes *OsLsi1* and *OsLsi2* involved in the uptake of Si, Ge and As (III), *OsNramp5* for Mn and Cd uptake was significantly lower in *dice1* than in the WT. In addition, the localization of Si transporter OsLsi1 was altered in *dice1* mutant; OsLsi1 localized at the root exodermis of the WT was changed to be localized to other cell layers of the mutant roots.

dice2 is characterized by having a short primary root and crown roots. Anatomical analysis showed that the cortex cell length was significantly shorter in the mutant than in WT, while the root cell types did not differ between *dice2* mutant and WT. Furthermore, the short-root phenotype of the mutant was partially recovered when grown at a high temperature. Mineral profile analysis revealed that the concentration of most mineral elements in the shoots was lower in *dice2* mutant than in the WT, but the uptake based on root dry weight did not differ between two lines, indicating that the function for mineral element uptake was not altered in *dice2* mutant. Map-based cloning combined with complementation test revealed that the short-root phenotype was caused by a nucleotide substitution of a gene being annotated to encode Lysine Ketoglutarate Reductase Trans-Splicing related 1 (*OsLKRT1*),

resulting in a premature stop. There are 10 *OsLKRT1* homologous genes in rice genome, but none of them have been functionally characterized. *OsLKRT1* was expressed in different organs through whole growth period. Subcellular localization analysis in rice protoplasts showed that OsLKRT1 was localized in the cytosol. Furthermore, immunostaining with an antibody against GFP showed that OsLKRT1 was highly expressed in all cells of the root tip region, but only in central cylinder of mature root region in transgenic lines carrying *OsLKRT1* promoter fused with GFP.

These results indicated that both OsGlu3 and OsLKRT1 are required for root development in different ways; OsGlu3 is involved in both cell elongation and differentiation of the roots, while OsLKRT1 is only involved in root cell elongation. Furthermore, the results revealed that a normal root structure is required for maintaining the expression and localization of transporters involved in the mineral element uptake in rice

References

Ahamed A, Murai-Hatano M, Ishikawa-Sakurai J, Hayashi H, Kawamura Y, Uemura M (2012) Cold stress-induced acclimation in rice is mediated by root-specific aquaporins. Plant Cell Physiol 53: 1445-1456

Agabian N (1990) Trans splicing of nuclear pre-mRNAs. Cell 61: 1157-1160

Araya T, Miyamoto M, Wibowo J, Suzuki A, Kojima S, Tsuchiya Y N, Sawa S, Fukuda H, von Wirén N, Takahashi H (2014) CLE-CLAVATA1 peptide-receptor signaling module regulates the expansion of plant root systems in a nitrogen-dependent manner. Proc Natl Acad Sci USA 111: 2029-2034

Arite T, Kameoka H, Kyozuka J (2012) Strigolactone positively controls crown root elongation in rice J Plant Growth Regul 31: 165-172

Atkinson J A, Rasmussen A, Traini R, Voß U, Sturrock C, Mooney S J, Wells D M, Bennett M J (2014) Branching out in roots: uncovering form, function, and regulation. Plant Physiol 166: 538-550

Azhiri-Sigari T, Yamauchi A, Kamoshita A, Wade L J (2000) Genotypic variation in response of rainfed lowland rice to drought and rewatering: II. Root growth. Plant Prod Sci 3: 180-188

Barberon M (2017) The endodermis as a checkpoint for nutrients. New Phytol 213: 1604-1610

Barberon M, Geldner N (2014) Radial transport of nutrients: the plant root as a polarized epithelium. Plant Physiol 166: 528-537

Barkan A, Klipcan L, Ostersetzer O, Kawamura T, Asakura Y, Watkins K P (2007) The CRM domain: an RNA binding module derived from an ancient ribosome-associated protein. RNA 13: 55-64

Benfey P N, Linstead P J, Roberts K, Schiefelbein J W, Hauser M T, Aeschbacher R A (1993) Root development in Arabidopsis: four mutants with dramatically altered root morphogenesis. Development 119: 57-70

Bouguyon E, Perrine-Walker F, Pervent M, Rochette J, Cuesta C, Benkova E, Martinière A, Bach L, Krouk G, Gojon A, Nacry P (2016) Nitrate controls root development through posttranscriptional regulation of the NRT1.1/NPF6.3 transporter/sensor. Plant Physiol 172: 1237-1248

Boyer J S (2009) Cell wall biosynthesis and the molecular mechanism of plant enlargement. Funct Plant Biol 36: 383-394

Che J, Yamaji N, Ma J F (2018) Efficient and flexible uptake system for mineral elements in plants. New Phytol 219: 513–517

Che J, Yamaji N, Shen R F, Ma J F (2016) An Al-inducible expansin gene, OsEXPA10 is involved in root cell elongation of rice. Plant J 88: 132-142

Chen C W, Yang Y W, Lur H S, Tsai Y G, Chang M C (2006) A novel function of abscisic acid in the regulation of rice (*Oryza sativa* L.) root growth and development. Plant Cell Physiol 47: 1-13

Chen N, Xu Y Y, Wang X, Du C, Du J Z, Yuan M, Xu Z H, Chong K (2011) *OsRAN2*, essential for mitosis, enhances cold tolerance in rice by promoting export of intranuclear tubulin and maintaining cell division under cold stress. Plant Cell Environ 34: 52-64

Chen S, Tao L, Zeng L, Vega-Sanchez ME, Umemura K, Wang GL (2006) A highly efficient transient protoplast system for analyzing defence gene expression and protein-protein interactions in rice. Mol Plant Pathol 7: 417-427

Chen X N, Shi J, Hao X, Liu H L, Shi J H, Wu Y R, Wu Z C, Chen M X, Wu P, Mao C Z (2013) *OsORC3* is required for lateral root development in rice. Plant J 74: 339-350

Chen Y H, Chao Y Y, Hsu Y Y, Hong C Y, Kao C H (2012) Heme oxygenase is involved in nitric oxide-and auxin-induced lateral root formation in rice. Plant Cell Rep 31: 1085-1091

Chen Y, Yang Q F, Sang S H, Wei Z Y, Wang P (2017) Rice inositol polyphosphate kinase (OsIPK2) directly interacts with OsIAA11 to regulate lateral root formation. Plant Cell Physiol 58: 1891-1900

Chen Z C, Yamaji N, Fujii-Kashino M, Ma J F (2016) A cation-chloride cotransporter gene is required for cell elongation and osmoregulation in rice. Plant Physiol 171: 494-507

Cheng C, Yun K Y, Ressom H W, Mohanty B, Bajic V B, Jia Y L, Yun S J, de los Reyes B G (2007) An early response regulatory cluster induced by low temperature and hydrogen peroxide in seedlings of chilling-tolerant japonica rice. BMC Genomics 8: 175

Cheng S F, Gutmann B, Zhong X, Ye Y T, Fisher M F, Bai F Q, Castleden I, Song Y, Song B, Huang J Y, Liu X, Xu X, Lim B L, Bond C S, Yiu S M, Samll I (2015) Redefining the structural motifs that determine RNA binding and RNA editing by pentatricopeptide repeat proteins in land plants. Plant J 85: 532-547

Cheng Y F, Dai X H, Zhao Y D (2004) AtCAND1, a heat-repeat protein that participates in auxin signaling in Arabidopsis. Plant Physiol 135: 1020-1026

Chern M, Bai W, Sze-To W H, Canlas P E, Bartley L E, Ronald P C (2012) A rice transient

assay system identifies a novel domain in NRR required for interaction with NH1/OsNPR1 and inhibition of NH1-mediated transcriptional activation. Plant Methods 8: 6

Chinnusamy V, Zhu J, Zhu J K (2007) Cold stress regulation of gene expression in plants. Trends Plant Sci 12: 444-451

Considine M J, Foyer C H (2014) Redox regulation of plant development. Antioxid Redox Sign 21: 1305-1326

Cornwell W K, Grubb P J (2003) Regional and local patterns in plant species richness with respect to resource availability. Oikos 100: 417-428

Cosgrove D J (2005) Growth of the plant cell wall. Nat Rev Mol Cell Bio 6: 850

Coudert Y, Périn C, Courtois B, Khong N G, Gantet P (2010) Genetic control of root development in rice, the model cerea. Trends Plant Sci 15: 219-226

Courtois B, Ahmadi N, Khowaja F, Price A H, Rami J F, Frouin J, Hamelin C, Ruiz M (2009) Rice root genetic architecture: meta-analysis from a drought QTL database. Rice 2: 115

Courtois B, Shen L, Petalcorin W, Carandang S, Mauleon R, Li Z (2003) Locating QTLs controlling constitutive root traits in the rice population IAC165×Co39. Euphytica 134: 335–345

Cui P, Liu H B, Ruan S L, Ali B, Gill R A, Ma H S, Zheng Z F, Zhou W J (2017) A zinc finger protein, interacted with cyclophilin, affects root development via IAA pathway in rice. J Integr Plant Biol 59: 496-505

Dazzo F B, Truchet G L, Sherwood J E, Hrabak E M, Abe M, Pankratz S H (1984) Specific phases of root hair attachment in the *Rhizobium trifolii*-clover symbiosis. Appl Environ Microbiol 48: 1140–1150

Ding W N, Yu Z M, Tong Y L, Huang W, Chen H M, Wu P (2009) A transcription factor with a bHLH domain regulates root hair development in rice. Cell Res 19: 1309

Dropkin V (1969) The necrotic reaction of tomatoes and other hosts resistant to Meloidogyne: reversal by temperature. Phytopathology 59: 1632–1637

Enstone D E, Peterson C A, Ma F S (2002) Root endodermis and exodermis: structure, function, and responses to the environment. J Plant Growth Regul 21: 335-351

Felcon de Longevialle A, Meyer E H, Andrés C, Taylor N L, Lurin C, Millar A H, Small I D (2007) The pentatricopeptide repeat gene *OTP43* is required for trans-splicing of the mitochondrial *nad1* intron 1 in *Arabidopsis thaliana*. Plant Cell 19: 3256-3265

Fukai S, Cooper M (1995) Development of drought-resistant cultivars using physiomorphological traits in rice. Field Crop Res 40: 67-86

Fuse T, Sasaki T, Yano M (2001) Ti-plasmid vectors useful for functional analysis of rice genes. Plant Biotechnol 18: 219-222

Galili G, Tang G L, Zhu X H, Gakiere B (2001) Lysine catabolism: a stress and development super-regulated metabolic pathway. Curr Opin Plant Biol 4: 261-266

Gao S, Fang J, Xu F, Wang W, Sun X H, Chu J F, Cai B D, Feng Y Q, Chu C C (2014) Cytokinin oxidase/dehydrogenase4 integrates cytokinin and auxin signaling to control rice crown root formation. Plant Physiol 165: 1035-1046

Geldner N (2013) The endodermis. Annu Rev Plant Biol 64: 531-558

Giehl R F H, von Wirén N (2014) Root nutrient foraging. Plant Physiol 166: 509-517

Gilroy S, Jones D L (2000) Through form to function: root hair development and nutrient uptake. Trends Plant Sci 5: 56–60

Gu M, Zhang J, Li H H, Meng D Q, Li R, Dai X L, Wang S C, Liu W, Qu H Y, Xu G H (2017) Maintenance of phosphate homeostasis and root development are coordinately regulated by MYB1, an R2R3-type MYB transcription factor in rice. J Exp Bot 68: 3603-3615

Hiei Y, Ohta S, Komari T, Kumashiro T (1994) Efficient transformation of rice (*Oryza-Sativa* L) mediated by *Agrobacterium* and sequence-analysis of the boundaries of the T-DNA. Plant J 6: 271-282

Hoshikawa K (1989) The growing rice plant: an anatomical monograph. pp171-198

Hosmani P S, Kamiya T, Danku J, Naseer S, Geldner N, Guerinot M L, Salt D E (2013) Dirigent domain-containing protein is part of the machinery required for formation of the lignin-based Casparian strip in the root. Proc Natl Acad Sci USA 110: 14498–14503

Hsu Y Y, Chao Y Y, Kao C H (2013) Methyl jasmonate-induced lateral root formation in rice: the role of heme oxygenase and calcium. J Plant Physiol 170: 63-69

Huang C F, Yamaji N, Nishimura M, Tajima S, Ma J F (2009) A rice mutant sensitive to Al toxicity is defective in the specification of root outer cell layers. Plant Cell Physiol 50:976-985

Huang C F, Yamaji N, Ono K, Ma J F (2012) A leucine-rich repeat receptor-like kinase gene is involved in the specification of outer cell layers in rice roots. Plant J 69: 565-576

Inukai Y, Sakamoto T, Morinaka Y, Miwa M, Kojima M, Tanimoto E, Yamanoto H, Sato K, Katayama Y, Matsuoka M, Kitano H (2012) Root growth inhibiting, a rice endo-1, 4-β-D-glucanase, regulates cell wall loosening and is essential for root elongation. J Plant Growth Regul 31: 373-381

Inukai Y, Sakamoto T, Ueguchi-Tanaka M, Shibata Y, Gomi K, Umemura I, Hasegawa Y, Ashikari M, Kitano H, Matsuoka M (2005) Crown rootless1, which is essential for crown root formation in rice, is a target of an auxin response factor in auxin signaling. Plant Cell 17: 1387-1396

Ito M, Sentoku N, Nishimura A, Hong S K, Sato Y, Matsuoka M (2002) Position dependent expression of *GL2*-type homeobox gene, *Roc1*: significance for protoderm differentiation and radial pattern formation in early rice embryogenesis. Plant J 29: 497-507

Ito M, Sentoku N, Nishimura A, Hong S K, Sato Y, Matsuoka M (2003) Roles of rice *GL2*-type homeobox genes in epidermis differentiation. Breeding Sci 53: 245-25

Jeuken M J W, Zhang N W, McHale L K, Pelgrom Koen, Boer E D, Lindhout P, Michelmore R W, Visser R G F, Niks R E (2009). Rin4 causes hybrid necrosis and race-specific resistance in an interspecific lettuce hybrid. Plant Cell 21: 3368-3378

Jia L Q, Zhang B T, Mao C Z, Li J H, Wu Y R, Wu P, Wu Z C (2008) OsCYT-INV1 for alkaline/neutral invertase is involved in root cell development and reproductivity in rice (*Oryza sativa* L.). Planta 228: 51-59

Jiang C, Gao X H, Liao L L, Harberd N P, Fu X D (2007) Phosphate starvation root architecture and anthocyanin accumulation responses are modulated by the gibberellin-DELLA signaling pathway in Arabidopsis. Plant Physiol 145: 1460-1470

Jiang H W, Wang S M, Dang L, Wang S F, Chen H M, Wu Y R, Jiang X H, Wu P (2005) A novel short-root gene encodes a glucosamine-6-phosphate acetyltransferase required for maintaining normal root cell shape in rice. Plant Physiol 138: 232-242

Jing H W, Yang X L, Zhang J, Liu X H, Zheng H K, Dong G J, Nian J Q, Feng J, Xia B, Qian Q, Li J Y, Zuo J R (2015) Peptidyl-prolyl isomerization targets rice Aux/IAAs for proteasomal degradation during auxin signalling. Nature Commun 6: 7395

Johnson N A (2002) Sixty years after “Isolating mechanisms, evolution and temperature”: Muller's legacy. Genetics 161: 939-944

Jones J D G, Dangl J L (2016) The plant immune system. Nature 444: 323

Jung J K H, McCouch S (2013) Getting to the roots of it: genetic and hormonal control of root architecture. Front Plant Sci 4: 186

Kamiya T, Borghi M, Wang P, Danku J M, Kalmbach L, Hosmani P S, Naseer S, Fujiwara T, Geldner N, Salt D E (2015) The MYB36 transcription factor orchestrates Casparian strip formation. Proc Natl Acad Sci USA 112: 10533–10538

Kang B, Zhang Z C, Wang L L, Zheng L B, Mao W H, Li M F, Wu Y R, Wu P, Mao X R (2013) OsCYP2, a chaperone involved in degradation of auxin-responsive proteins, plays crucial roles in rice lateral root initiation. Plant J 74: 86-97

Kawai M, Samarajeewa P K, Barrero R A, Nishiguchi M, Uchimiya H (1998) Cellular dissection of the degradation pattern of cortical cell death during aerenchyma formation of rice roots. Planta 204: 277–287

Kawakatsu T, Takaiwa F (2010) Differences in transcriptional regulatory mechanisms functioning for free lysine content and seed storage protein accumulation in rice grain. Plant Cell Physiol 51: 1964-1974

Kim C M, Park S H, Je B I, Park S H, Park S J, Piao H L, Eun M Y, Dolan L, Han C D (2007) OsCSLD1, a cellulose synthase-like D1 gene, is required for root hair morphogenesis in rice. Plant Physiol 143: 1220-1230

Kitomi Y, Inahashi H, Takehisa H, Sato Y, Inukai Y (2012) OsIAA13-mediated auxin signaling is involved in lateral root initiation in rice. Plant Sci 190: 116-122

Kitomi Y, Ito H, Hobo T, Aya K, Kitano H, Inukai Y (2011) The auxin responsive AP2/ERF transcription factor crown rootless5 is involved in crown root initiation in rice through the induction of OsRR1, a type-A response regulator of cytokinin signaling. Plant J 67: 472-484

Kitomi Y, Ogawa A, Kitano H, Inukai Y (2008) CRL4 regulates crown root formation through auxin transport in rice. Plant Root 2: 19-28

Kong X Q, Gao X H, Sun W, An J, Zhao Y X, Zhang H (2011) Cloning and functional characterization of a cation–chloride cotransporter gene OsCCC1. Plant Mol Biol 75: 567-578

Krouk G, Lacombe B, Bielach A, Perrine-Walker F, Malinska K, Mounier E, Hoyerova K, Tillard P, Leon S, Ljung K, Zazimalova E, Benkova E, Nacry P, Gojon A (2010) Nitrate-regulated auxin transport by NRT1. 1 defines a mechanism for nutrient sensing in plants. Dev Cell 18: 927-937

Kubo H, Hayashi K (2011) Characterization of root cells of anl2 mutant in *Arabidopsis thaliana*. Plant Sci 180: 679–685

Kumar S, Stecher G, Tamura K (2016) MEGA7: molecular evolutionary genetics analysis version 7.0 for bigger datasets. Mol Biol Evol 33: 1870-1874

Lasda E L, Blumenthal T (2011) Trans-splicing. Wiley Interdisciplinary Reviews: RNA 2: 417-434

Lee K, Park S J, Colas des Francs-Small C, Whitby M, Small I, Kang H (2019) The coordinated action of PPR 4 and EMB 2654 on each intron half mediates trans-splicing of *rps12* transcripts in plant chloroplasts. Plant J 100: 1193-1207

Lee Y, Rubio M C, Alassimone J, Geldner N (2013) A mechanism for localized lignin deposition in the endodermis. Cell 153: 402-412

Liberman L M, Sparks E E, Moreno-Risueno M A, Petricka J J, Benfey P N (2015) MYB36 regulates the transition from proliferation to differentiation in the Arabidopsis root. Proc Natl Acad Sci USA 112: 12099-12104

Li J T, Zhao Y, Chu H W, Wang L K, Fu Y R, Liu P, Upadhyaya N, Chen C L, Mou T M, Feng Y Q, Kumar P, Xi J (2015a) SHOEBOX modulates root meristem size in rice through dose-dependent effects of gibberellins on cell elongation and proliferation. PLoS Gene 11: e1005464

Li J Z, Han Y C, Liu L, Chen Y P, Du Y X, Zhang J, Sun H Z, Zhao Q Z (2015b) qRT9, a quantitative trait locus controlling root thickness and root length in upland rice. J Exp Bot 66: 2723–2732

Li J, Zhu S H, Song X W, Shen Y, Chen H M, Yu J, Yi K K, Liu Y F, Karplus V J, Wu P, Deng X W (2006) A rice glutamate receptor-like gene is critical for the division and survival of individual cells in the root apical meristem. Plant Cell 18: 340-349

Li Z C, Mu P, Li C P, Zhang H L, Li Z K, Gao Y M, Wang X K (2005) QTL mapping of root traits in a doubled haploid population from a cross between upland and lowland japonica rice in three environments. Theor Appl Genet 110: 1244-1252

Liu H J, Wang S F, Yu X B, Yu J, He X W, Zhang S L, Shou H X, Wu P (2005) ARL1, a LOB-domain protein required for adventitious root formation in rice. Plant J 43: 47-56

Liu S P, Wang J R, Wang L, Wang X F, Xue Y H, Wu P, Shou H X (2009) Adventitious root formation in rice requires OsGNOM1 and is mediated by the OsPINs family. Cell Res 19: 1110-1119

López-Bucio J, Cruz-Ramırez A, Herrera-Estrella L (2003) The role of nutrient availability in regulating root architecture. Curr Opin Plant Biol 6: 280-287

Lorković Z J, Wieczorek Kirk D A, Lambermon M H L, Filipowicz W, (2000) Pre-mRNA splicing in higher plants. Trends Plant Sci 5: 160–167

Ma J F, Tamai K, Yamaji N, Mitani N, Konishi S, Katsuhara M, Ishiguro M, Murata Y, Yano M (2006) A silicon transporter in rice. Nature 440: 688–691

Ma J F, Yamaji N (2015) A cooperative system of silicon transport in plants. Trends Plant Sci 20: 435–442

Ma J F, Yamaji N, Mitani N, Tamai K, Konishi S, Fujiwara T, Katsuhara M, Yano M (2007) An efflux transporter of silicon in rice. Nature 448: 209–212

Ma J F, Yamaji N, Mitani N, Xu X Y, Su Y H, McGrath S P, Zhao F J (2008) Transporters of arsenite in rice and their role in arsenic accumulation in rice grain. Proc Natl Acad Sci USA 105: 9931–9935

Mao C Z, Wang S M, Jia Q J, Wu P (2005) OsEIL1, a rice homolog of the Arabidopsis EIN3 regulates the ethylene response as a positive component. Plant Mol Biol 61: 141

Marschner H (2011) Marschner's mineral nutrition of higher plants. Cambridge, MA, USA: Academic Press

Meng F, Xiang D, Zhu J S, Li Y, Mao C Z (2019) Molecular mechanisms of root development in rice. Rice 12: 1

McGee J D, Hamer J E, Hodges T K (2001) Characterization of a *PR-10* pathogenesis-related gene family induced in rice during infection with Magnaporthe grisea. Mol Plant Microbe In 14: 877-886

Mori M, Nomura T, Ooka H, Ishizaka M, Yokota T, Sugimoto K, Okabe K, Kajiwara H, Satoh K, Yamamoto K, Hirochika H, Kikuchi S (2002) Isolation and characterization of a rice dwarf mutant with a defect in brassinosteroid biosynthesis. Plant Physiol 130: 1152-1161

Nakamura A, Umemura I, Gomi K, Hasegawa Y, Kitano H, Sazuka T, Matsuoka M (2006) Production and characterization of auxin-insensitive rice by overexpression of a mutagenized rice IAA protein. Plant J 46: 297-306

Naseer S, Lee Y, Lapierre C, Franke R, Nawrath C, Geldner N (2012) Casparian strip diffusion barrier in *Arabidopsis* is made of a lignin polymer without suberin. Proc Natl Acad Sci USA 109: 10101-10106

Nemoto H, Suga R, Ishihara M, Okutsu Y (1998) Deep rooted rice varieties detected through the observation of root characteristics using the trench method. Breed Sci 48: 321-324

Nicol F, His I, Jauneau A, Vernhettes S, Canut H, Höfte H (1998) A plasma membrane-bound putative endo-1, 4-β-d-glucanase is required for normal wall assembly and cell elongation in Arabidopsis. EMBO J 17: 5563-5576

Ni J, Wang G H, Zhu Z X, Zhang H H, Wu Y R and Wu P (2011) OsIAA23-mediated auxin signaling defines postembryonic maintenance of QC in rice. Plant J 68: 433-442

Niones J M, Inukai Y, Suralta R R, Yamauchi A (2015) QTL associated with lateral root plasticity in response to soil moisture fluctuation stress in rice. Plant soil 391: 63–75

Qi X P, Wu Z C, Li J H, Mo X R, Wu S H, Chu J, Wu P (2007) AtCYT-INV1, a neutral invertase, is involved in osmotic stress-induced inhibition on lateral root growth in Arabidopsis. Plant Mol Biol 64: 575-587

Qi Y H, Wang S K, Shen C J, Zhang S N, Chen Y, Xu Y X, Liu Y, Wu Y R, Jiang D A (2012) OsARF12, a transcription activator on auxin response gene, regulates root elongation and affects iron accumulation in rice (*Oryza sativa*). New Phytol 193: 109-120

Qin C, Li Y Y, Gan J, Wang W X, Zhang H H, Liu Y, Wu P (2015) OsDGL1, a homolog of an oligosaccharyltransferase complex subunit, is involved in N-glycosylation and root development in rice. Plant Cell Physiol 54: 129-137

Rebouillat J, Dievart A, Verdeil J L, Escoute J, Giese G, Breitler J C, Gantet P, Espeout E, Périn G C (2009) Molecular genetics of rice root development. Rice 2: 15–34

Reddy K R, Patrick W H, Broadbent F E (1984) Nitrogen transformations and loss in flooded soils and sediments. Crit Rev Env Sci Tec 13: 273-309

Robbins N E, Trontin C, Duan L, Dinneny J R (2014) Beyond the barrier: communication in the root through the endodermis. Plant Physiol 166: 551-559

Roppolo D, De Rybel B, Tendon V D, Pfister A, Alassimone J, Vermeer J E M, Yamazaki M, Stierhof Y D, Beeckman T, Geldner N (2011) A novel protein family mediates Casparian strip formation in the endodermis. Nature 473: 380

Sanghera G S, Wani S H, Hussain W, Singh B B (2011) Engineering cold stress tolerance in crop plants. Curr Genomics 12: 30

Sakurai G, Satake A, Yamaji N, Mitani-Ueno N, Yokozawa M, Feugier F G, Ma J F (2015) In silico simulation modeling reveals the importance of the casparian strip for efficient silicon uptake in rice roots. Plant Cell Physiol 56: 631–639

Sasaki A, Yamaji N, Ma, J F (2016) Transporters involved in mineral nutrient uptake in rice. J Exp Bot 67: 3645–3653

Sasaki A, Yamaji N, Xia J X, Ma J F (2011) OsYSL6 is involved in the detoxification of excess manganese in rice. Plant Physiol 157: 1832-1840

Sasaki A, Yamaji N, Yokosho K, Ma J F (2012) Nramp5 is a major transporter responsible for manganese and cadmium uptake in rice. Plant Cell 24: 2155-2167

Schmitz-Linneweber C, Williams-Carrier R E, Williams-Voelker P M, Kroeger T S, Vichas A, Barkan A (2006) A pentatricopeptide repeat protein facilitates the trans-splicing of the maize chloroplast *rps12* pre-mRNA. Plant Cell 18: 2650-2663

Shao J F, Yamaji N, Shen R F, Ma J F (2017) The key to Mn homeostasis in plants: regulation of Mn transporters. Trends Plant Sci 22: 215–224

Shao Y L, Zhou H Z, Wu Y R, Zhang H, Lin J, Jiang X Y, He Q J, Zhu J S, Li Y, Yu H, Mao C Z (2019) OsSPL3, an SBP-domain protein, regulates crown root development in rice. Plant Cell 31: 1257-1275

Shikata M, Matsuda Y, Ando K, Nishii A, Takemura M, Yokota A, Kohchi T (2004) Characterization of *Arabidopsis* ZIM, a member of a novel plant-specific GATA factor gene family. J Exp Bot 55: 631-639

Sun H W, Bi Y, Tao J Y, Huang S J, Hou M M, Xue R, Liang Z H, Gu P Y, Yoneyama K, Xie X N, Shen Q R, Xu G H, Zhang Y L (2016) Strigolactones are required for nitric oxide to induce root elongation in response to nitrogen and phosphate deficiencies in rice. Plant Cell Environ 39: 1473-1484

Sun H W, Tao J Y, Hou M M, Huang S J, Chen S, Liang Z H, Xie T N, Wei Y Q, Xie X N, Yoneyama K, Xu G H, Zhang Y L (2015) A strigolactone signal is required for adventitious root formation in rice. Ann Bot 115: 1155-1162

Tabata R, Sumida K, Yoshii T, Ohyama K, Shinohara H, Matsubayashi Y (2014) Perception of root-derived peptides by shoot LRR-RKs mediates systemic N-demand signaling. Science 346: 343-346

Takahashi E, Syo S, Miyake Y (1976a) Effect of germanium on the growth of plants with special reference to the silicon nutrition (Part 1). J Sci Soil Manure Jpn 47: 183-190

Takahashi E, Syo S, Miyake Y (1976b) Effect of germanium on the growth of plants with special reference to the silicon nutrition (Part 2). J Sci Soil Manure Jpn 47: 191-197

Takken F L W, Goverse A (2012) How to build a pathogen detector: structural basis of NB-LRR function. Curr Opin Plant Biol 15: 375-384

Tang G L, Zhu X H, Gakiere B, Levanony H, Kahana A, Galili G (2002) The bifunctional *LKR/SDH* locus of plants also encodes a highly active monofunctional lysine-ketoglutarate

reductase using a polyadenylation signal located within an intron. Plant Physiol 130: 147-154

Teo Y H, Beyrouty C A, Norman R J, Gbur E E (1995) Nutrient uptake relationship to root characteristics of rice. Plant Soil 171: 297-302

Tsukagoshi H, Busch W, Benfey P N (2010) Transcriptional regulation of ROS controls transition from proliferation to differentiation in the root. Cell 143: 606-616

Ueno D, Sasaki A, Yamaji N, Miyaji T, Fujii Y, Takemoto Y, Moriyama S, Che J, Moriyama Y, Iwasaki K, Ma J F (2015) A polarly localized transporter for efficient manganese uptake in rice. Nat Plants 1: 15170

Uga Y, Kitomi Y, Yamamoto E, Kanno N, Kawai S, Mizubayashi T, Fukuoka S (2015) A QTL for root growth angle on rice chromosome 7 is involved in the genetic pathway of deeper rooting 1. Rice 8: 8

Uga Y, Okun K, Yano M (2011) Dro1, a major QTL involved in deep rooting of rice under upland field conditions. J Exp Bot 62: 2485–2494

Uga Y, Sugimoto K, Ogawa S, Rane J, Ishitani M, Hara N, Kitomi Y, Inukai Y, Ono K, Kanno N, Inoue H, Takehisa H, Motoyama R, Nagamura Y, WU J Z, Matsumoto T, Takai T, Okuno K, Yano M (2013) Control of root system architecture by deeper rooting 1 increases rice yield under drought conditions. Nature Genet 45: 1097–1102

Wang J Z, Wang J, Hu M J, Wu S, Qi J F, Wang G X, Han Z F, Qi Y J, Gao N, Wang H W, Zhou J M, Chai J J (2019a) Ligand-triggered allosteric ADP release primes a plant NLR complex. Science 364: eaav5868

Wang H, Inukai Y, Yamauchi A (2006) Root development and nutrient uptake. Crit Rev Plant Sci 25: 279–301

Wang S K, Xu Y X, Li Z L, Zhang S N, Lim J M, Lee K O, Li C Y, Qian Q, Jiang D A, Qi Y H (2014b) OsMOGS is required for N-glycan formation and auxin-mediated root development in rice (*Oryza sativa* L.). Plant J 78: 632-645

Wang X F, He F F, Ma X X, Mao C Z, Hodgman C, Lu C G, Wu P (2011) OsCAND1 is required for crown root emergence in rice. Mol Plant 4: 289-299

Wang Y, Ma N N, Qiu S C, Zou H Y, Zang G C, Kang Z H, Wang G X, Huang J L (2014a) Regulation of the α-expansin gene OsEXPA8 expression affects root system architecture in transgenic rice plants. Mol Breeding 4: 47-57

Wang Y H, Wang D, Gan T, Liu L L, Long W H, Wang Y L, Niu M, Li X H, Zheng M, Jiang L, Wan J M (2016) CRL6, a member of the CHD protein family, is required for crown root development in rice. Plant Physiol Biochem 105: 185-194

Wang Z, Yamaji N, Huang S, Zhang X, Shi M X, Fu S, Yang G Z, Ma J F, Xia J X (2019b) OsCASP1 is required for Casparian strip formation at endodermal cells of rice roots for selective uptake of mineral element. Plant Cell 31: 2636-2648

Wen W W, Jin M, Li K, Liu H J, Xiao Y J, Zhao M C, Alseekh S, Li W Q, Lima F, Brotman Y, Willmitzer L, Fernie A R, Yan J B (2018) An integrated multi-layered analysis of the metabolic networks of different tissues uncovers key genetic components of primary metabolism in maize. Plant J 93: 1116-1128

White D W R (2006) PEAPOD regulates lamina size and curvature in *Arabidopsis*. P Natl Acad Sci USA 103: 13238-13243

Williamson L C, Ribrioux S P C P, Fitter A H, Leyser H M O (2001) Phosphate availability regulates root system architecture in Arabidopsis. Plant Physiol 126: 875-882

Xia J X, Yamaji N, Che J, Shen R F, MA J F (2014) Normal root elongation requires arginine produced by argininosuccinate lyase in rice. Plant J 78: 215-226

Xiao G Q, Qin H, Zhou J H, Quan R D, Lu X Y, Huang R F, Zhang H W (2016) OsERF2 controls rice root growth and hormone responses through tuning expression of key genes involved in hormone signaling and sucrose metabolism. Plant Mol Biol 90: 293-302

Xu W F, Jia L G, Shi W M, Liang J S, Zhou F, Li Q F, Zhang J H (2013) Abscisic acid accumulation modulates auxin transport in the root tip to enhance proton secretion for maintaining root growth under moderate water stress. New Phytol 197: 139-150

Yamada S, Kano A, Tamaoki D, Miyamoto A, Shishido H, Miyoshi S, Taniguchi S, Akimitsu K, Gomi K (2012) Involvement of OsJAZ8 in jasmonate-induced resistance to bacterial blight in rice. Plant Cell Physiol 53: 2060-2072

Yamaguchi M, Sharp R E (2010) Complexity and coordination of root growth at low water potentials: recent advances from transcriptomic and proteomic analyses. Plant Cell Environ 33: 590-603

Yamaji N, Sasaki A, Xia J X, Yokosho K, Ma J F (2013) A node-based switch for preferential distribution of manganese in rice. Nat Commun 4: 2442

Yamaji N, Ma JF (2007) Spatial distribution and temporal variation of the rice silicon transporter Lsi1. Plant Physiol 143: 1306-1313

Yokosho K, Yamaji N, Mitani-Ueno N, Shen RF, Ma JF (2016) An aluminum-inducible IREG gene is required for internal detoxification of aluminum in buckwheat. Plant Cell Physiol

57: 1169-1178

Yoo S C, Cho S H, Paek N C (2013) Rice WUSCHEL-related homeobox 3A (OsWOX3A) modulates auxin-transport gene expression in lateral root and root hair development. Plant Signal Behav 8: e25929

Yoshida K, Imaizumi N, Kaneko S, Kagagoe Y, Tagiri A, Tanaka H, Nishitani K, Komae K (2006) Carbohydrate-binding module of a rice endo-β-1, 4-glycanase, OsCel9A, expressed in auxin-induced lateral root primordia, is post-translationally truncated. Plant Cell Physiol 47: 1555-1571

Yoshinari A, Takano J (2017) Insights into the mechanisms underlying boron homeostasis in plants. Front Plant Sci 8: 1951

Yuan Y X, Wu J, Sun R F, Zhang X W, Xu D H, Bonnema G, Wang X W (2009) A naturally occurring splicing site mutation in the *Brassica rapa FLC1* gene is associated with variation in flowering time. J Exp Bot 60: 1299–1308

Yuan Y X, Zhong S H, Li Q, Zhu Z R, Lou Y G, Wang L Y, Wang J J, Wang M Y, Li Q L, Yang D L, He Z H (2007). Functional analysis of rice NPR1-like genes reveals that OsNPR1/NH1 is the rice orthologue conferring disease resistance with enhanced herbivore susceptibility. Plant Biotechnol J 5: 313-324

Yu C L, Sun C D, Shen C J, Wang S K, Liu F, Liu Y, Chen Y L, Li C Y, Qian Q, Aryal B, Geisler M, Jiang D A, Qi Y H (2015) The auxin transporter, OsAUX1, is involved in primary root and root hair elongation and in Cd stress responses in rice (*Oryza sativa* L.). Plant J 83: 818-830

Yu H S, Kong X F, Huang H, Wu W W, Park J, Yun A J, Lee B, Shi H Z, Zhu J K (2020) *STCH4/REIL2* confers cold stress tolerance in Arabidopsis by promoting rRNA processing and CBF protein translation. Cell Rep 30: 229-242

Yu P, Gutjahr C, Li C J, Hochholdinger F (2016) Genetic control of lateral root formation in cereals. Trends Plant Sci 21: 951-961

Yu Z, Kang B, He X, Lv S, Bai Y, Ding W, Chen M, Cho HT, Wu P (2011) Root hairspecific expansins modulate root hair elongation in rice. Plant J 66:725–734

Zhang H M, Han W, De Smet I, Talboys P, Loya R, Hassan A, Rong H L, Jurgens G, Knox J P, Wang M H (2010) ABA promotes quiescence of the quiescent centre and suppresses stem cell differentiation in the Arabidopsis primary root meristem. Plant J 64: 764-774

Zhang J W, Xu L, Wu Y R, Chen X A, Liu Y, Zhu S H, Ding W N, Wu P, Yi K K (2012) OsGLU3, a putative membrane-bound endo-1, 4-beta-glucanase, is required for root cell elongation and division in rice (*Oryza sativa* L.). Mol Plant 5: 176-186

Zhang W P, Shen X Y, Wu P, Hu B, Liao C Y (2001) QTLs and epistasis for seminal root length under a different water supply in rice (*Oryza sativa* L.). Theor Appl Genet 103: 118-123

Zhao Y, Hu Y F, Dai M Q, Huang L M, Zhou D X (2009) The WUSCHEL-related homeobox gene WOX11 is required to activate shoot-borne crown root development in rice. Plant Cell 21: 736-748

Zhao Y, Cheng S F, Song Y L, Huang Y L, Zhou S L, Liu X Y, Zhou D X (2015) The interaction between rice ERF3 and WOX11 promotes crown root development by regulating gene expression involved in cytokinin signaling. Plant Cell 27: 2469-2483

Zheng B S, Yang L, Zhang W P, Mao C Z, Wu Y R, Yi K K, Liu F Y, Wu p (2003) Mapping QTLs and candidate genes for rice root traits under different water-supply conditions and comparative analysis across three populations. Theor Appl Genet 107: 1505–1515

Zheng H K, Li S J, Ren B, Zhang J, Ichii M, Taketa S, Tao Y Z, Zuo J R, Wang H (2013) Lateral rootless2, a cyclophilin protein, regulates lateral root initiation and auxin signaling pathway in rice. Mol Plant 6: 1719-1721

Zheng Z, Wang Z, Wang X Y, Liu D (2019) Blue light-triggered chemical reactions underlie phosphate deficiency-induced inhibition of root elongation of Arabidopsis seedlings grown in petri dishe. Mol Plant 12: 1515-1523

Zhou H L, He S J, Cao Y R, Chen T, Du B X, Chu C C, Zhang J S, Chen S Y (2006) OsGLU1, A putative membrane-bound Endo-1, 4-ß-D-glucanase from rice, affects plant internode elongation. Plant Mol Biol 60: 137-151

Zhu J S, Li Y, Lin J, Wu Y R, Guo H X, Shao Y L, Wang F, Wang X F, Mo X R, Zheng S J, Yu H, Mao C Z (2019) CRD1, an Xpo1 domain protein, regulates miRNA accumulation and crown root development in rice. Plant J 100: 328-342

Zhu J K (2001) Plant salt tolerance. Trends Plant Sci 6: 66-71

Zhu J K (2002) Salt and drought stress signal transduction in plants. Annu Rev Plant Biol 53: 247-273

Zhu Y, Qian W Q, Hua J (2010) Temperature modulates plant defense responses through NB-LRR proteins. Plos Pathog 6: e1000844

Zhu Z X, Liu Y, Liu S J, Mao C Z, Wu Y R, Wu P (2012) A gain-of-function mutation in OsIAA11 affects lateral root development in rice. Mol Plant 5: 154-161

Zuo J R, Niu Q W, Nishizawa N, Wu Y, Kost B, Chua N H (2000) KORRIGAN, an Arabidopsis endo-1, 4-β-glucanase, localizes to the cell plate by polarized targeting and is essential for cytokinesis. Plant Cell 12: 1137-1152

Zou H Y, Wenwen Y H, Zang G C, Kang Z H, Zhang Z Y, Huang J L, Wang G X (2015) OsEXPB2, a β-expansin gene, is involved in rice root system architecture. Mol Breeding 35: 41

Acknowledgements

First of all, I would like to express my sincere gratitude to my supervisor Dr. Jian Feng Ma, who gives me the valuable opportunity to study in his lab. I appreciate his valuable guidance and insightful comments on my experiments.

I also sincerely thank to my co-supervisors Drs. Takashi Hirayama and Yamaji Naoki for their useful suggestions and technical support. Especial thanks are given to all members in my lab, for their great helps.

I also thank to my parents, without their support, I would not go that far.

Finally, I would like to thank the JASSO Honors Scholarship, Ohara Scholarship, and Monbukagakusho (MEXT) Scholarship for the financial support during my study in Japan.